DENDI KRISNA NUGRAHA

INTERACTION BETWEEN *BORDETELLA BRONCHISEPTICA* AND *ACANTHAMOEBA* AS A TRANSIENT HOST IN THE NATURAL ENVIRONMENT

GRADUATE SCHOOL OF FRONTIER BIOSCIENCES

OSAKA UNIVERSITY

2022

INTERACTION BETWEEN *BORDETELLA BRONCHISEPTICA* AND *ACANTHAMOEBA* AS A TRANSIENT HOST IN THE NATURAL ENVIRONMENT

DOCTORAL DISSERTATION

Submitted as partial fulfillment of the requirement to obtain

Doctor of Philosophy Degree from Graduate School of Frontier

Biosciences, Osaka University, Japan

March 2022

Dendi Krisna Nugraha

32A17072

Prof. Yasuhiko Horiguchi, Ph.D., D.V.M.

Supervisor

ABSTRACT

INTERACTION BETWEEN *BORDETELLA BRONCHISEPTICA* AND *ACANTHAMOEBA* AS A TRANSIENT HOST IN THE NATURAL ENVIRONMENT

DENDI KRISNA NUGRAHA

Bordetella bronchiseptica (*Bb*) is a Gram-negative bacterium, which causes respiratory diseases in pigs, dogs, cats, and occasionally humans. In addition to infecting hosts, *Bb* is considered to survive in the environment persistently, which may provide a source of infection; however, the environmental lifestyle of *Bb* is poorly understood. In general, environmental bacteria survive in a dormant state or proliferate with or without interacting with other living organisms, such as protozoa.

In this study, I explored the possible interaction between *Bb* and *Acanthamoeba castellanii* (*Ac*) as a representative of environmental protozoa. Unlike bacteria that serve as amoeba food sources, *Bb* phagocytosed by the amoeba resisted digestion and escaped to extracellular milieu through contractile vacuoles (CVs), intracellular compartments involved in osmoregulation. Furthermore, *Bb* survived and proliferated for at least 28 days of co-culture with the amoeba. The Bordetellae harbors the *Bordetella* virulence gene (BvgAS) two-component system, which controls the reversible phenotypic conversions between an avirulent phenotype known as Bvg^- phase and the virulent Bvg^+ phase. A mutant of *Bb* locked in the Bvg^- phase but not in the Bvg^+ phase was found to survive and proliferate in the co-culture with the amoeba. Microscopic analyses revealed that the Bvg^+ phase-locked mutant was more efficiently internalized and transported to the intracellular digestion pathway than the Bvg^- phase-locked mutant. After seven days of co-culture, the dead cells of the Bvg^+ phase-locked mutant were accumulated in giant food

vacuoles (GFVs), which were previously reported as a specific compartment in the amoeba phago-endosomal pathway. These data suggest that *Bb* resists predation by *Ac* in a Bvg phase-dependent manner. By screening variants of the Bvg^+ phase-locked mutant in which Bvg^+-specific genes were deleted, I found that deletion mutants deficient in bacterial adhesion molecules, FhaB and fimbriae, survived in the co-culture with the amoeba similar to the WT strain, indicating that the adhesion molecules are targeted for predation by the amoeba.

The present study indicates that *Bb* survives from *Ac* predation by concealing FhaB and fimbriae, which are major bacterial adhesins contributing to the establishment of bacterial colonization in infection to mammalian hosts. *Ac* could be a transient host in the natural environment, which supports the propagation of the bacteria. This study also provides a new perspective for understanding the ecology of *Bb* during the lifecycle outside the mammalian hosts.

LIST OF ABBREVIATIONS

Ac: *Acanthamoeba castellanii*

Bb: *Bordetella bronchiseptica*

BG: Bordet-Gengou

BscN: *Bordetella* secretion gene *n* (Type III Secretion System ATPase)

BvgAS: Bordetella virulence gene A (response regulator)/ S (histidine kinase)

CFU: Colony Forming Unit

CV: Contractile Vacuole

Dd: *Dictyostelium discoideum*

DNT: Dermonecrotic Toxin

Ec: *Escherichia coli*

FhaB: Filamentous hemagglutinin gene *b*

FimBCD: Fimbriae gene *b*, *c* and *d*

FV: Food Vacuole

GFP: Green Fluorescent Protein

GFV: Giant Food Vacuole

GPA: Gentamicin Protection Assay

HG: Hepes-Glucose (50 mM Hepes pH 7.4 and 5 mM glucose) medium

HOS: High Osmolarity Solution (50 mM magnesium chloride and 10% glucose)

LB: Luria Broth

MOI: Multiplicity of Infection

OD: Optical density

Prn: Pertactin

PYG: Peptone Yeast Glucose

SS: Stainer-Scholte

TCS: Two Component System

WT: wildtype

TABLE OF CONTENTS

LIST OF FIGURES

LIST OF TABLES

CHAPTER 1 - GENERAL INTRODUCTION

1.1 *Bordetella bronchiseptica* (*Bb*)

Bordetella bronchiseptica (*Bb*) is an aerobic Gram-negative coccobacillus with about 0.5-1 µm in diameter and 1 µm in length. Its optimal growth temperature is 35-37℃. Since 1910, even though it did not bear its present name, *Bb* has been known as a respiratory tract pathogen in various domestic animals such as swine, dogs, cats, and later is known to infect immunocompromised humans occasionally (*1*, *2*). Among them, highly contagious kennel cough in dogs is characterized by congestion of the mucosal trachea and bronchi. On the other hand, atrophic rhinitis, mainly found in young piglets, is characterized by sneezing and coughing, followed by deformity of the bone structure of the nose and therefore easily observed as a twisted snout (*3*). *Bb* is closely related to a human-adapted *Bordetella pertussis* and *Bordetella parapertussis,* which cause whooping cough. These three bacteria are categorized as the classical *Bordetellea* (*4*).

1.1.1 Virulence factors and their regulation in *Bb*

The successful establishment of infection in the animal hosts is facilitated by various virulence factors expressed by *Bb*. These virulence factors can be divided into several classes, such as adhesins, autotransporters, toxins, and others which include lipopolysaccharide (LPS), secretion systems, and flagella (**Table 1.1**) (*5*). Three types of adhesins expressed by *Bb,* such as filamentous hemagglutinin (FHA), fimbriae (FIM), and pertactin (PRN), have been studied extensively (*6–8*). Several *Bordetella* proteins with predicted autotransporter ability include pertactin, virulence-associated-gene 8 (Vag8), *Bordetella* resistance to killing A (BrkA), and subtilisin-like protein SphB1 (*3*, *9–11*). Two major toxins, such as adenylate cyclase toxin (CyaA) and dermonecrotic toxin (DNT), were well-characterized and have been shown to be implicated in significant clinical manifestation of the diseases (*12*, *13*). Although harbors an intact 12 kbp *ptx–ptl* operon, *Bb* does not express Pertussis toxin (PTX) due to an inactive *ptx* promoter (P*ptx*) (*14*). The replacement with a functional *ptx* promoter from *B. pertussis* directly upstream of the *ptx-ptl* region of *Bb* resulted in both production and efficient secretion of the toxin (*15*). *Bb* also possesses a Type III secretion system that secretes effector proteins directly into host

cells and contribute to the persistence of the bacteria in the lower respiratory tract of swine (*16*). Some of the above-mentioned major virulence factors produced by *Bb* are briefly discussed below.

Table 1.1 Function information for various virulence determinants in *Bordetellae*

Virulence determinant	Description	Gene expression	
		B. pertussis	*B. bronchiseptica*
Adhesins			
Filamentous hemagglutinin (FHA)	220-kDa surface-associated and secreted protein; dominant adhesin; required for tracheal colonization; highly immunogenic; primary component of acellular pertussis vaccines	+	+
Fimbriae (FIM)	Filamentous cell surface structures; required for persistent tracheal colonization; component of some acellular pertussis vaccines: required for protective immunity to infection	+	+
Autotransporters			
Pertactin (PRN)	68–70-kDa surface protein; mediates eukaryotic cell binding in vitro; enhances protective immunity	+	+
Vag8	95-kDa outer membrane protein	+	+
BrkA	73-kDa surface-associated N-terminal passenger domain with 30-kDa outer membrane C-terminal protein; putative adhesin; confers serum resistance and protection against antimicrobial peptides in *B. pertussis*	+	+
SphB1	Subtilisin-like Ser protease/lipoprotein required for FHA maturation in *B. pertussis*	+	+
Tracheal colonization factor (TcfA)	60-kDa secreted protein; role in tracheal colonization in murine model	+	−
Toxins			
Pertussis toxin (PT)	A-B-toxin; ADP-ribosylates G proteins; responsible for pertussis-associated lymphocytosis; strong adjuvant and primary component of pertussis vaccines	+	−
Adenylate cyclase (CyaA)	Calmodulin-activated RTX family toxin with dual adenylate cyclase/hemolysin activity; acts as anti-inflammatory and antiphagocytic factor during infection	+	+
Type III secretion	Allows *Bordetella* to translocate effector proteins directly into host cells; required for persistent tracheal colonization; inhibits host immune response; activates ERK1/2; mislocalizes NF-κB; causes caspase-independent cell death	+	+
Dermonectrotic toxin (DNT)	160-kDa heat-labile secreted toxin; activates Rho; induces necrosis in vitro	+	+
Tracheal cytotoxin (TCT)	Disaccharide-tetrapeptide monomeric by-product of peptidoglycan synthesis; causes mitochondrial bloating, disruption of tight junctions, damage to cilia, IL-1α and $NO^{\cdot}$ production	+	+

LPS			
wlb locus	Consists of 12 genes required for LPS (band A) biosynthesis	+	+
wbm locus	Encodes O antigen; may be important for confering serum resistance	−	+
PagP	Mediates palmitoylation modification of lipid A; may be important for persistence and resistance to serum killing	−	+
Additional loci			
Flagella	Peritrichous cell surface appendages required for motility; highly antigenic; ectopic expression of flagella in the Bvg^+ phase is detrimental to the infection cycle	−	+
Type IV pili	Polar pili usually with an N-methylated phenylalanine as the N-terminal residue; possible functions include adherence, twitching motility, and DNA uptake	Δ	ND
Capsule	A type II polysaccharide coat predicted to be comprised of an *N*-acetylgalactosaminuronic acid Vi antigen-like polymer; possible role in protection against host defense mechanisms or survival in the environment	Δ	ND
Alcaligin	A siderophore for complexing iron, which is internalized through outer membrane receptors (*B. bronchiseptica* encodes 16 such receptors while *B. pertussis* encodes 12); iron uptake may be important for survival within mammalian hosts	+	+
Vrg loci	Several loci of uncharacterized function	+	−

+, *positive for expression;* –, *no expression;* Δ, *genome contains deletion mutations in these genes; ND, not determined* (taken from (5))

FHA is a ~220 kDa surface-associated and highly immunogenic secreted protein, which is commonly shared by *Bb*, *B. pertussis*, and *B. parapertusis* (*1*, *3*, *7*). In 1983, Weiss *et al.* identified the genetic locus responsible for FHA production in a *B. pertussis* mutant due to insertion of Tn5 transposon that was unable to agglutinate sheep erythrocytes (*17*). Mature FHA contains an Arg-Gly-Asp (RGD) tripeptide motif which was reported to facilitate adherence of the bacteria to the integrin and complement receptor type 3 (CR3) of macrophages to promote phagocytosis (*18*, *19*). *In vitro* studies also suggested that FHA possesses a carbohydrate recognition domain (CRD), which facilitates adherence to ciliated respiratory epithelial cells and macrophages (*20*). In addition, FHA also displays a lectin-like activity for heparin and other sulfated carbohydrates, which mediate attachment to non-ciliated epithelial cell lines. This heparin-binding site is dependent from the RGD or CRD site and is required for FHA-induced hemagglutination (*21*).

Another major adhesin produced by *Bb* is FIM, a filamentous complex of polymeric proteins presented on the bacterial cell surface. The two predominant subunits, Fim2 and Fim3 (AGG2 and AGG3), mainly compose pilins in *Bordetella* (*22*). Other important pilins such as FimX, FimN, and FimA are also expressed in *Bb* (*23*, *24*). The fimbrial

biogenesis operon is composed of *fimBCD* genes located downstream of the *fhaB* gene, which encodes FHA (*3*, *6*). It has been shown that *Bb* strain lacking FIM due to an in-frame deletion mutation of the *fimBCD* genes but with intact FHA production was defective in its ability to adhere ciliated rabbit tracheal explants, indicating that FIM may mediate adherence specifically to cilia (*25*). Together with FHA, FIM are required for the persistent colonization of the trachea in mice and may play a role in the development of a humoral immune response to *Bordetella* infection (*26*).

Autotransporter proteins also compose a group of virulence factors of *Bb*. The name "autotransporter" came from their characteristic feature to be autonomously exported to the outer membrane. In addition, the *Bordetella* autotransporter family, includes functionally diverse proteins, such as proteases, adhesins, toxins, and lipases (*3*, *27*). PRN, the autotransporter firstly identified and described in *Bordetella*, is known to function as a non-fimbrial adhesin. The size of mature PRN in *Bb* is ~68 kDa (*8*), ~69 kDa in *B. pertussis* (*28*), and 70 kDa in *B. parapertussis* (*29*). Similar to FHA and FIM, PRN also facilitates attachment to mammalian cells via its RGD sequence (*30*, *31*). Besides the RGD sequence, pertactin also contains proline-rich region and leucine-rich repeats, conserved motifs found in molecules that mediate protein-protein interactions involved in eukaryotic cell binding (*32*). BrkA, Vag8, and SphB1 are also secreted proteins with predicted ability as autotransporter, characterized by highly significant sequence similarity in the C-terminal region and contain at least one RGD motif (*33*–*35*).

CyaA possesses bifunctional modules: an adenylate cyclase (AC) domain which is sensitive to calmodulin activation and catalyzes the unregulated production of cyclic AMP (cAMP), and a repeat-in-toxin (RTX) hemolytic domain, which facilitates toxin binding to target cells and translocating the AC domain into the cytosol by cation-selective pore formation (*36*, *37*). CyaA is a ~216 kD secreted protein produced by all *Bordetella* species except *B. avium* (*38*, *39*). CyaA has a unique enzymatic activity that facilitates the formation of ion-permeable pores on the target cell membranes. In erythrocytes, this action causes hemolysis, which is characterized by the formation of a clear zone surrounding grown *Bb* colonies on the BG agar supplemented with horse or sheep blood cells (*40*, *41*).

A *Bb* mutant lacking CyaA was defective in colonization, indicating that this toxin is essential for establishing early colonization (*42*).

Dermonecrotic toxin (DNT) is a ~160 kDa intracellular, heat-labile, and mitogenic toxin produced by *Bordetella*. DNT impairs osteoblastic differentiation and is implicated in atrophic rhinitis in pigs (*43*, *44*). Despite well-studied mechanism by which the toxin enters target cells, nothing is known about its secretion pathway from the bacterial cell body. A possible explanation is that DNT may be released following cell lysis (*3*, *37*, *45*–*47*). DNT is cytotoxic for preosteoblast, kidney epithelial, fibroblast, and embryonic bovine lung cells (*48*). Upon entry to target cells through the T-type voltage-gated Ca^{2+} channel $Ca_V3.1$ as its receptor (*49*), DNT deamidates 63rd glycine residue (Gln-63) of small G-protein Rho or Gln-61 of Rac or Cdc42 to Glu and causes assembly of actin stress fibers and focal adhesions (*50*, *51*). DNT from *Bordetellea* has structural and functional homology to the *Escherichia coli* cytotoxic necrotizing factor 1 (CNF1) (*48*, *52*).

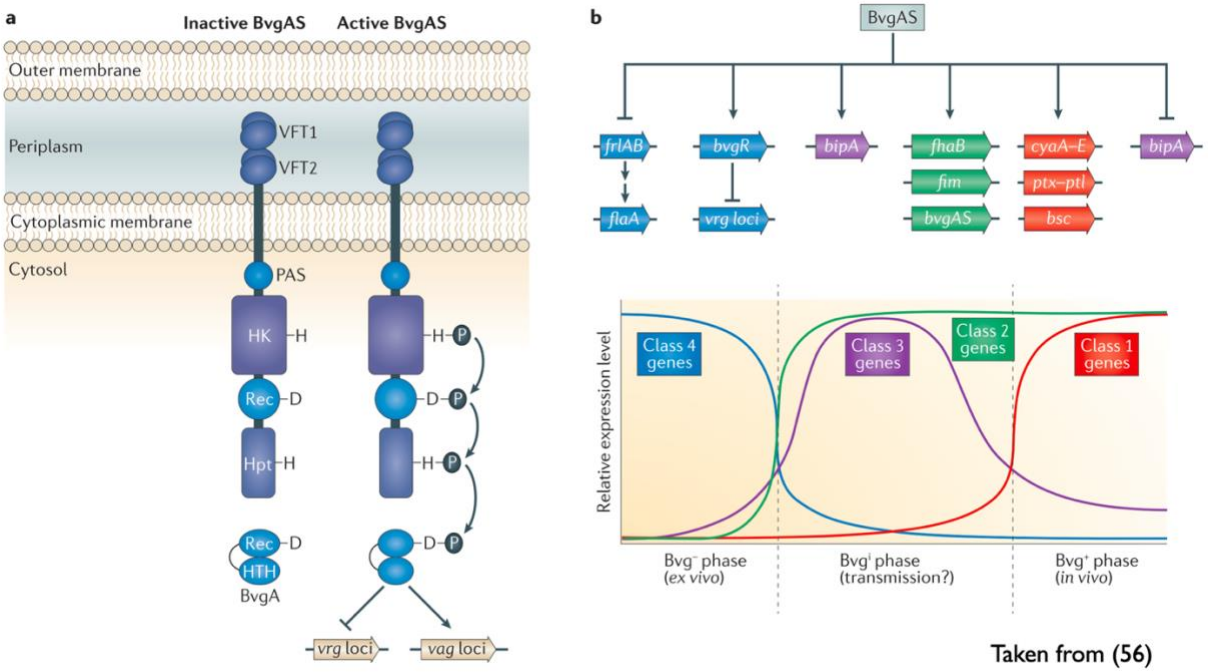

Figure 1.1 The BvgAS two-component system in *Bordetellae*

A two-component system (TCS) termed as BvgAS system, which is encoded by *Bordetella* virulence genes (Bvg) locus, regulates the expression of major virulence factors mentioned above (**Fig. 1.1**). Like other bacterial two-component signal transduction

systems, the *Bordetella* Bvg regulon uses a sensor kinase (BvgS) to deliver signals to a response regulator (BvgA) via a four-step His-Asp-His-Asp phosphorelay signaling. When grown at 37℃, the BvgAS system is activated (Bvg^+ phase). Once phosphorylated by BvgS, BvgA promotes the transcription of Bvg^+ phase-specific genes (most of the virulence factors) by binding to their promoter regions. At lower temperature (20-25℃) or in the presence of a low concentration of modulating agents such as nicotinic acid and magnesium sulfate, the BvgAS system is inactivated (Bvg^- phase), resulting in upregulation of the expression of Bvg^- phase-specific genes, such as genes related in chemotaxis and motility (*53–56*). *Bordetella* also has a third intermediate phase called Bvg^i that displays reduced survival *in vivo* but increased ability to survive nutrient deprivation (*57*). In *Bb*, the Bvg^+ phase is required to establish respiratory tract infection in the rabbit, while the Bvg^- phase may contribute to environmental survival and persistence (*58*).

1.1.2 Intracellular survival within the host

Bb is exposed to various host immune barriers upon entry to the mammalian hosts, including macrophages, dendritic cells, monocytes, and neutrophils, which phagocytizes and digests bacteria using an endocytic processing pathway (*59*). Despite being considered an extracellular pathogen, *Bb* has been shown to survive intracellularly in a Bvg^+ phase-dependent manner (*60*). *In vitro* experiments have demonstrated that *Bb* invaded into and survived in mouse dendritic cells and macrophages (*61–63*). However, it is poorly understood how *Bb* survives in the cells. Transmission electron microscopy analysis of mouse dendritic cells infected with *Bb* revealed that the proliferated bacteria were present in phagosomes, which had fused with lysosomes during the initial infection period (*64*). Another TCS called RisAS, which was found only in *Bb*, is responsible for acid phosphatase production. Mutation within the genetic locus encoding RisAS impaired the persistence of *Bb* in peritoneal macrophages. This mutant exhibited a lower ability to colonize the lung of BALB/c mice (*65*). These results suggest that the acid phosphatase production may confer resistance on *Bb* to phagosome acidification and reactive oxygens intermediates (*65, 66*).

1.1.3 Ecology and environmental survival of *Bb*

Bb was reported to grow well in the soil extract similar to *B. petrii* isolated from the environment, indicating that pathogenic *Bordetella* may have retained the ability to proliferate in the environment, besides the mammalian-adapted pathogen. Another study reported that *Bb* survived up to 45 days after incubated in soil extract. This result prompts the hypothesis that *Bb* may originate from an environmental *Bordetella* ancestor and suggests that *Bb* may be found transiently in soil, for example, at farms with suitable animal hosts such as cattle, swine, sheep, and horses (*67*, *68*). It was also demonstrated that *Bb* persisted and proliferated up to 1,000-fold after incubation for 48 hours at 37℃ in the natural lake and pond water (*69*). At 10℃ or less, *Bb* was reported to survive up to 24 weeks in lake water (*70*). *Bb* is considered to survive under these conditions through environmental adaptations, such as highly efficient scavenging of trace nutrients, reductive cell division, endogenous respiration, and re-utilization of nutrients from dead bacteria debris (*69*). These results showed that *Bb* may survive in environments outside of the mammalian hosts. It is intriguing to consider that extra-host or environmental reservoirs may be a potential risk of *Bb* infection.

1.2 Introduction to *Acanthamoeba*

Acanthamoeba is a genus of free-living amoeba (FLA) that are ubiquitously found in various natural water or soils (*71*). *Acanthamoeba* occasionally causes blinding keratitis and fatal granulomatous encephalitis in immunocompromised humans, and therefore designated as a protist pathogen (*72*). Despite its pathogenicity, *Acanthamoeba* is increasingly used as a model organism for studying cellular differentiation mechanisms, motility, phagocytosis, and bacterial pathogenesis (*73*). Based on the 18S ribosomal RNA (rRNA) sequences, *Acanthamoeba* strains are classified into 18 genotypes, from T1 to T18; the disease-causing isolates mostly belong to T4 (*74*, *75*). Among them, *Acanthamoeba castellanii* was used for the present study.

1.2.1 *Acanthamoeba castellanii* (*Ac*)

In 1930, Aldo Castellani isolated an amoeba from a contaminated *Cryptococcus pararoseus* culture that was later named after him, *Acanthamoeba castellanii* (*Ac*), which

is distinctly characterized by the spike-like protrusions called acanthopodia on their surface. These cytoplasmic protrusions are involved in capturing prey, motility, and adherence. *Ac* has two life stages: a metabolically active, vegetative form, called a trophozoite, and a dormant form, called a cyst (**Fig. 1.2**). In the presence of food sources and under optimal growth conditions, *Ac* takes on the trophozoite form ranging from 15 to 50 μm in size. This form of *Ac* contains at least one contractile vacuole (CV), involved in osmoregulation, digestive vacuoles, lysosomes, and glycogen-containing vacuoles (*73*). Under optimal growth conditions, i.e., neutral pH, incubation temperature between 25-30°C, and osmolarity between 50-80 milliosmole (mOsmol), *Ac* trophozoites divide by binary fission with a doubling time of 8-24 h (*71*). When exposed to unfavorable conditions, such as poor nutrition, extreme pH and temperature, or in the presence of toxic chemical substances, *Ac* trophozoites become cysts through the process called encystation, by which *Acanthamoeba* converts into the dormant state. During encystation, *Ac* produces a double-layered cyst wall, which comprises an external wall (ectocyst) and an inner wall (endocyst). The ectocyst mainly composed of lipids and proteins, organizes a wrinkled layer, while the endocyst containing cellulose varies in shape (*76*). When returning to favorable conditions, cysts revert to the active trophozoite form by the process called excystment (*71*, *76*, *77*).

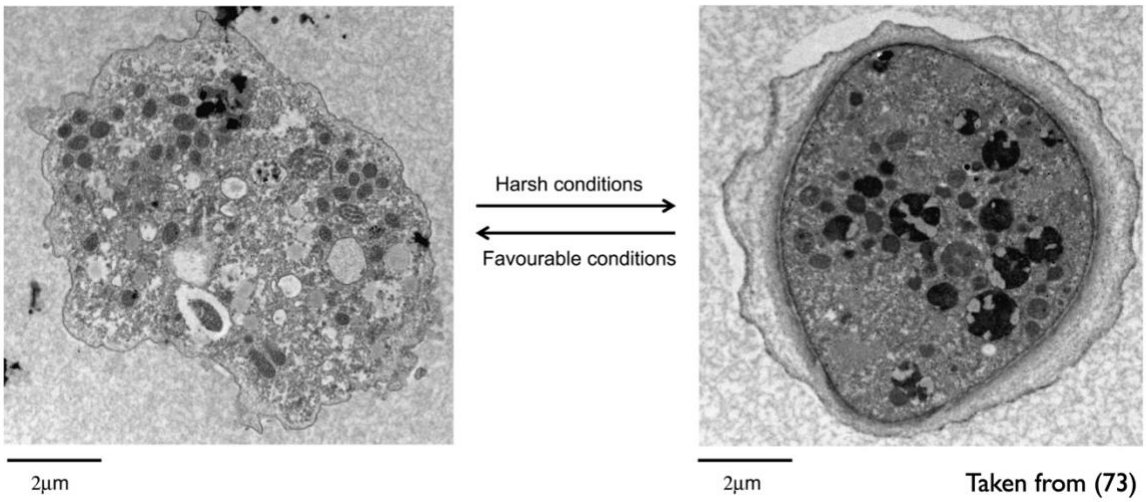

Figure 1.2 Life cycle of *Acanthamoeba* spp

1.2.2 Feeding systems

FLA, including *Ac*, is the predator that feeds on microorganisms such as bacteria, yeasts, archaea, and other protists in soil or freshwater (*71*, *78–80*). *Ac* trophozoites phagocytize them, similar to mammalian macrophages, by employing acanthopodia (**Fig. 1.3**). After internalized, these microorganisms are transported to the phagolysosome and killed by digestive enzymes (*81*). This activity reduces ~60% of the bacterial population in the natural environment and makes *Acanthamoeba* spp the primary bacterial predator in nature (*73*, *82*). Gram-negative bacteria, especially *Escherichia coli* or *Enterobacter aerogenes*, serve as their major grazing target, although *Ac* does not choose which bacteria to eat (*83*). The phagocytosis by *Ac* is mediated mainly by a receptor that recognizes mannose-rich elements on the surface of their prey. *Ac* also possesses chemosensory receptor(s) in its plasma membrane to detect chemo-attractants produced by bacteria, such as lipopolysaccharide (LPS), lipid A, cyclic AMP (cAMP), lipoteichoic acid, N-acetyl glucosamine, and chemotactic peptide formyl-methionyl-leucyl-phenylalanine (*83*, *84*). *Acanthamoeba* spp. also uptake large solute and food particles through the non-specific 'drinking' process called pinocytosis which involves invagination of the membrane (*85*).

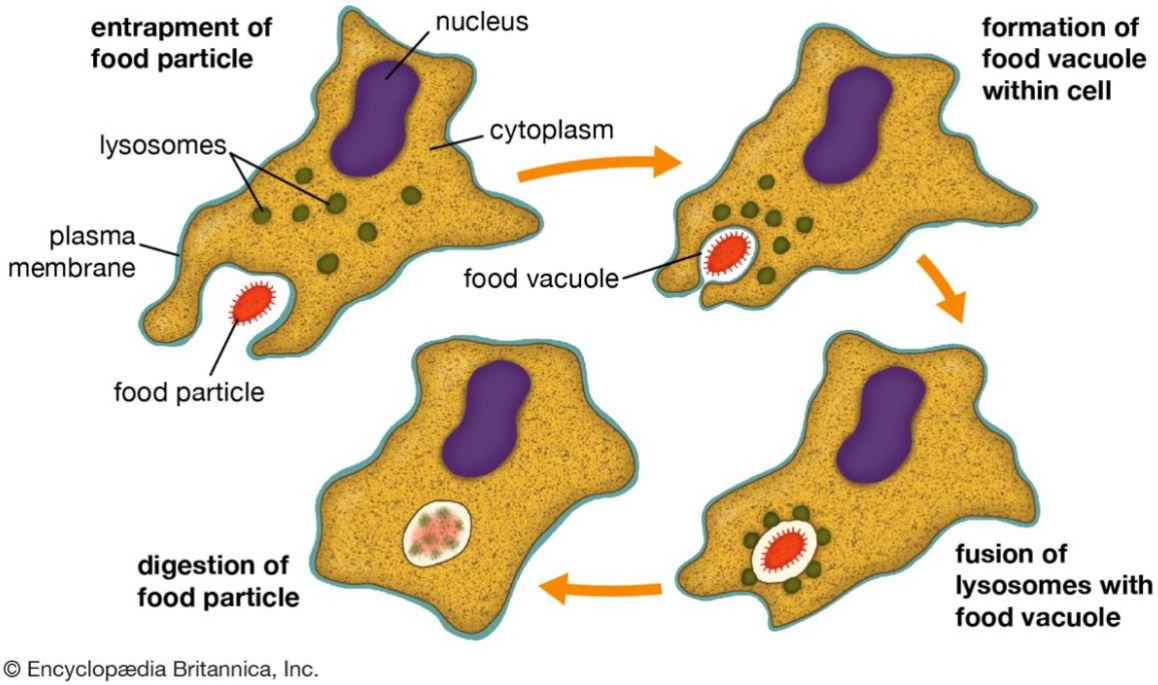

Figure 1.3 Phagocytosis and digestion of food particles in amoeba

1.2.3 Ecology

Although *Acanthamoeba* spp. are commonly found in various ecosystems such in soil or water bodies (*71*), it is also isolated from air conditioning systems and humidifiers (*86*, *87*), tap water (*88*), water bottles (*89*), sewages (*90*), animal feces (*91*), beaches (*92*), surgical tools (*91*), contact lenses, and human tissues (*93*). Besides being the primary bacterial population control, *Ac* also plays a vital role in nitrogen mineralization essential for soil fertility. Indeed, several key enzymes involved in the nitrogen metabolism were found in *Ac* (*94*).

1.3 Bacteria – Amoebae interaction

It is hypothesized that bacteria interacted with amoebae long before encountering animals and humans, and making the amoeba as a potentially important reservoir for the many mammalian and human pathogenic bacteria. Their long interactions result in a complex relationship, where the amoeba have evolved different mechanisms to digest bacteria, while bacteria also developed strategies to resist amoeba predation and sometimes to infect and kill the amoeba (*81*). There are three types of ecological interaction between amoebae and bacteria: predation, parasitism, and mutualism (**Fig. 1.4**).

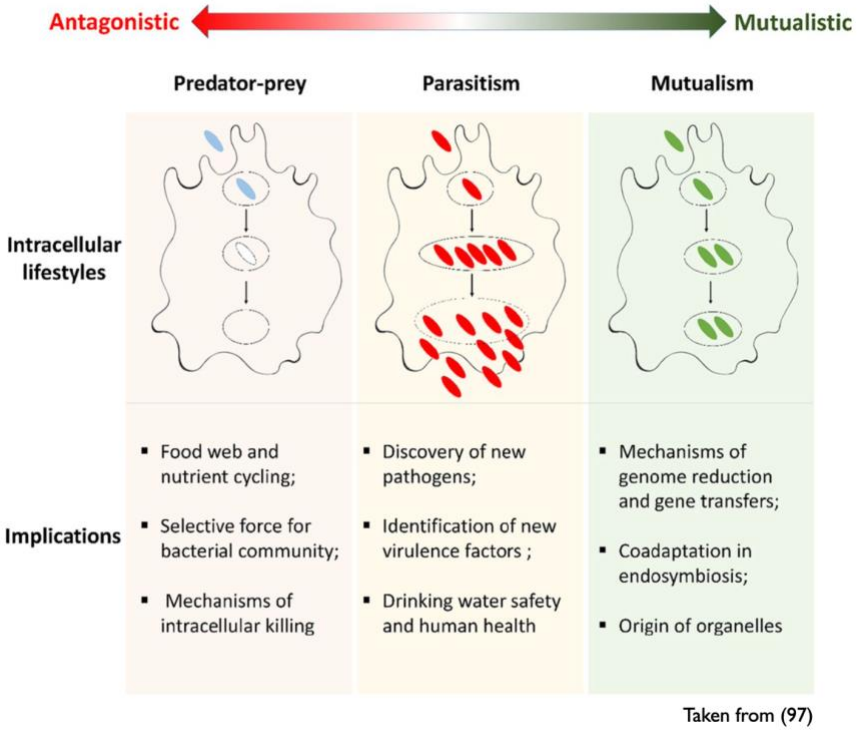

Figure 1.4 Three types of ecological interaction between amoebae and bacteria

In the predator-prey relationship, as its name implies, amoebae consume bacteria as their nutritional source. Bacteria evolved to avoid predation by amoebae, and some bacteria even gained the ability to re-invade amoebae. This type of bacteria is called amoebae-resisting bacteria (ARB), which utilize amoebae as their environmental host or vector (parasitic). In general, ARB that escape amoeba predation possess pathogenicity to mammalians or humans (*95*). Some ARBs that establish a stable long-term interaction with amoebae, both in the trophozoites and cysts forms, are called endosymbionts. It was reported that 25% of *Acanthamoeba* isolates harbor obligate endosymbionts (*96*). The emerge of different types of interactions between bacteria and amoebae under selective pressures indicates that their interactions are continuous rather than discontinuous (*97*).

1.3.1 Amoebae prey on bacteria

Among those three types of interactions between amoebae and bacteria, predation is dominant. Historically, it has been described that amoebae graze on bacteria as their nutritional resources and control the bacterial population in the environments (*98*, *99*). Therefore, bacteria constantly need to evade amoeba predation, leading to developing resistance to it. This process for adaptation might evolve pathogenicity toward other eukaryotes (*100*, *101*).

1.3.2 Bacteria invade amoebae

ARBs escape the phagocytosis, or survive, replicate, and escape from amoebae after internalization (**Fig. 1.5**). With these strategies, many ARBs that are pathogenic to mammalians or humans survive in the environments by invading and utilizing amoebae as their environmental reservoirs. There are two survival styles of ARBs in amoebae: survival with or without proliferation (*95*, *102*, *103*). In both cases, ARBs utilize the amoebae as reservoirs. In addition, the proliferating ARBs cause amoebae lysis (*104*). The bacteria occasionally exploit amoeba cysts to survive for a longer period under harsh environmental conditions (i.e., extreme temperatures, nutrient deprivation, etc.) (*105*, *106*).

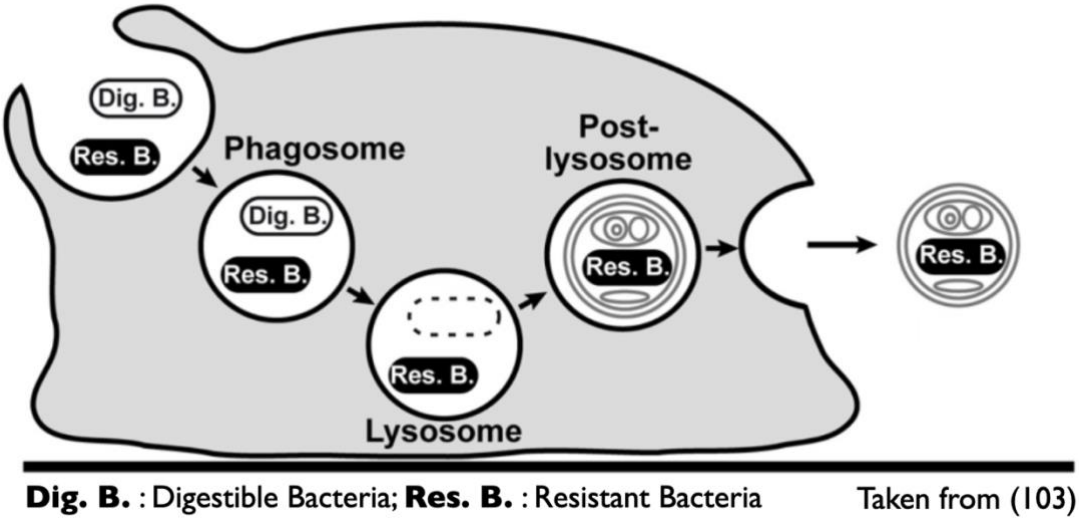

Figure 1.5 Fate of bacteria within amoeba

1.3.3 Bacterial infection facilitated by *Acanthamoeba*

As mentioned above, *Acanthamoeba* spp. serve as environmental shelters or niches for bacteria, and vectors of dissemination which facilitates transmission and infection to animals or humans (*98*). One of the most studied bacteria-amoebae interactions is *Legionella pneumophila* and *Acanthamoeba*. *L. pneumophila* is a Gram-negative, non-encapsulated, aerobic rod bacterium that resides in aquatic environments, where it interacts with amoebae and ciliated protozoa as the natural hosts. *L. pneumophila* is the causative agent of Legionnaires' disease (LD), characterized by fever, cough, pneumonia, or Pontiac fever, a milder illness without pneumonia (*107*). Since *L. pneumophilla* and amoebae share similar aquatic niches, it is hypothesized that the interaction with free-living amoebae facilitates *Legionella* growth and protects the bacteria from environmental stresses (chemical, physical, and microbial competition) (*108, 109*). Amoebae belonging to genera of *Acanthamoeba* and *Naegleria* often serve as hosts for *L. pneumophila* in the environments. It has been shown that *L. pneumophilla* interacts with *Acanthamoeba* in a similar manner to mammalian-phagocytic cells (*107*). Therefore, it is considered that common bacterial factors are involved in the interactions with amoebae and mammalian macrophages (*110*). Amoebae and their secreted vesicles containing bacteria could be the source of infection rather than free-living bacteria (*111*).

1.3.4 Interaction between *Bb* and amoebae

As mentioned in the previous section, *Bb* survives in natural freshwater samples or soil extract (*67–70*). Since amoebae and *Bb* share similar environmental niches, I considered that there should be mutual interactions between them; however, our understanding of these issues is poor. Only one study has shown that *Bb* survived in soil-amoeba *Dictyostelium discoideum* (*Dd*), as examined by gentamicin protection assay (GPA) (*112*). In contrast, *Klebsiella pneumoniae* (a common food bacterium given to *D. discoideum*) was eradicated by the amoeba in one hour GPA. *Bb* was also shown to survive and proliferate in the fruiting bodies, which appear during the amoeba social stage. They found that *Bb* in the Bvg^- phase was more advantageous for surviving and proliferating in the amoeba. *Bb* that survived through seven passages of the amoeba spores still retained the ability to infect mouse respiratory tracts (*112*).

1.4 The objectives of this study

Even though the biological interaction between *Bb* and *Dd* was reported (*112*), there is still a lack of detailed analyses if similar interactions were observed in other amoebae genera, i.e., *Acanthamoeba* spp., which is more ubiquitous in aquatic or terrestrial environments. Using more common FLA might increase the awareness of the pathogen risk, since the chance of finding similar occurrences between observed laboratory results and the actual natural phenomenon is high. *Acanthamoeba* may act as a reservoir, protective host, and virulence training ground for bacteria, there is a growing concern that they may play a role in the transmission and persistence of *Bb* in the farm-related environments. The objective of this doctoral research is to investigate the nature of interactions between *Bb* and a common representative of FLA, *Ac* that are co-cultured *in vitro*. In addition, the intracellular survival mechanisms by which *Bb* survived within *Dd* is still unknown. If the results obtained in this study show that *Bb* has similar ability to survive within *Ac*, further experiments could be directed to dissect these mechanisms.

CHAPTER 2 - MATERIALS AND METHODS

2.1 Bacterial cultures and plasmids

All bacterial strains and plasmids used in this study are listed in **Table 2.1**. *Bb* strain RB50 was provided by Peggy A. Cotter (University of North Carolina, USA), and *Bb* strain S798 was provided by N. Terakado (National Institute of Animal Health, Ibaraki, Japan). *Bb* was grown at 37℃ in Stainer-Scholte (SS) broth or BG agar plate (Becton Dickinson) containing 0.4% (w/v) hipolypeptone (Wako), 1% glycerol (v/v), 15% defibrinated horse blood (v/v), and ceftibuten at a final concentration of 10 μg/ml. *Escherichia coli* strains were grown at 37℃ on LB agar plate or LB broth. Growth media were supplemented with antibiotics at the following concentrations when necessary: gentamicin (Gm), 10 μg/ml; ceftibuten, 10 μg/ml; ampicillin, 50 μg/ml; kanamycin (Km), 30 and 50 μg/ml for *Bb* and *E. coli*, respectively. The bacterial numbers of *Bb* were estimated from optical density values at 650 nm (OD_{650}) in SS medium, according to the following equation: $OD_{650}\ 1.0 = 3.3 \times 10^9$ cells/ml. This equation was obtained from a calibration curve with known concentrations of the bacterial cells versus OD_{650} values.

2.2 Cultivation of *Ac*

Ac strain C3 (ATCC 50739) was maintained axenically in Peptone-Yeast-Glucose (PYG) broth as described previously at 20℃ in a T-25 culture flask (Cellstar) without shaking (*73*). After 4- to 6-day incubation, the grown amoebae were detached by vigorously shaking the flasks and centrifuged at 1,200 rpm for 3 min at room temperature (RT). After discarding the supernatant, amoebae pellets were suspended in a fresh PYG medium. The viability of *Ac* trophozoites was confirmed by staining with 0.2% trypan blue. The amoebae numbers were

enumerated using a Bürker-Türk type cell-counting chamber (Watson). The amoebae at the indicated numbers were seeded into a well of a 24-well tissue culture plate (Iwaki).

2.3 Determination of a suitable infection medium

Ac suspension in 50 mM HEPES buffer, pH 7.4 which is supplemented with different concentrations of glucose (0, 5, 20, and 80 mM) and NaCl (0, 80, 135 mM) was seeded into each well of a 24-well plate at a density of 1×10^5 cells. The culture plates were then incubated at 20℃ for 7 days. *Ac* morphology was observed using an inverted microscope (CKX53, Olympus) at day 7 of incubation.

2.4 Generation of mutant strains through homologous recombination

All the mutant strains of *Bb* RB50 and S798 listed in **Table 2.1** were constructed as described previously (*113*). The primers used in this study are listed in Table **2.2**. PCR was performed using with KOD Fx Neo (Toyobo). For example, a BB1281-deficient mutant (RB50 Δ*A*) was generated as follows. Approximately 1,000 bp of 5'- and 3'- flanking regions of the target *BB1281* gene (named BB1281-upstream and BB1281-downstream fragment) were amplified by PCR with *Bb* genomic DNA (gDNA) as a template and a combination of the primers BD192-F and BD193-R, and another combination of the primers BD194-F and BD195-R. Primers BD193-R and BD194-F include ~15-40 overlapped regions (bold) to allow a combination of two fragments through overlap PCR. Furthermore, BB1281-upstream and BB1281-downstream fragments contain ~20-25 bp of homologous sequences to the 5' or 3'-terminal of linearized pABB-CRS2-Gm (primer set of BD85-R and BD86-F). The connected BB1281-upstream and -downstream fragment (~2 kbp) was then ligated into pABB-CRS2-

Gm via the homology sequences (underlined) using an In-Fusion HD cloning kit (Clontech) according to the manufacturer's instructions. The resultant plasmid (pABB-CRS2-Gm-Δ*BB1281* (Δ*A*)) was introduced into *E. coli* S17-1 λpir and then transferred to strain RB50 by biparental conjugation. The *BB1281* gene was deleted in strain RB50 by a two-step homologous recombination with 10% sucrose for the counter-selection. Other mutants were also generated from RB50 by the same method using the suicide vectors listed in **Table 2.1** and primers listed in **Table 2.2**.

A Bvg$^-$ phase-locked strain in RB50 was constructed as previously described (*114*). The *bvgS* region was amplified by PCR with *Bb* RB50 WT gDNA as a template and a combination of primers BD117-F and BD120-R. The resultant fragment was inserted into the linearized pABB-CRS2-Gm using an In-Fusion HD cloning kit, and the plasmid was designated as pABB-CRS2-Gm-$bvgS_{full}$. Then, inverse PCR was carried out with the primers BD118-R and BD119-F and pABB-CRS2-Gm-$bvgS_{full}$, which resulted in deletion of the gene corresponding to region from 541 to 1020 amino acid positions (aa) of BvgS. The resultant PCR products were self-ligated by T4 Polynucleotide Kinase (Takara), designated as pABB-CRS2-Gm-Δ*bvgS*.

Bvg$^+$ phase-locked mutants in RB50 or S798 strain were constructed as previously described with slight modifications (*114*, *115*). The *bvgS* gene was amplified by PCR with *Bb* gDNA WT as a template and a combination of the primers BD117-F and BD120-R or primers BD218-F and BD219-R for RB50 or S798 strain, respectively. The DNA fragment was inserted into the linearized pABB-CRS2-Gm using an In-Fusion HD cloning kit. The *bvgS*-

C3 mutation (R570H) was introduced into the resultant plasmid using primers BD121-F and BD122-R, and the plasmid was designated as pABB-CRS2-Gm-*bvgS*-C3. The Bvg^+ phase-locked strain was generated by two-step homologous recombination using pABB-CRS2-Gm-*bvgS*-C3. The *bvgS*-C3 mutation was confirmed by sequencing.

2.5 Generation of reporter-expressing *Bb* using transposon mutagenesis

Stable GFP expression was achieved by integrating P*tac*-GFP fragment into a random region of the *Bb* genome. The plasmid pMariK-GFP used for this purpose was constructed as follows. Linearized pMariK plasmid (*116*) was obtained by performing inverse PCR using a combination of primer BD41-F and BS179-R. P*tac*-GFP fragment from pBBR1MCS-5-P*tac*-GFP (*114*) was amplified using a combination of primer BD42-F and BD43-R. P*tac*-GFP fragment was ligated to the linearized pMariK plasmid and the resulted plasmid was designated as pMariK-GFP. This plasmid was introduced into donor strain *Escherichia coli* S17-1 λpir and transferred to *Bb* by biparental conjugation. Integration of KmR-P*tac*-GFP fragment into the *Bb* genome was confirmed by colony PCR using a combination of primer BS333-F and BS334-R. The site of KmR-P*tac*-GFP integration was determined as previously described (*116*). Briefly, a single mutant grew on the plate after conjugation was cultured overnight. The genomic DNA was isolated using the DNeasy Blood & Tissue Kit (Qiagen) according to the manufacturer's protocol. Bacterial genomic DNA was digested with *Sau3AI* (TaKaRa), self-ligated with T4 DNA ligase (Promega), and used as templates for PCR. Inverse PCR was carried out using a combination of primer Mari5 and Mari7. The PCR products were purified using MinElute PCR Purification Kit (Qiagen) and subjected for sequencing analyses. DNA sequences were analyzed using SnapGene (GSL Biotech) to determine the location of

transposon insertion sites through mapping to the *Bb* RB50 genome (NCBI accession no. NC_002927.3) as a reference.

Bb stably expressing mCherry was constructed through integration of P*tac*-mCherry-KmR fragment into the identical site where the transposon carrying GFP-KmR fragment was integrated (at 763rd nucleotide position of BB4978). Briefly, P*tac*-mCherry from pBBR1MCS-5-P*tac*-mCherry was amplified using a combination of primers BD216-F and BD217-R and ligated to the linearized pMariK plasmid (BD41-F and BS179-R). The resulted plasmid was designated as pMariK-mCherry. A suicide plasmid for knock-in was constructed as mentioned above using a pABB-CRS2-Gm plasmid. Approximately 2.2 kbp of BB4977-4979 fragment was amplified by PCR with *Bb* RB50 gDNA as a template and a combination of primers BD168-F and BD169-R. The fragment was ligated into linearized pABB-CRS2-Gm, resulting in pABB-CRS2-Gm-RB50-BB4978. Then, inverse PCR was performed using pABB-CRS2-Gm-RB50-BB4978 as a template to obtain linearized pABB-CRS2-Gm-RB50-BB4978 using a combination of primers BD222-F and BD223-R. KmR-P*tac*-mCherry without mariner repeat (MR) from pMariK-mCherry plasmid was amplified using a combination of primers BD224-F and BD225-R and ligated to the linearized pABB-CRS2-Gm-RB50-BB4978 plasmid. The resulted plasmid was designated as pABB-CRS2-Gm-RB50-BB4978-mCherry. This plasmid was introduced into *E. coli* S17-1 λpir and then transferred to strain RB50 by biparental conjugation. The KmR-P*tac*-mCherry gene was inserted in the genome of strain RB50 by a two-step homologous recombination through the counter-selection with 10% sucrose. The GFP and mCherry expression was observed and analyzed using a confocal laser scanning

microscope (LSM880 Zeiss) and image processing software, ImageJ (NIH; https://imagej.nih.gov/ij/docs/intro.html).

2.6 Effect of *Bb* on *Ac* viability

Amoebae (1×10^5 cells) were co-cultured with *Bb* (1×10^7 CFU) for 1 h at 20℃ in 500 µl of PYG medium. After the extracellular bacteria were killed by treatment with a fresh PYG medium containing 300 µg/ml of Gm for 3 h at 20℃, the amoebae were washed to remove antibiotic traces. After final washing, 500 µl of fresh PYG medium were added, and the amoebae were detached by vigorous pipetting. Ten microliters of the amoeba suspension were aliquoted for counting the cell numbers. The remaining solution was transferred to a T-25 culture flask and incubated for the indicated periods. At each point of incubation, 200 µl bacteria-amoeba solution was taken out and centrifuged at 8,000 rpm for 5 min. The pellets were resuspended in 0.2% trypan blue, and the trophozoite cells were counted using an inverted microscope (CKX53, Olympus).

2.7 Intracellular survival of *Bb* in *Ac*

The ability of bacteria to survive in *Ac* trophozoites was evaluated by the method described previously (*112*). Briefly, the amoebae (2×10^5 cells) were infected with *Bb* (2×10^7 CFU) in a well of 24-well plates. The plates were centrifuged (200×*g*, 10 min, RT) and incubated for 1 h at 20℃ to allow the amoebae-bacterial interaction. After 1 h, the medium was replaced with PYG containing 300 µg/ml of Gm and incubated for 3 h at 20℃. Antibiotic traces were eliminated by washing with phosphate-buffered-saline (PBS; 137 mM NaCl, 2.7 mM KCl, 8 mM $Na_2HPO_4 \cdot 12H_2O$, 1.47 mM KH_2PO_4) at least twice. The amoebae cells in each well

were allowed to be lysed by incubation in 200 µl of 0.1% Triton X-100 at 20℃ for 10 min. Three hundred microliters of PBS were added to each well to make the final volume of 500 µl. The lysed-amoebae suspension was collected and serially diluted, and 50 µl of the dilution was plated on a BG plate. After incubation at 37℃ for 48 h, the numbers of grown colonies were counted.

2.8 Co-culture assay

Co-culture assay was performed in a 24-well plate using 50 mM HEPES, pH 7.4, supplemented with 5 mM glucose, which was used as the infection medium. The amoeba (1×10^5 cells) was infected with *Bb* (1×10^5 CFU) for 7 days at 20℃. The number of *Bb* was estimated based on OD_{650} values as mentioned above. For total bacteria enumeration, the bacteria and amoebae suspension were collected at indicated periods of incubation, and the amoebae were lysed with a 27-gauge syringe (Terumo). The intracellular bacteria were recovered after treating the bacteria and amoebae suspension according to the protocol described in section **2.7** above.

2.9 Fluorescence microscopy for the localization of *Bb* in *Ac*

The intracellular localization of GFP-expressing *Bb* in *Ac* trophozoites was analyzed by a confocal microscope (LSM880 Zeiss). The amoebae cultivated in a 35-mm glass base dish (Eppendorf) were inoculated with bacteria at an indicated multiplicity of infection (MOI) (1,000 or 3,000) in 2 ml of PYG or the infection medium containing 40 µg/ml of Alexa Fluor 647-labeled dextran (size: 10,000 molecular weights, Life Technologies) and incubated at 20℃ for 3-6 h.

For the intracellular localization of GFP-expressing *Bb* in *Ac* cysts, the amoebae (1×10^5 cells) were infected with bacteria (1×10^7 CFU) in a well of 24-well plates. The plates were centrifuged (200×*g*, 10 min, RT) and incubated for 1 h at 20℃. After 1 h, the medium was replaced with PYG containing 300 μg/ml of Gm and incubated at 20℃ for 3 h. After washing with PBS, the amoebae were incubated in 500 μl of PBS containing 50 mM $MgCl_2$ and 10% glucose (high osmolarity solution, HOS (*117*)) for 3 days at 20℃ to allow the encystation of amoebae. After the incubation, all cyst suspensions were transferred to a 35-mm glass base dish (Eppendorf) for microscopy.

For microscopy of the bacteria localized in the contractile vacuole (CV), the amoebae were infected with the bacteria in a 35-mm glass base dish (Eppendorf) at an MOI of 1 in the infection medium for 7 days at 20℃. For time-lapse imaging, pictures were taken every 10 s at selected time points using a confocal microscope (LSM880 Zeiss). All taken images were processed using ImageJ.

2.10 Negative screening: Preparation of transposon-sequencing (Tn-seq) mutant library

For the construction of pMariG plasmid to deliver mariner transposon containing the gentamicin resistance gene (Gmr), a ~0.6 kbp of DNA fragment encoding Gmr was amplified from pABB-CRS2-Gm by PCR using a combination of primers pABB-Gm-S and pABB-Gm-AS. Inverse PCR was also performed using pMariK (*116*) as the template with primers pMariK-S and pMariK-AS to obtain linearized pMariK. These PCR products were then ligated using an In-Fusion HD Cloning Kit. The resultant plasmid was designated as pMariG, carrying Gmr in place of the kanamycin resistance gene (Kmr) in the pMariK backbone (*118*).

The transposon mutant library was generated as follows: *E. coli* S17-1 λpir transformed with pMariG as a donor strain was mixed with a recipient strain *Bb* RB50 at a ratio of 3:1 and incubated for 6 h at 37℃ to allow conjugation. After the incubation, the bacterial suspension was collected, resuspended in 1 ml of SS medium, spread onto BG agar plate containing ceftibuten and Gm to select transconjugants. After 2-3 days of incubation at 37℃, the transconjugants were scraped off the plates using a sterile spatula and suspended in 10 ml of SS medium. After 4 h of incubation at 37℃ for the enrichment step, the bacterial suspensions were aliquoted and stored in 40% glycerol at -80℃. gDNA of the aliquoted bacteria was extracted using DNeasy Blood & Tissue Kit (Qiagen), according to the manufacturer's protocol. These extracted gDNA samples were designated as input gDNA libraries.

2.11 Negative screening: Tn-seq screening and data analyses

Aliquots of the input library were thawed and resuspended to a concentration of ~10^9 CFU/ml in SS medium and incubated with shaking at 37 ℃ for 3 h. The bacteria were diluted to give a concentration of 2.0×10^8 cells/ml and co-cultured with the amoebae as described above. After 5 days of incubation at 20℃, bacteria and amoeba suspensions were collected in a 50-ml tube. The amoebae and bacteria suspension was roughly separated by centrifugation at 150 × *g* for 2 min RT. The supernatants were subsequently filtered through 5 μm- and 1.2 μm-pore syringe filters (Whatman) to remove residual amoeba cells. The flowthrough fractions were centrifuged at 12,850 × *g* for 2 min RT to collect extracellular bacteria. The amoebae in the pellets after the first centrifugation were suspended in 2 ml of the infection medium, and disrupted by passing through a 27-gauge syringe (Terumo) for ~15 times. The amoeba cell debris was removed by centrifugation at 150 × *g* for 2 min RT, and the collected supernatant

was filtered through 5 μm- and 1.2 μm-pore syringe filters and centrifuged at 12,850 × *g* for 2 min RT to collect the intracellular bacteria. The collected extracellular and intracellular bacteria were mixed and subjected to the second round of screening. After the secondary screening, extracellular and intracellular bacteria were separated again by the same method. The collected bacteria were enriched by incubation at 37℃ for 3 h in SS medium. gDNA of extracellular and intracellular bacteria was extracted using DNeasy Blood & Tissue Kit (Qiagen) according to the manufacturer's protocol. These extracted gDNA were designated as output gDNA libraries. Purified input and output gDNAs were subjected to next generation sequencing (NGS) as described previously (*119*). Briefly, 3 μg of gDNA was digested with *MmeI* (New England Biolabs) for 2.5 h, treated with rAPID alkaline phosphatase (Roche), and the digested short fragments were purified with a phenol-chloroform extraction reagent (Nacalai Tesque). Adapter oligonucleotides (BD182-F and BD183-R) were ligated to the short fragments with T4 DNA ligase (New England Biolabs) at 16℃ overnight. The resultant fragments were amplified by PCR using a combination of primers, one of which contains a specific index sequence (6 nucleotides): i.e., a combination of primers BD184 and BD187 produce a PCR product that contains ATCACG (greyed) as a specific index derived from BD184. Approximately 120 bp-long fragments of PCR products were gel-extracted using QIAquick Gel Extraction Kit (Qiagen) and submitted to the NGS Core Facility, Research Institute for Microbial Diseases, Osaka University for sequencing and quality control analyses. Reads were separated into three groups based on the specific index sequences, and adapter sequences were trimmed to obtain 16-17 bp fragments of *Bb* genomic DNA. The obtained short reads were mapped to the *Bb* RB50 reference genome (NCBI accession no. NC_002927.3). EdgeR (*120*) was used to determine genes required for *Bb* survival after co-

culture assay by examining differences in the numbers of each read between input and output gDNA library. When the read numbers were changed three or more log-fold (Log2FC), the corresponding genes were picked up as candidate genes. The picked up genes were grouped into Bvg^+- or Bvg^--phase specific genes based on the previous microarray data (*121*).

2.12 Positive screening: co-culture assay

Positive screening was performed using variant of mutants of the *Bb* S798 strain listed in **Table 2.1**. The Bvg^+ phase-locked strain was generated by two-step homologous recombination with pABB-CRS2-Gm-*bvgS*-C3. Co-culture assay was performed to screen candidate genes as described above. Briefly, *Bb* (1×10^5 CFU) was incubated with the amoeba (1×10^5 cells) in the infection medium in a well of 24-well plates for 7 days at 20°C. On day 7, the bacteria and amoebae suspension were collected and the total bacteria were enumerated after the amoeba cells were disrupted with a 27-gauge syringe. Variant of *Bb* mutants with recovered viability similar to WT was designated as a candidate.

2.13 Statistical analyses

Statistical analyses were performed using Prism 8 (GraphPad Software). The data are from three independent experiments and expressed as mean ± SD of experimental triplicates. $p < 0.05$ was taken to indicate statistical significance.

Table 2.1 Strains and plasmids used in this study

Strain or plasmid	Description	Source or reference
B. bronchiseptica		
RB50	WT	P. A. Cotter
RB50 BB4978::KmR-GFP	RB50 derivative	This study
RB50 BB4978::KmR-GFP Bvg$^+$ phase-locked	RB50 derivative	This study
RB50 BB4978::KmR-GFP Bvg$^-$ phase-locked	RB50 derivative	This study
RB50 BB4978::KmR-mCherry	RB50 derivative	This study
RB50 Δ*BB1281* (Δ*A*)	RB50 derivative	This study
RB50 Δ*BB2796* (Δ*B*)	RB50 derivative	This study
RB50 Δ*BB4462* (Δ*C*)	RB50 derivative	This study
RB50 Δ*BB0019* (Δ*D*)	RB50 derivative	This study
RB50 Δ*BB3917* (Δ*E*)	RB50 derivative	This study
RB50 Δ*BB0824* (Δ*F*)	RB50 derivative	This study
RB50 Bvg$^-$ phase-locked	RB50 derivative	This study
RB50 Bvg$^+$ phase-locked	RB50 derivative	This study
RB50 Δ*fhaB* Bvg$^+$ phase-locked	RB50 derivative	This study
RB50 Δ*fimBCD* Bvg$^+$ phase-locked	RB50 derivative	This study
RB50 Δ*fhaB*Δ*fimBCD* Bvg$^+$ phase-locked	RB50 derivative	This study
S798	WT, Clinical isolate	(*122*)
S798 Δ*bscN*Δ*dnt*Δ*prn*Δ*cyaA* (Δ4) Bvg$^+$ phase-locked	S798 derivative	This study
S798 Δ4Δ*fhaB* (Δ5) Bvg$^+$ phase-locked	S798 derivative	This study
S798 Δ5Δ*fimBCD* (Δ6) Bvg$^+$ phase-locked	S798 derivative	This study
S798 Δ6Δ*vag8* (Δ7) Bvg$^+$ phase-locked	S798 derivative	This study
S798 Δ7Δ*fhaS* (Δ8) Bvg$^+$ phase-locked	S798 derivative	This study
S798 Δ8Δ*fhaL* (Δ9) Bvg$^+$ phase-locked	S798 derivative	This study
S798 Δ9Δ*brtA* (Δ10) Bvg$^+$ phase-locked	S798 derivative	This study
E. coli		
S17-1 λpir	K-12 cloning strain for plasmid with R6K origin with genome-integrated conjugation apparatus	Lab collection
Plasmids		
pBBR1MCS-5-P*tac*-GFP	pBBR1MCS-5 carrying *tac* promoter, *gfp* and *trpA* terminator	(*114*, *123*)
pBBR1MCS-5-P*tac*-mCherry	pBBR1MCS-5 carrying *tac* promoter, *mCherry* and *trpA* terminator	Lab collection
pBBR1MCS-5-KmR-P*tac*-GFP	pBBR1MCS-5 carrying *tac* promoter, KmR, *mCherry* and *trpA* terminator	This study
pMariK	Mariner transposon vector carrying KmR	(*116*)
pMariK-GFP	pMariK carrying *tac* promoter, *gfp* and *trpA* terminator	This study
pMariK-mCherry	pMariK carrying *tac* promoter, *gfp* and *trpA* terminator	This study
pMariG	Mariner transposon vector carrying KmR	(*118*)
pABB-CRS2-Gm	Gm^r, R6K-derived suicide vector	Laboratory collection
pABB-CRS2-Gm-RB50-BB4978	*BB4978* fragment cloned into pABB-CRS2-Gm	This study
pABB-CRS2-Gm-RB50-BB4978-mCherry	P*tac*-mCherry fragment at *BB4978* site cloned into pABB-CRS2-Gm	This study
pABB-CRS2-Gm-Δ*BB1281* (Δ*A*)	*BB1281* deletion cloned into pABB-CRS2-Gm	This study
pABB-CRS2-Gm-Δ*BB2796* (Δ*B*)	*BB2796* deletion cloned into pABB-CRS2-Gm	This study

pABB-CRS2-Gm-Δ*BB4462* (Δ*C*)	*BB4462* deletion cloned into pABB-CRS2-Gm	This study
pABB-CRS2-Gm-Δ*BB0019* (Δ*D*)	*BB0019* deletion cloned into pABB-CRS2-Gm	This study
pABB-CRS2-Gm-Δ*BB3917* (Δ*E*)	*BB3917* deletion cloned into pABB-CRS2-Gm	This study
pABB-CRS2-Gm-Δ*BB0824* (Δ*F*)	*BB0824* deletion cloned into pABB-CRS2-Gm	This study
pABB-CRS2-Gm-Δ*fhaB*	*FhaB* deletion cloned into pABB-CRS2-Gm	This study
pABB-CRS2-Gm-Δ*fimBCD*	*FimBCD* deletion cloned into pABB-CRS2-Gm	This study
pABB-CRS2-Gm-$bvgS_{full}$	*BvgS* fragment cloned into pABB-CRS2-Gm	This study
pABB-CRS2-Gm-Δ*bvgS*	*bvgS* deletion cloned into pABB-CRS2-Gm ($\Delta_{541-1020}$)	This study
pABB-CRS2-Gm-*bvgS*-C3	*bvgS*-C3 mutation cloned into pABB-CRS2-Gm (R570H)	This study
pABB-CRS2-Gm-Δ4 (S798)	Δ*bscN*Δ*dnt*Δ*prn*Δ*cyaA* deletion cloned into pABB-CRS2-Gm	Lab collection
pABB-CRS2-Gm-Δ5 (S798)	Δ4 and *FhaB* deletion cloned into pABB-CRS2-Gm	Lab collection
pABB-CRS2-Gm-Δ6 (S798)	Δ5 and *FimBCD* deletion cloned into pABB-CRS2-Gm	Lab collection
pABB-CRS2-Gm-Δ7 (S798)	Δ6 and *Vag8* deletion cloned into pABB-CRS2-Gm	Lab collection
pABB-CRS2-Gm-Δ8 (S798)	Δ7 and *FhaS* deletion cloned into pABB-CRS2-Gm	Lab collection
pABB-CRS2-Gm-Δ9 (S798)	Δ8 and *FhaL* deletion cloned into pABB-CRS2-Gm	Lab collection
pABB-CRS2-Gm-Δ10 (S798)	Δ9 and *BrtA* deletion cloned into pABB-CRS2-Gm	Lab collection

Table 2.2 Primers and oligonucleotides used in this study

Name	Sequence (5' to 3')	Application
BD28-F	CGTTGCTGCTCCATAACATC	Construction of pBBR1MCS-5-KmR-P*tac*-GFP
BD29-R	CAATTCGTTCAAGCCGAGAT	
BD26-F	TGTTATGGAGCAGCAACGATGAGCCATATTCAACGGG	
BD27-R	CTCGGCTTGAACGAATTGTTAGAAAAACTCATCGAGCATC	
BD41-F	CCAATTCTGATTAGAAAAACTCATCGA	Construction of pMariK-GFP
BS179-R	TTAATTGGTTGTAACACTGGCAGAG	
BD42-F	TTTCTAATCAGAATTGGGGCAAATATTCTGAAATGAGC	
BD43-R	TGTTACAACCAATTAATTCTCCTACATGTTCGCC	
BD216-F	CGATGAGTTTTTCTAATCAGAATTGGTGCGCCGACATCATAACGG	Construction of pMariK-mCherry
BD217-R	CTGCCAGTGTTACAACCAATTAACGGTTCTCCTACATGTTCGCCT	
BD85-R	GGGAGAGCTCGGATCCACTAGT	Construction of pABB-CRS2-Gm-RB50-BB4978
BD86-F	GGGAATTCCACAAATTGTTATCCGCT	
BD168-F	AGGCCATGCACGAGGATATCATGGTCTAGAGTCGACCTCGAGG	
BD169-R	CGGTTGGCGTAACCCTGGAACGGTTCTCCTACATGTTCGCCT	
BD222-F	TTCCAGGGTTACGCCAACCG	Construction of pABB-CRS2-Gm-RB50-BB4978-mCherry
BD223-R	GATATCCTCGTGCATGGCCTCG	
BD224-F	AGGCCATGCACGAGGATATCATGGTCTAGAGTCGACCTCGAGG	
BD225-R	CGGTTGGCGTAACCCTGGAACGGTTCTCCTACATGTTCGCCT	
Mari5	GACTCTAGACCATGGTTGTGTC	Determination of transposon insertion site
Mari7	ATGCCTCTTCCGACCATCAAGC	
BS333-F	GACACAACCATGGTCTAGAGTCGACCTC	Colony PCR to check P*tac*-GFP integration
BS334-R	CCCTTCAAGAGCGATACCCGAGC	
BD192-F	TAGTGGATCCGAGCTCTCCCATCCTCCTGCAAGGCAACGT	Construction of pABB-CRS2-Gm-Δ*BB1281* (Δ*A*)
BD193-R	**CCGGTTCGGATAGATTCACATATCAAGACAACGGAGGGAG**C	
BD194-F	**CTCCCTCCGTTGTCTTGATATGTGAATCTATCCGAACCGG**GACT	
BD195-R	TAACAATTTGTGGAATTCCCCGTTCGAGTGCGACCACTT	
BD196-F	TAGTGGATCCGAGCTCTCCCGGTATGGCTACAATTGCGG	Construction of pABB-CRS2-Gm-Δ*BB2796* (Δ*B*)
BD197-R	**GCCCCGGCTTACTGGTCGTCCATGCCAGGGGTT**CCC	
BD198-R	TAACAATTTGTGGAATTCCCCCCATGCCGGCGAAATGC	
BD199-F	**AACCCCTGGCATGGACGACCAGTAAGCCGGGGC**C	
BD200-F	TAGTGGATCCGAGCTCTCCCCGCTGGGTCATGGTCAAGG	Construction of pABB-CRS2-Gm-Δ*BB4462* (Δ*C*)
BD201-R	**CGCCGGTTCAGTTGCGCATGGTTCAGAATTTGAACT**GGGATACGG	
BD202-F	**AGTTCAAATTCTGAACCATGCGCAACTGAACCGGCG**C	
BD203-R	TAACAATTTGTGGAATTCCCGTCGTTCGCCAAGATCGGC	

BD204-F	TAGTGGATCCGAGCTCTCCCTTTGAGACAGTGTGGCGCG	
BD205-R	**CGGCGCACCTTAGAATTCCGGCCGAATCATGAACTTC**TCT	Construction of pABB-CRS2-Gm-Δ*BB0019* (Δ*D*)
BD206-F	**GAAGTTCATGATTCGGCCGGAATTCTAAGGTGCGCCGCC**	
BD207-R	TAACAATTTGTGGAATTCCCCACACCTGGCCAAAGCGCA	
BD208-F	TAGTGGATCCGAGCTCTCCCCGGGCATCGAACCGGTTC	
BD209-R	**TCGGTTCGGAAGCGTCAGGCGTTCATCAGAATTTCT**CCGG	Construction of pABB-CRS2-Gm-Δ*BB3917* (Δ*E*)
BD210-F	**AGAAATTCTGATGAACGCCTGACGCTTCCGAACCGA**GA	
BD211-R	TAACAATTTGTGGAATTCCCTCTTGTCCAGCAGCAGGACG	
BD212-F	TAGTGGATCCGAGCTCTCCCGGCCTGGAAACGCGACATC	
BD213-R	**CGGTATGCGCTCAGAGCAAGGGCGGGACTCCTG**CA	Construction of pABB-CRS2-Gm-Δ*BB0824* (Δ*F*)
BD214-F	**CAGGAGTCCCGCCCTTGCTCTGAGCGCATACCG**CATG	
BD215-R	TAACAATTTGTGGAATTCCCCCAGGCGCACCATGACATG	
fhaB-US	TAGTGGATCCGAGCTCTCCCGTGAAAAGAAAGAAATGGAAAACAA	
fhaB-UAS	**TATGAAACCAACAAA**TAGGTAGTCGCTGCC	Construction of pABB-CRS2-Gm-Δ*fhaB* (RB50)
fhaB-DS	**TTTGTTGGTTTCATA**GCCCGCACACGCCAA	
fhaB-DAS	TAACAATTTGTGGAATTCCCGCGTACTGTCGCTCTTGGCG	
fimBCD-US	TAGTGGATCCGAGCTCTCCCGAAACTGCGCGAA	
fimBCD-UAS	**GTCGACAGTACTCTCGA**GACCTTGAACTATGACTGACG	Construction of pABB-CRS2-Gm-Δ*fimBCD* (RB50)
fimBCD-DS	**TCGAGAGTACTGTCGAC**ACAAGCGTATGTATTCATG	
fimBCD-DAS	TAACAATTTGTGGAATTCCCATTGCAGCCCATCCTTT	
BD117-F	TAGTGGATCCGAGCTCTCCCACGCTGCATTACTTCCCATC	Construction of pABB-CRS2-Gm-*bvgS*$_{full}$ (RB50)
BD120-R	AACAATTTGTGGAATTCCCTTACCGTCAGTACGTTCGATG	
BD118-R	CTCGTTGCGGTAGGCGTA	Construction of pABB-CRS2-Gm-Δ*bvgS* (RB50)
BD119-F	ATCACCGATTGCAACATGCC	
BD121-F	GGCGCCAGATCCGCCAGCACAAGCGGGCCGAGCGGG	Construction of pABB-CRS2-Gm-*bvgS*-C3 (RB50 and S798)
BD122-R	CCGCTCGGCCCGCTTGTGCTGGCGGATCTGGCGCC	
BD218-F	TAGTGGATCCGAGCTCTCCCACGCTGCATTACTTCCCATCAT	Construction of pABB-CRS2-Gm-*bvgS*$_{full}$ (S798)
BD219-R	ATAACAATTTGTGGAATTCCCTCAGGTCCACCGAAACCGTT	
BD182-F	ACACGACGCTCTTCCGATCTGGAACTCCTACTGACNN	Adapter sequences for Tn-Seq
BD183-R	p-GTCAGTAGGAGTTCCAGATCGGAAGAGCGTCGTGTAGGGA-p	
BD184	CAAGCAGAAGACGGCATACGAGATATCACGAGACCGGGGACTTATCATCCAACCTGT	Index sequences for NGS sample multiplexing
BD185	CAAGCAGAAGACGGCATACGAGATCGATGTAGACCGGGGACTTATCATCCAACCTGT	
BD186	CAAGCAGAAGACGGCATACGAGATTTAGGCAGACCGGGGACTTATCATCCAACCTGT	
BD187	AATGATACGGCGACCACCGAGATCTACACTCTTTCCCTACACGACGCTCTTCCGATCT	

Underlined are sequences for In-Fusion; Bold are sequences for overlap-extension PCR; Greyed are index sequences

CHAPTER 3 - RESULTS

3.1 Preliminary experiments to optimize conditions for infection

3.1.1 Medium

Peptone Yeast Glucose (PYG) is a common medium used for culturing *Acanthamoeba* sp. Several pathogenic bacteria such as *Vibrio parahaemolyticus*, *Campylobacter jejuni*, *Helicobacter pylori,* and *Vibrio cholerae* did not grow when incubated in PYG alone. Therefore PYG is a suitable infection medium for co-culture study with *Acanthamoeba* sp. (*124–127*). It was reported that PYG medium was also used to study a short-term interaction (~4 h) between *Bordetella bronchiseptica* (*Bb*) and *Ac* (*112*); however, *Bb* was found to proliferate in PYG medium after four-day incubation at 20℃ (**Fig. 3.1A**), which may lead to biased interpretations as to whether the bacteria grow by the aid of amoebae. Therefore, I considered that PYG is unsuitable for studying long-term interaction between *Bb* and *Ac*, and started to search for a suitable infection medium, in which *Bb* cannot grow but remains viable upon prolonged incubation at 20℃. The medium also should support the viability of *Ac* in the metabolically active trophozoite form.

The new infection medium should be isotonic with viable cells and contain a carbon source. Glucose, which is a common carbon source for *Ac*, is included in the PYG medium (*128*). Therefore, I chose glucose as the main carbon source, and also used sodium chloride (NaCl) as the osmolyte and source for inorganic ions (*129*). Different concentrations of glucose (0, 5, 20, and 80 mM) and NaCl (0, 80, 135 mM) were mixed in 50 mM HEPES buffer pH 7.4 as a base solution. The combination of 50 mM HEPES buffer pH 7.4 with 5 mM of glucose maintained *Ac* trophozoite form after 7 days of incubation, indicating that this medium was

suitable for *Ac*. A higher concentration of glucose (80 mM) and NaCl (135 mM) caused *Ac* encystation after 7 days incubation at 20℃, as judged by the round morphology of cysts (**Fig. 3.1B**). From this result, I decided to use the combination of 50 mM HEPES buffer pH 7.4 with 5 mM of glucose as the new infection medium (named as 'HG medium'). It was also confirmed that *Bb* did not grow but remained viable after incubation for 7 days at 20℃ in HG medium (data not shown).

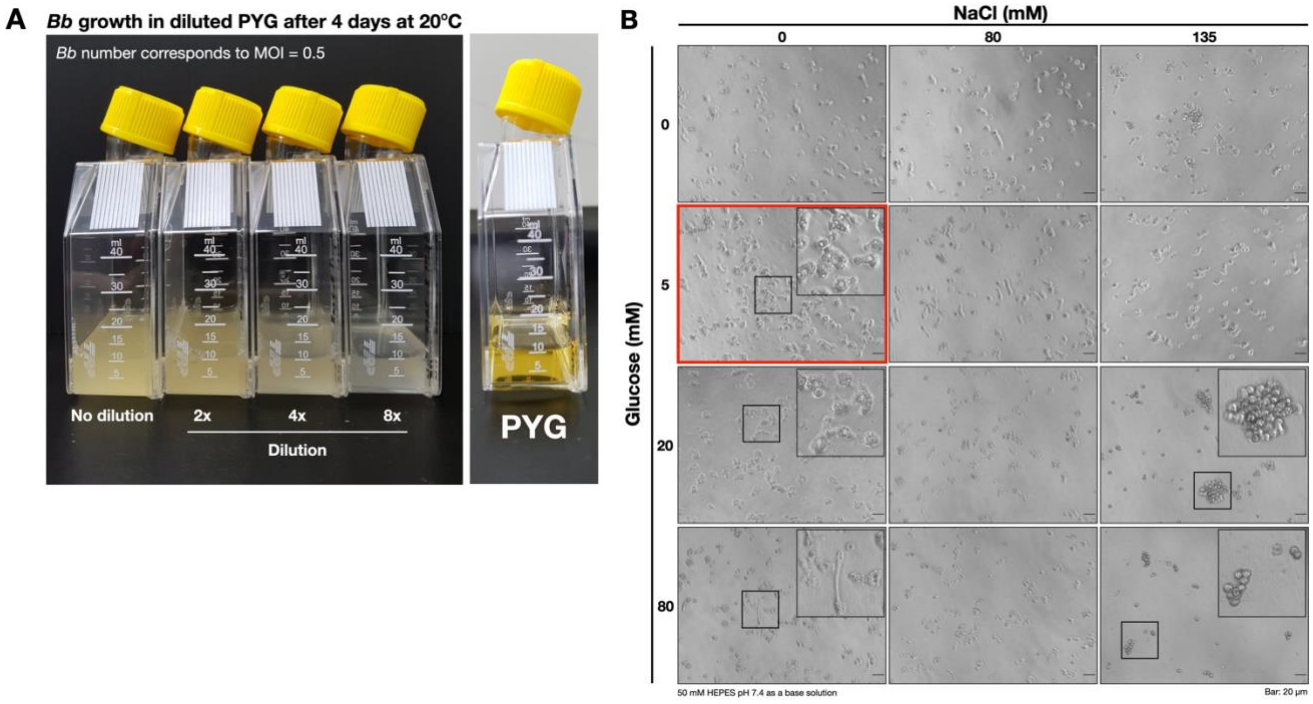

Figure 3.1 Searching for a suitable infection medium for co-culture assay

A. *Bb* growth in PYG medium (1, 2, 4, and 8x dilution) after four days of incubation at 20℃ indicated by the turbidity of the medium. PYG medium as a control remained clear.

B. Different concentrations of glucose and sodium chloride (NaCl) were used to search a new infection medium. *Ac* was seeded at a 1×10^5 cells/well density and the plates were incubated at 20℃. After 7 days of incubation, the images from each well were taken.

Representative images are shown for each treatment. A red box indicates the suitable combination for the new infection medium. Bar: 20 µm.

3.1.2 Generation of stable green fluorescent protein (GFP)-expressing *Bb*

Initially, I used a GFP-expressing *Bb* harboring the expression plasmid but obtained inconsistent results. The plasmid-containing *Bb* showed high GFP intensity at 37℃, but the fluorescence became undetectable in 7 days of incubation at 20℃ (data not shown). I suspected that incubation in the HG medium at low temperature did not allow *Bb* to maintain the plasmid probably because it metabolically burdens to the bacteria. The absence of antibiotics as selective pressure during incubation may cause plasmid loss (*130*). Therefore, I constructed a more stable GFP-expressing *Bb* strain by integrating a *gfp* gene into the *Bb* genome by using a transposon-based system. Even after 144 h of incubation in the HG medium at 20℃, GFP expression was strongly detectable compared to that of the plasmid-based *Bb*, indicating that genome integrated *gfp* is more suitable for this study (**Fig. 3.2A**). *Mariner* transposon used for developing a stable GFP-expressing *Bb* strain was incorporated in the region of *BB4978* gene corresponding to the 254th amino acid between isoleucine and tyrosine of BB4978 protein that is a hypothetical protein with unknown function. There was no growth difference between WT (WT) and the GFP-expressing strain at 37℃ and 20℃, as judged by similar optical density (OD_{650}) values at each time point (**Fig. 3.2B**).

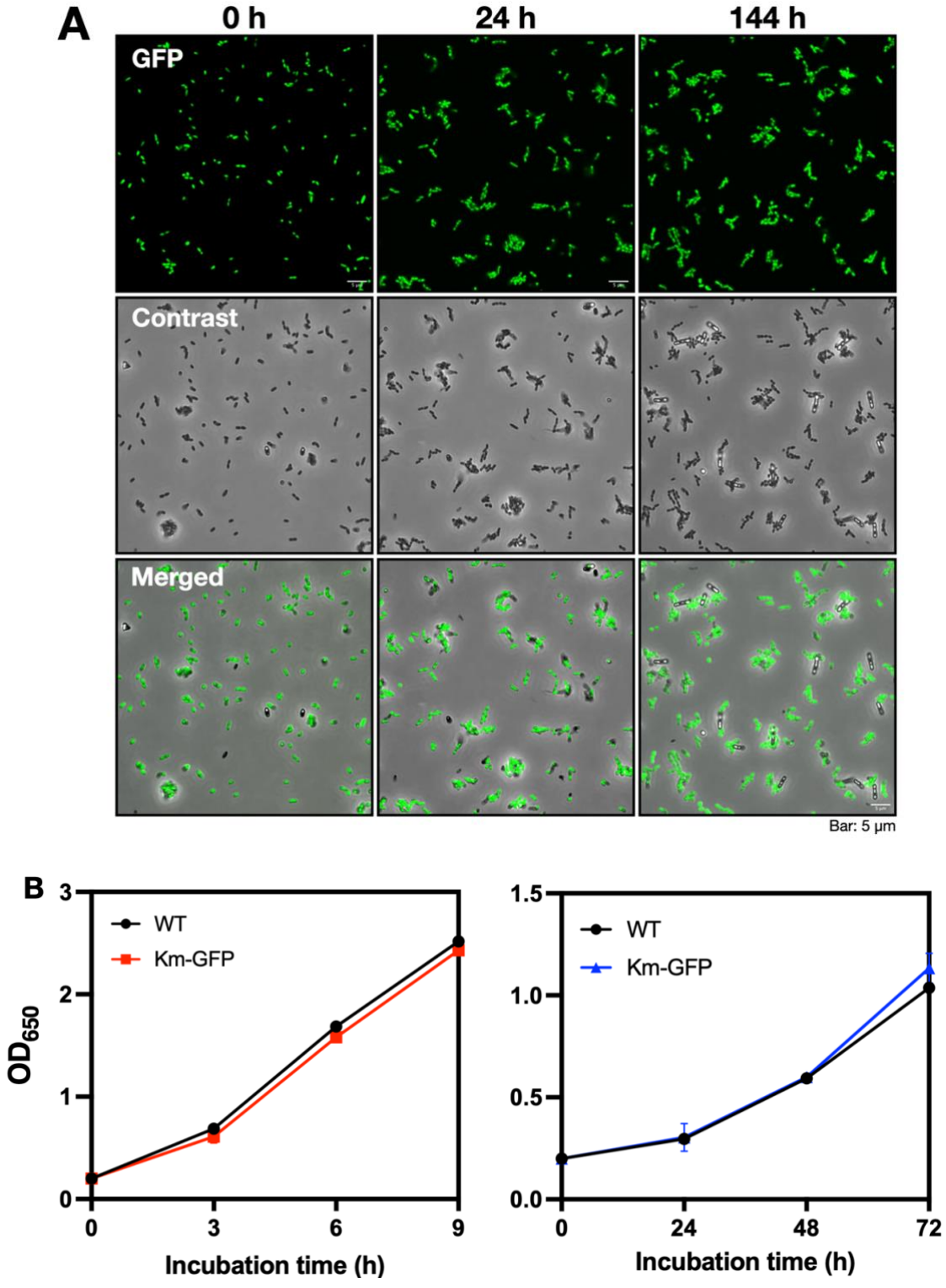

Figure 3.2 Development of more stable GFP-expressing *Bb*

A. GFP expression of at 0, 24, and 144 h post-incubation in HG medium at 20℃. Bar: 5 μm.

B. OD_{650} values of WT and GFP-expressing strain at 0, 3, 6, 9, and 24 h post-incubation at 37℃ (left) and 20℃ (right). Bacterial suspension was adjusted at OD650 = 0.01 and 0.15 for 37℃ and 20℃, respectively. Values of each time point are the mean ± standard deviation (SD) (*n*=3).

3.2 Uptake of *Bb* by *Ac* trophozoites and cysts

The internalization of the GFP-expressing *Bb* by *Ac* was monitored by time-lapse imaging. The GFP-expressing *Bb* was efficiently internalized by *Ac* via its pseudopods (spike-like structures) (**Fig. 3.3A**). Once internalized, the bacteria were localized within small, bacterium-filled vacuole-like compartments involved in the amoeba digestion pathway (**Fig. 3.3B**). It seemed that the small bacterium-filled vacuoles fused into larger vacuole-like compartments (**Fig. 3.3C**). The GFP-expressing *Bb* cells located in the *Ac* cytosol of the trophozoites was not found, indicating that internalized *Bb* essentially resides in intracellular vacuoles.

In high osmolarity solution (HOS), approximately 90% of the trophozoites encysted in 3 days, as judged by their morphology: cysts represent the dormant state of *Ac*, showing the spherical morphology with a double wall. The bacteria that were internalized by trophozoites still expressed GFP even after encystation (**Fig. 3.3C, Left**). It was likely that *Bb* intracellularly proliferated even in the cysts because the intensity of GFP was apparently higher at day 7 than that at day 3 (**Fig. 3.3D, Right**). These results suggest that *Bb* is internalized by *Ac*

trophozoites, evades intracellular digestion, and remains viable or proliferates in *Ac* both in the trophozoite and cyst stages.

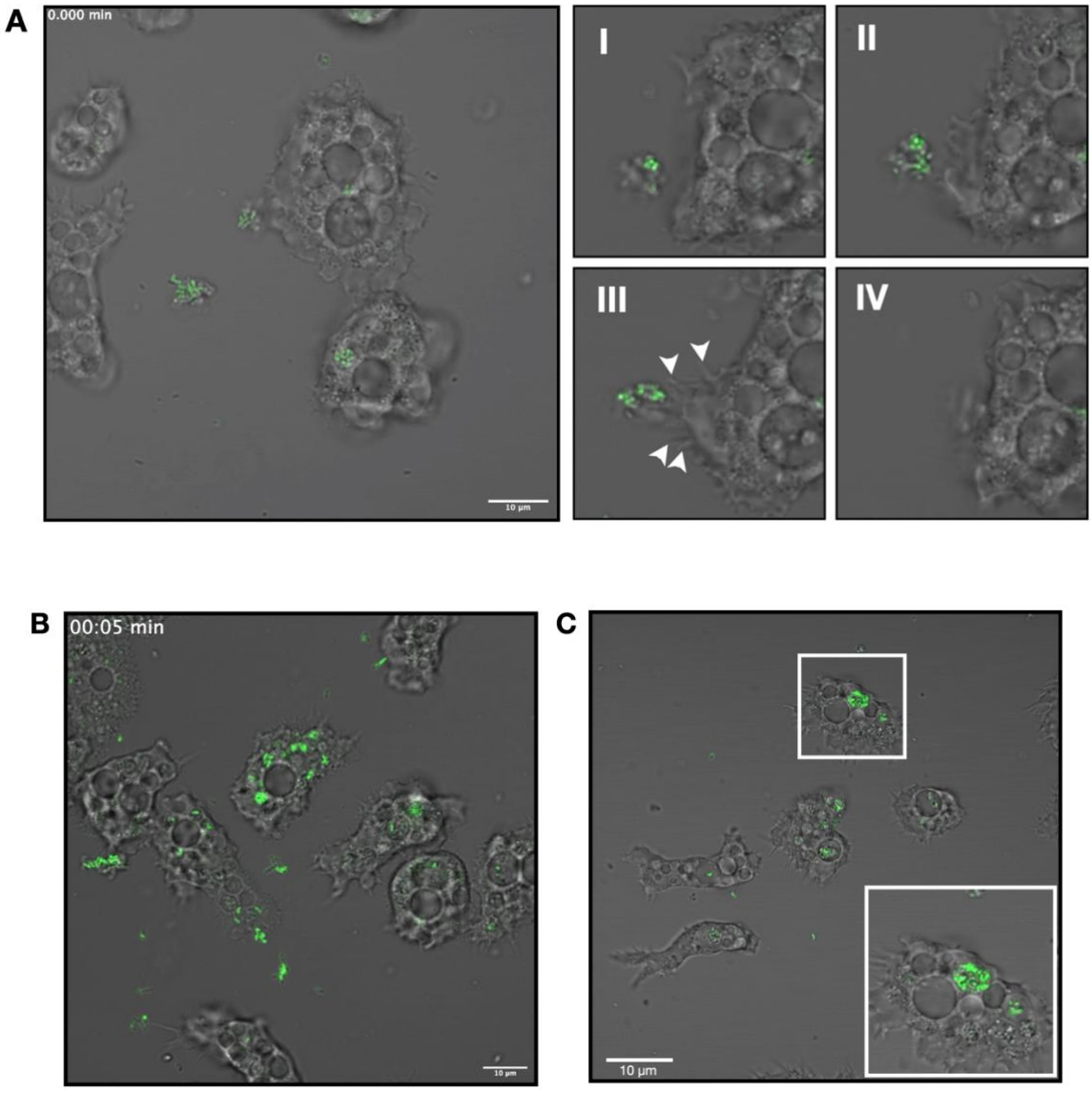

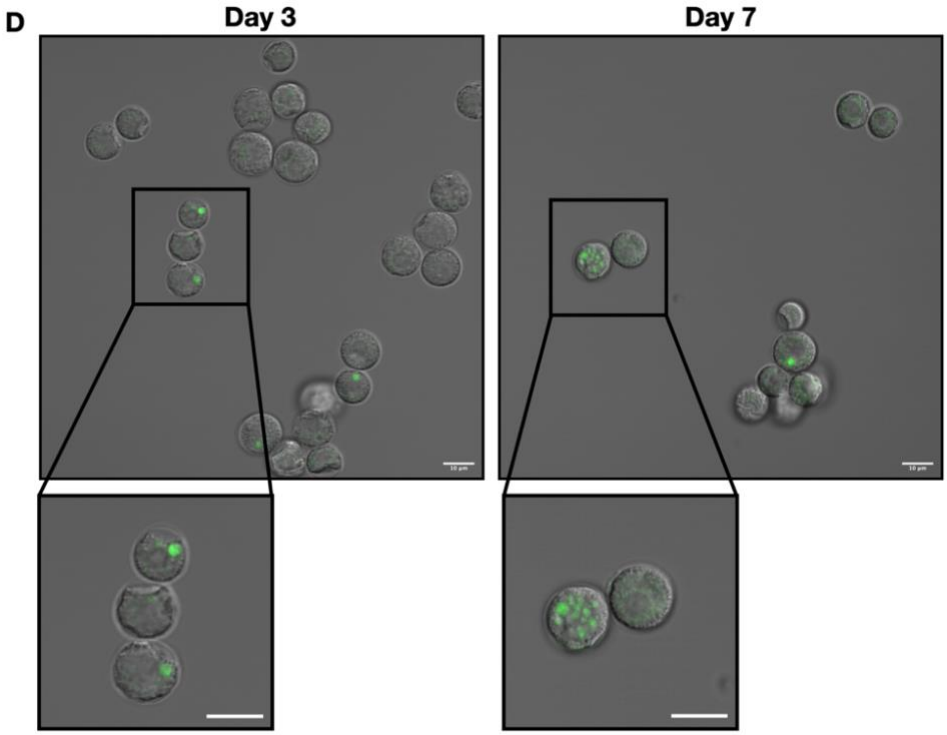

Figure 3.3 Visualization of GFP-expressing *Bb* within *Ac* trophozoites and cysts

A. Time-lapse microscopic imaging of *Ac* internalizing GFP-expressing *Bb* via active pseudopods (indicated by white arrowhead). The sequential uptake process is shown in images I-IV. Bar: 10 µm.

B. The accumulation of GFP-expressing *Bb* within small vacuoles of *Ac*, indicating active bacterial uptake by the amoebae. Bar: 10 µm.

C. GFP-expressing *Bb* was accumulated within a larger vacuole-like compartment. Squared are zoomed images. Bar: 10 µm.

D. *Ac* trophozoites containing internalized GFP-expressing *Bb* were treated with HOS (50 mM magnesium chloride and 10% glucose) for 3 days at 20℃ to induce encystation. Intracellular localization of *Bb* within *Ac* cysts was indicated by GFP expression. The increased of GFP intensity of intracellular *Bb* after 7 days suggests bacterial growth. Bar: 10 µm.

3.3 Survival of *Bb* in the presence of *Ac*

3.3.1 Intracellular survival of *Bb* in *Ac*

To examine whether internalized *Bb* was targeted by the amoeba digestion pathway, I used Alexa Fluor-labeled high molecular dextran. A previous study has shown that Alexa Fluor-labeled dextran is efficiently internalized and localized within the amoeba food vacuoles (FVs), which are involved in food digestion. Therefore, dextran is a suitable marker to follow the phago-endosomal pathway of *Ac* (*131*). At 3 h post-infection, a majority of GFP-expressing *Bb* was localized within vacuoles that did not contain the fluorescent dextran, implying that these vacuoles are independent of the amoeba phago-endosomal pathway (**Fig. 3.4A**). This result indicated that internalized *Bb* might survive by evading amoeba digestion.

To verify this hypothesis, I assessed the survival of intracellular bacteria by GPA to enumerate the intracellular bacteria recovered from the lysates of infected amoebae (*132*). After 3 h of gentamicin treatment, *Bb* was recovered from *Ac* at a high rate (at least 0.1% of inoculum), compared to *Escherichia coli* S17-1 λpir (*Ec*) as a negative control (less than 0.01% of inoculum) (**Fig. 3.4B**). Similar results were obtained in the prolonged co-culture of the bacteria with *Ac* (up to 30 h): For 30 h, the total number of *Bb* CFU remained almost constant, while the number of *Ec* were significantly decreased over time (**Fig. 3.4C, Top**). Both bacteria similarly grew in the absence of *Ac*, indicating that bacterial defect was not a factor causing low bacterial viability after co-culture with *Ac* (**Fig. 3.4C, Bottom**).

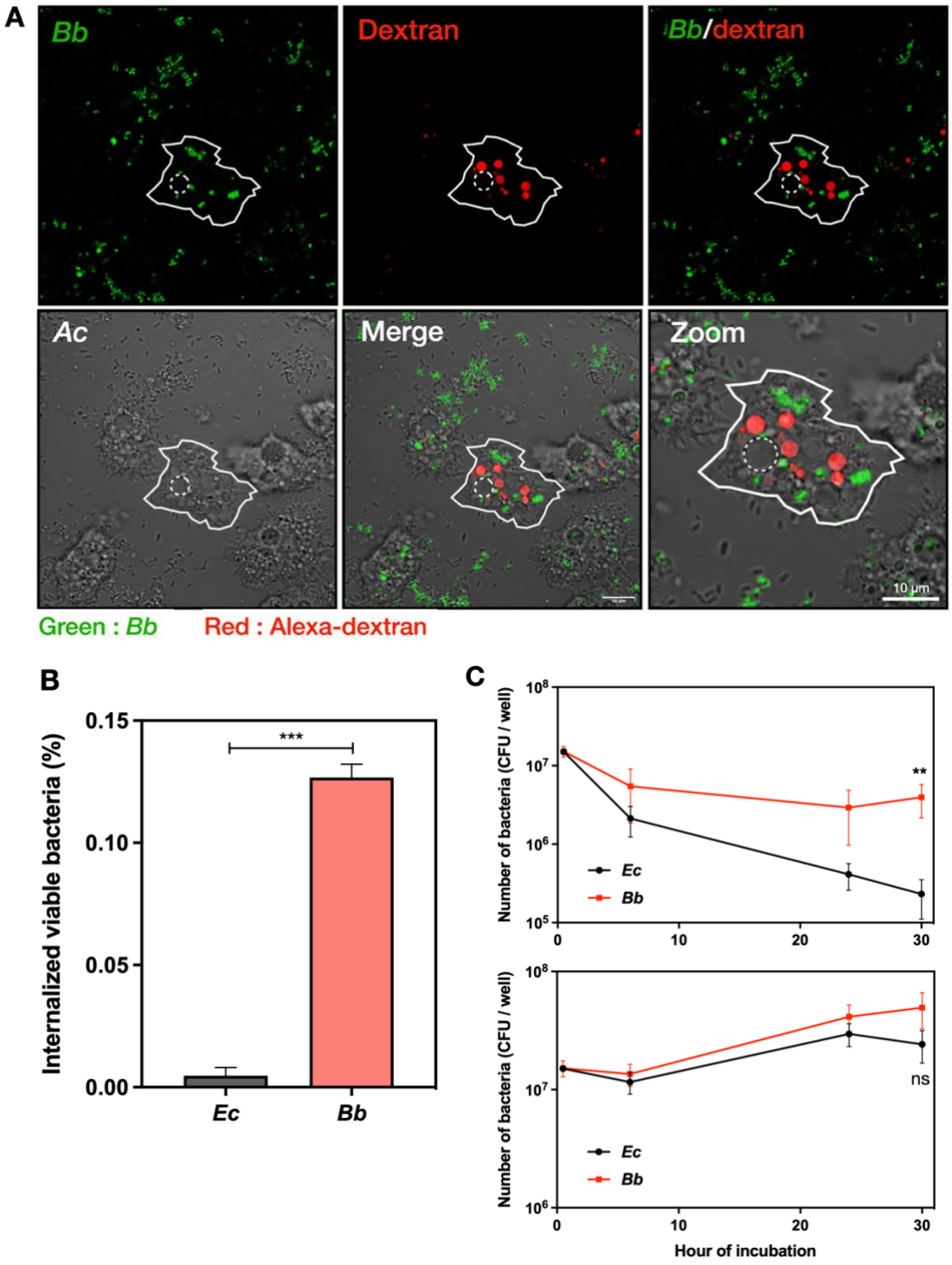

Figure 3.4 Internalized *Bb* did not colocalize with dextran

A. Internalized GFP-expressing *Bb* was localized in the vacuoles distinct from those containing dextran at 6 h post-infection. *Bb* was incubated with *Ac* at an MOI of 3000 in PYG medium containing 40 µg/ml of dextran. Bar: 10 µm.

B. *Bb* intracellularly survived within *Ac*. *Bb* was incubated for 1 h in the presence of *Ac* at an MOI of 100 and performed GPA for 3 h. Values are the mean ± standard deviation (SD) (n=3). *** denotes p<0.001.

C. *Bb*, but not *E. coli* S17-1 λpir (*Ec*) survived after prolonged incubation in the presence of *Ac* (above). Total CFU number of *Bb* and *Ec* were not significantly different in the absence of the amoebae, indicating that the low total number of *Ec* CFU was due to *Ac* and not bacterial growth defects (bottom). Values are the mean ± standard deviation (SD) (n=3). ** denotes p<0.05; ns: not significant.

3.3.2 Long-term survival of *Bb* in the presence of *Ac*

The pathogenic bacteria such as *Vibrio parahaemolyticus*, *Mycobacterium smegmatis*, *Mycobacterium bovis*, and *Listeria monocytogenes* were reported to survive for long periods of time in the presence of *Acanthamoeba* spp. (*124*, *133–135*). It has been shown that several intracellular pathogenic bacteria such as *Legionella pneumophilla* induced necrotic death of *Acanthamoeba polyphaga* cells in 48 h of infection (*136*). *Vibrio cholerae* has also been reported to cause *Ac* encystation and lysis of the cysts (*131*, *137*). These previous results prompted me to assess the effects of *Bb* on *Ac* viability after prolonged co-culture. The numbers of *Ac* in HG medium were unchanged in the presence or absence of *Bb* for 7 days of co-culture, suggesting that the bacteria did not affect the *Ac* viability (**Fig. 3.5A**). Furthermore,

the amoeba cysts were not found even in the presence of *Bb* (data not shown), suggesting that the bacteria did not induce encystation (data not shown).

The numbers of total bacteria recovered after co-culture with *Ac* in HG medium for 7 days were approximately 100 log-fold higher than those without the amoebae, indicating that *Ac* promoted *Bb* growth in HG medium, which is an unfavorable medium for *Bb* (**Fig. 3.5B**). Intracellular bacteria number recovered from *Ac* also significantly increased during co-culture, indicating that *Bb* did not only survive *Ac* digestion but also reside intracellularly within amoebae during co-culture (**Fig. 3.5C**). *Bb* proliferated within the first 7 days and survived at least for up to 4 weeks in the presence of *Ac*. *Bb* did not proliferate but survived even in HG medium in the absence of *Ac* (**Fig. 3.5D**). These results indicate that *Ac* trophozoites support bacterial growth and survival at higher bacterial numbers.

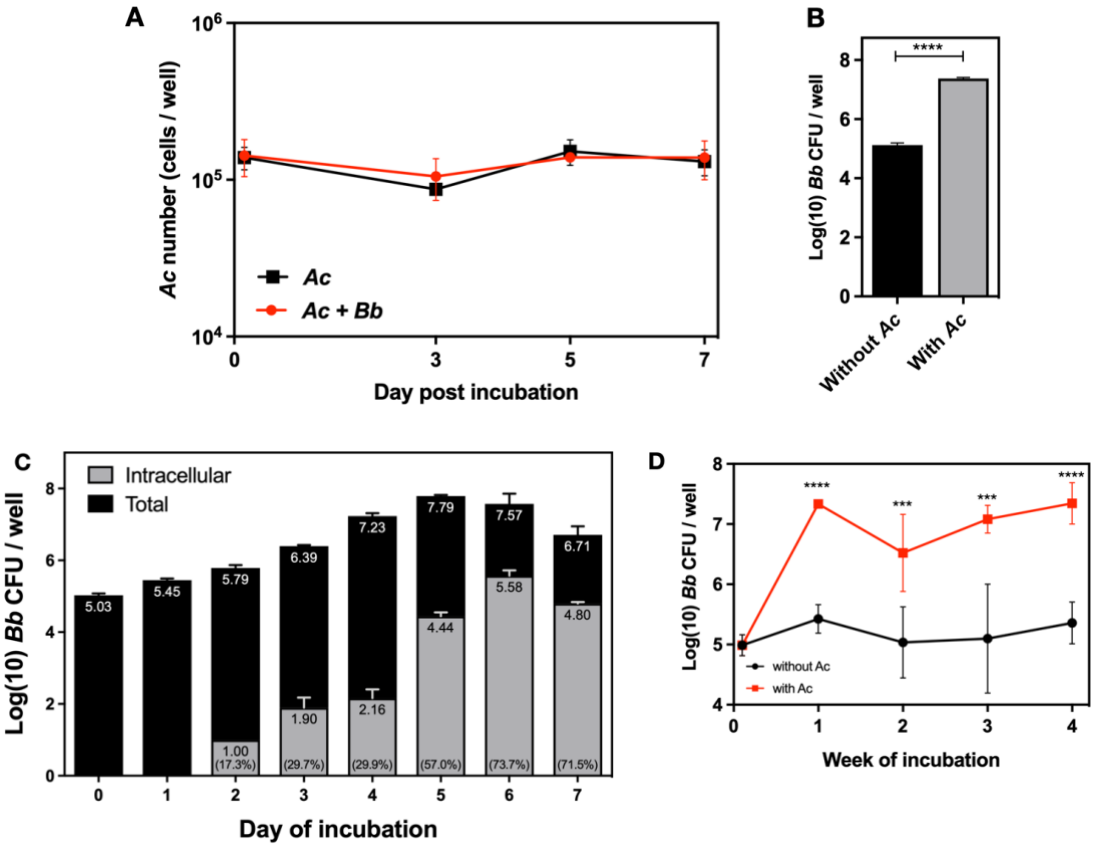

Figure 3.5 The presence of *Ac* stimulated *Bb* growth in HG medium

A. The total number of *Ac* trophozoites at each time point was unchanged in the presence or absence of *Bb*. *Ac* was incubated with *Bb* at an MOI of 100, and the total number of amoeba cells after 3, 5, and 7 days of incubation were counted using 0.1% of trypan blue. Values are the mean ± standard deviation (SD) (*n*=3).

B. The presence of *Ac* promoted *Bb* growth in HG medium. *Bb* was incubated for 4 weeks in the absence (black) or presence (grey) of *Ac* at an MOI of 1. Total and intracellular bacteria at each time point were enumerated. Values are the mean ± standard deviation (SD) (*n*=3). **** denotes $p<0.0001$.

C. The intracellular *Bb* (grey) was significantly increased during co-culture with *Ac* in HG medium for 7 days. *Bb* was incubated with *Ac* at an MOI of 1. Total and intracellular bacteria at each time point were enumerated. Values are the mean ± standard deviation (SD) (*n*=3).

D. Survival of *Bb* in the presence or absence of *Ac* in HG medium. *Bb* was incubated with *Ac* at an MOI of 1. The total CFU at each time point was enumerated. Values are the mean ± standard deviation (SD) (*n*=3). *** denotes $p<0.001$; **** denotes $p<0.0001$.

3.3.3 *Bb* escaped from *Ac* digestion by localizing in CV

Since previous results showed that intracellular *Bb* was constantly recovered from *Ac* (**Fig. 3.5C**), I tried to determine the fate of internalized *Bb* during co-culture. Microscopy revealed that GFP-expressing *Bb* was accumulated within amoeba CV at day 7 of co-culture (**Fig. 3.6A**). CV, which is readily visible as a large clear vacuole under a bright-field microscope (*138*, *139*), is known to regulate intracellular osmolarity of *Ac* by periodically collecting

excess cytosolic water and expelling it to the extracellular milieu (*71*). Therefore, I examined if *Bb* localized in CV escapes to the extracellular milieu by utilizing the CV function. Time-lapse imaging showed that the GFP-expressing bacteria accumulated within CV were expelled to the extracellular milieu along with the contents of CV (**Fig. 3.6B**).

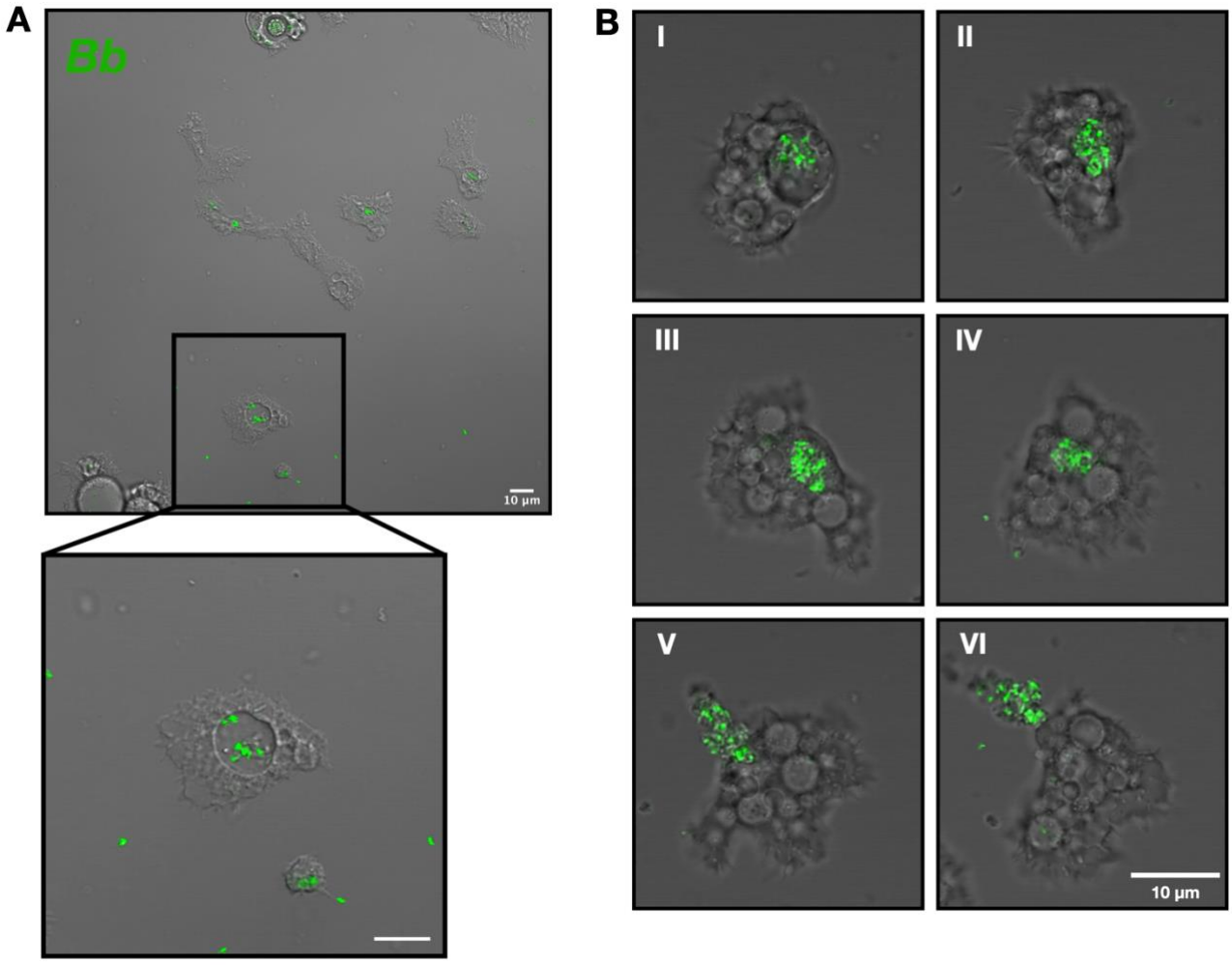

Figure 3.6 *Bb* utilized CV function to escape from *Ac*

A. GFP-expressing *Bb* was localized within amoeba CV, which is visible as a large clear vacuole. *Bb* was incubated with *Ac* at an MOI of 1000 in HG medium at 20℃ for 7 days. Bar: 10 µm.

B. Time-lapse images showing intracellular *Bb* escaped from CV through the water expulsion process. The relative time point is I, 0 min; II, 0.64 min; III, 1.44 min; IV, 3.84 min; V, 4.48 min; and VI, 5.44 min. Bar: 10 µm.

3.4 Effect of the *Bordetella virulence gene* (Bvg) phases on *Ac* viability

The pathogenicity of *Bb* is regulated by an intracellular TCS, called the *Bordetella* virulence gene (BvgAS) system, which controls phenotypic conversions of the bacteria between the virulent Bvg^+ phase and the avirulent Bvg^- phases. The Bvg^+ phase is essential for host infection (*58*, *140*), while the Bvg^- phase is considered to be necessary for environmental survival during the life cycle outside of the mammalian hosts (*58*). To address the latter point, I examined whether the intracellular survival of *Bb* depends on the Bvg phases. For this purpose, I utilized the *Bb* mutants, each of which is locked in the Bvg^+ or Bvg^- phase. None of *Bb* WT, Bvg^+ phase-locked-, and Bvg^- phase-locked-mutants affected the viability of the amoeba trophozoites (**Fig. 3.7**). These results suggest that major virulence factors, such as filamentous hemagglutinin (FHA), fimbriae, adenylate cyclase toxin (CyaA), pertactin, dermonecrotic toxin (DNT), and type III secretion system (*55*, *140*), did not affect *Ac* viability (**Fig. 3.7**).

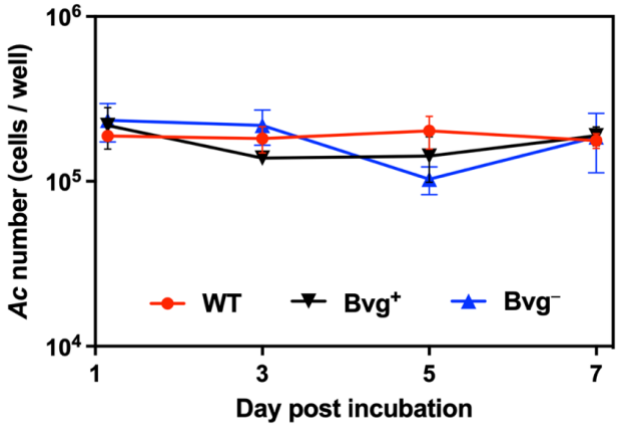

Figure 3.7 Viability of *Ac* was not affected in the presence of *Bb* WT, Bvg^+ phase-locked or Bvg^- phase-locked mutants

Ac was infected with *Bb* WT, *Bb* Bvg$^+$ phase-locked or *Bb* Bvg$^-$ phase-locked at an MOI of 100, and the total amoeba cells after 1, 3, 5, and 7 days of incubation were counted using 0.1% of trypan blue. Values are the mean ± standard deviation (SD) (n=3).

3.5 Bvg-phase dependency of intracellular survival of *Bb* in *Ac*

Next, I examined whether the intracellular survival of *Bb* is dependent on the Bvg phase. The Bvg$^-$ phase is reportedly important for *Bb* survival and growth in the soil amoeba, *Dictyostelium discoideum* (*Dd*) sori (*112*). I examined this point by using *Ac* instead of *Dd* and found that the Bvg$^-$ phase-locked, but not Bvg$^+$ phase-locked mutant, survived and proliferated after 7 days of co-culture with *Ac* (**Fig. 3.8A**). Prolonged incubation for up to 4 weeks in the presence of *Ac* resulted in the elimination of the Bvg$^+$ phase-locked mutant (**Fig. 3.8B**). The total number of the Bvg$^+$ phase-locked bacteria was unchanged for 4 weeks in HG medium, similar to *Bb* WT, indicating that *Ac* affected the survivability of the Bvg$^+$ phase-locked mutant (**Fig. 3.8C**).

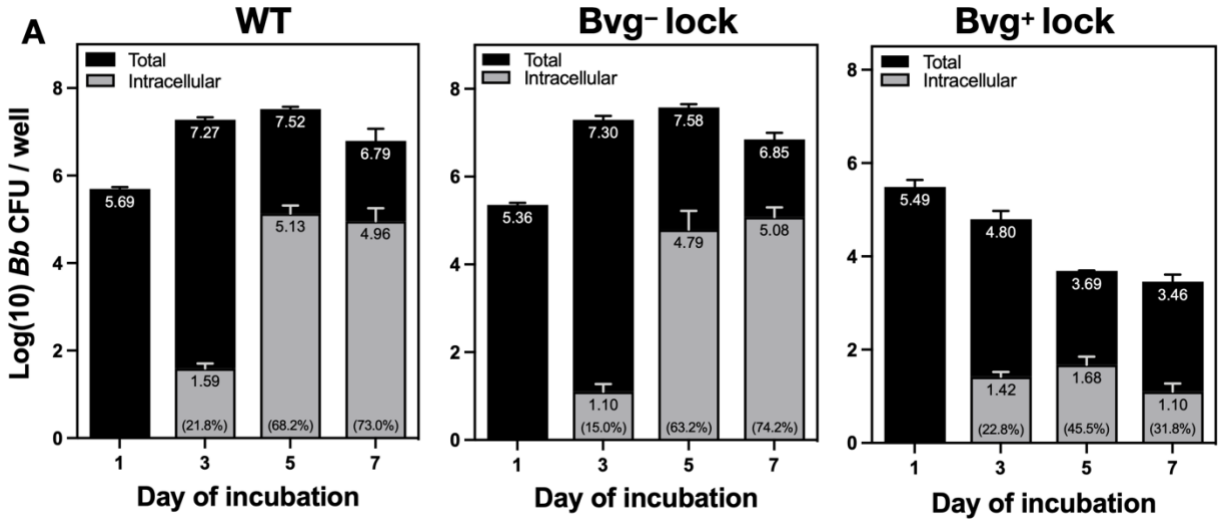

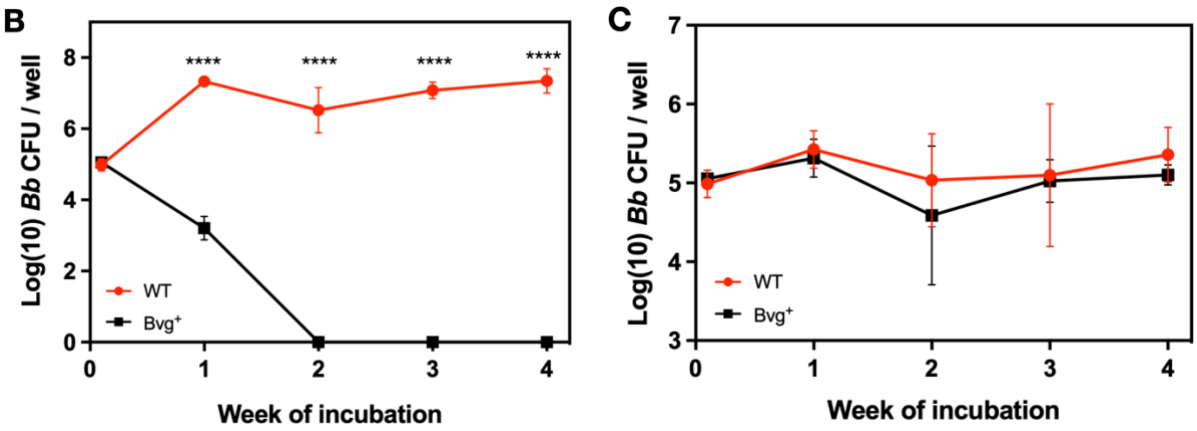

Figure 3.8 The Bvg^{-} phase facilitated *Bb* survival in the presence of *Ac*

A. The total (black) and intracellular (grey) bacterial number of WT, the Bvg^{-} phase-locked, and Bvg^{+} phase-locked mutants recovered from the co-culture with *Ac*. *Ac* was infected with WT-, the Bvg^{-} phase-locked-, and the Bvg^{+} phase-locked-mutants at an MOI of 1. The total and intracellular bacteria at each time point were enumerated. Values are the mean ± standard deviation (SD) (n=3).

B. Prolonged incubation significantly reduced the Bvg^{+} phase-locked-mutant. *Bb* WT or the Bvg^{+} phase-locked mutant was incubated for 4 weeks in the presence of *Ac* at an MOI of 1. The total bacteria at each time point were enumerated. Values are the mean ± standard deviation (SD) (n=3). **** denotes p<0.0001.

C. *Bb* WT and the Bvg^{+} phase-locked mutant similarly remained viable for 4 weeks without *Ac*. The total bacteria at each time point were enumerated. Values are the mean ± standard deviation (SD) (n=3).

3.6 Intracellular fate of the Bvg$^+$ and Bvg$^-$ phase-locked mutants within *Ac*

To understand why the Bvg$^+$ phase-locked mutant could not survive in *Ac*, I tried to track the fate of Bvg$^-$ and Bvg$^+$ phase-locked mutants internalized by *Ac*. In GPA, *Bb* WT and the Bvg$^-$ phase-locked mutant showed no significant differences in the number of the intracellular bacteria recovered after 4 h post gentamicin treatment, while the number of the recovered intracellular Bvg$^+$ phase-locked mutant was significantly reduced (**Fig. 3.9A**). Microscopic analyses revealed that the Bvg$^+$ phase-locked mutant was more efficiently internalized and transported to the intracellular digestion pathway where Alexa Fluor-labeled dextran was colocalized, compared to WT or the Bvg$^-$ phase-locked mutant (**Fig. 3.9B and 3.9F, Left**).

The Bvg$^-$ and Bvg$^+$ phase-locked mutants were differently localized in *Ac* at day 7 of co-culture: The Bvg$^-$ phase-locked mutant, but not the Bvg$^+$ phase-locked mutant, was transferred to CV similar to WT strain (**Fig. 3.9C and 3.9F, Middle**). These results imply that the Bvg$^+$ phase-locked mutant lost the CV localization ability (**Fig. 3.9B, Right**). When the GFP-expressing Bvg$^+$ phase-locked mutant was applied along with the mCherry-expressing *Bb* WT at 1:1 ratio to the co-culture with *Ac*, only mCherry-expressing *Bb* WT was observed in CV (indicated as a large clear vacuole) after 7 days of incubation. In addition, the GFP-expressing Bvg$^+$ phase-locked mutant was hardly observed in the extracellular medium after 7 days, suggesting that the Bvg$^+$ phase-locked mutant was phagocytized and digested by *Ac* (**Fig. 3.9D**). Indeed, after 7 days of co-culture, the dead cells of Bvg$^+$ phase-locked mutant were accumulated within giant food vacuoles (GFVs), which were previously reported as a specific compartment involved in the amoeba phago-endosomal pathway (*141*). These GFVs were distinct from the CV, since dextran was only accumulated within GFVs but not CVs. These dextran-filled GFVs contained granule-like substances that are possibly dead

bacteria (**Fig. 3.9E**). These granule-like substances within GFVs were not observed in the co-culture with WT or Bvg⁻ phase-locked mutant (**Fig. 3.9F, Right)**.

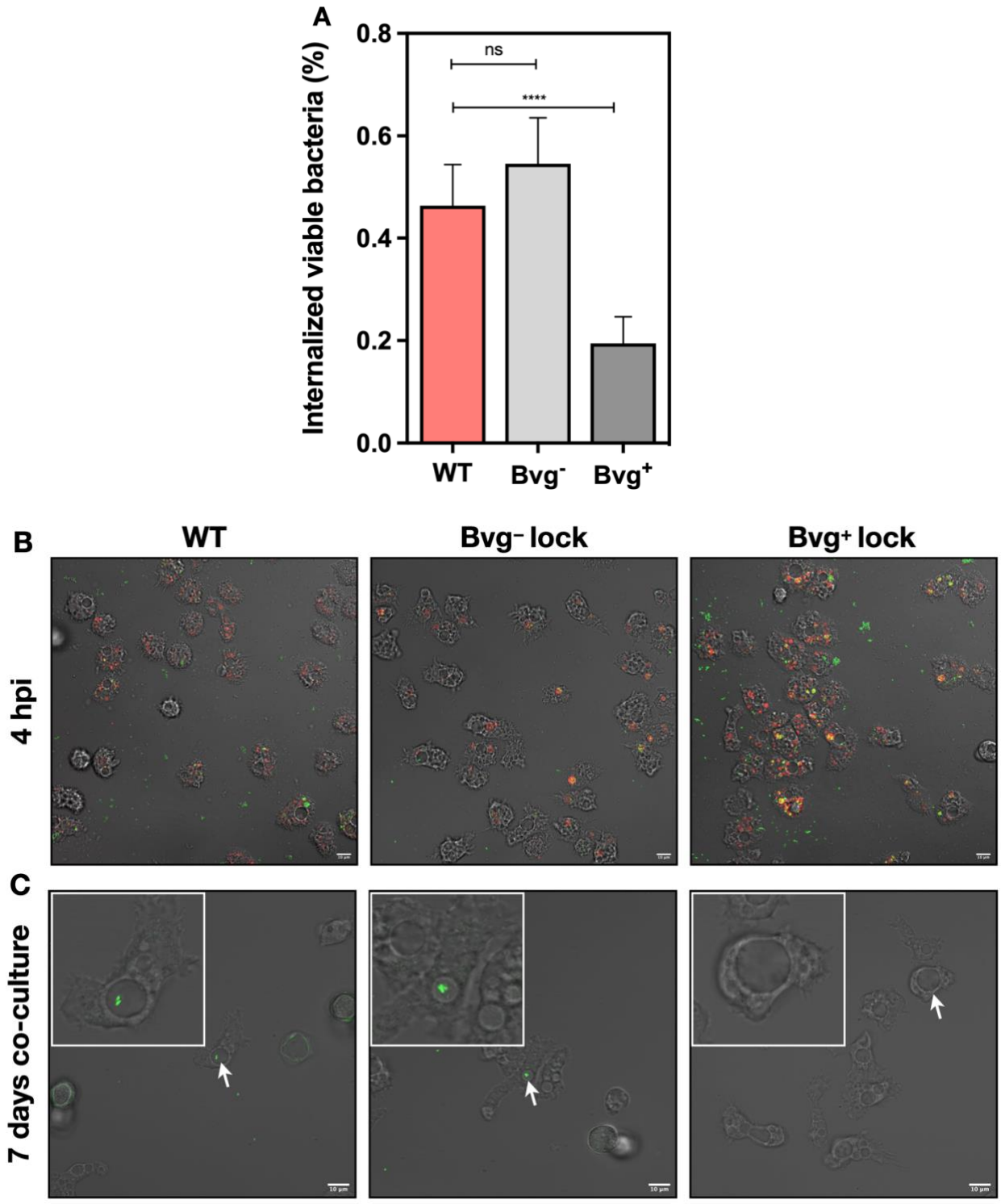

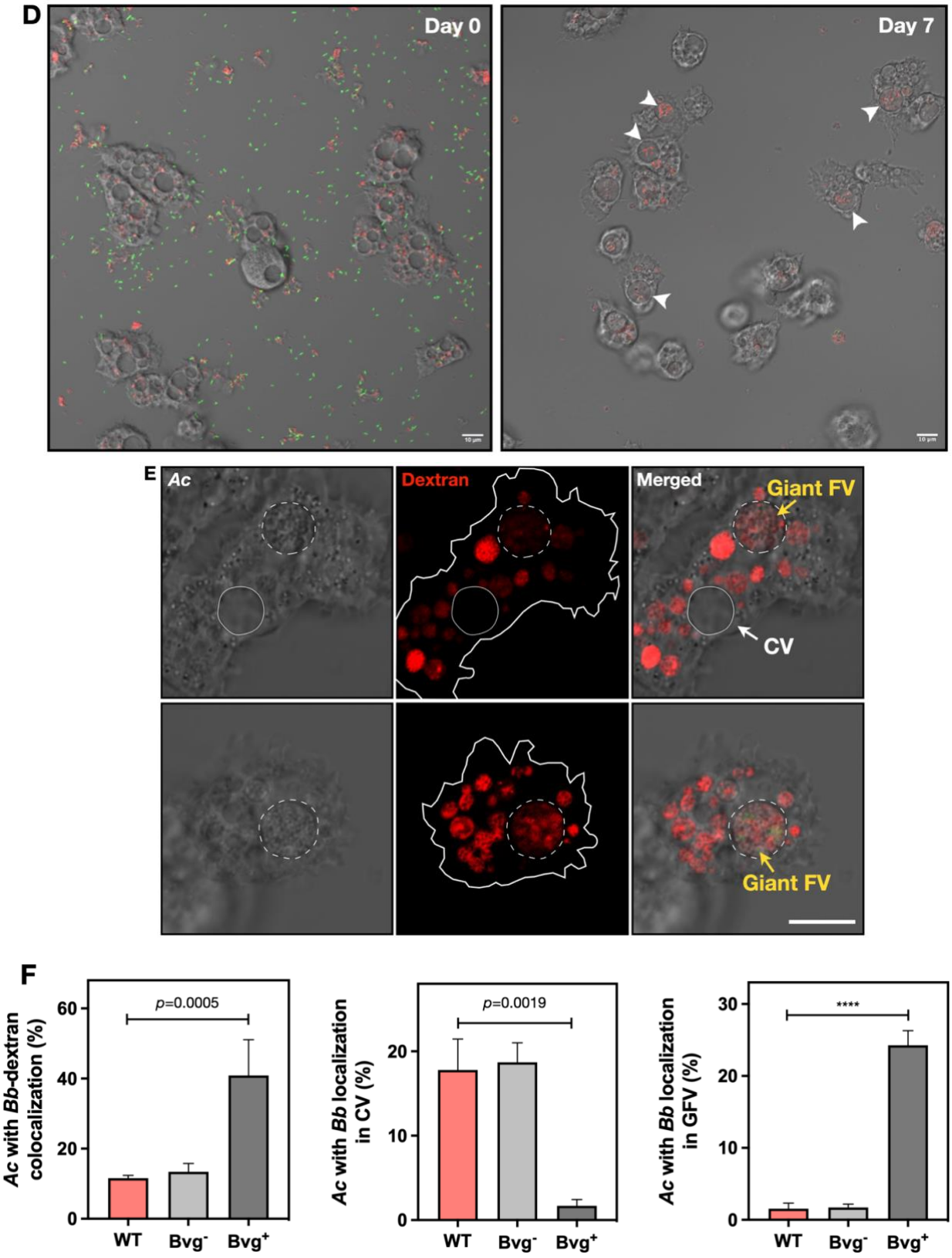

Figure 3.9 The fates of WT, Bvg⁻ phase-locked, and Bvg⁺ phase-locked mutants in *Ac*

A. The Bvg$^-$ phase-locked but not the Bvg$^+$ phase-locked mutant intracellularly survived within *Ac*. *Bb* strains were incubated for 1 h in the presence of *Ac* at an MOI of 100 and performed GPA for 4 h. Values are the mean ± standard deviation (SD) (*n*=3). *** denotes $p<0.001$. ns: not significant.

B. The GFP-expressing Bvg$^+$ phase-locked mutant was targeted by *Ac* digestion pathway. *Ac* was infected with *Bb* WT and the *Bb* mutants at an MOI of 1000 in HG medium supplemented with 40 μg/ml of dextran. Colocalization of the GFP-expressing *Bb* strains and dextran within FV was observed at 3 h post-infection (orange color). Bar: 10 μm.

C. The CV localization was observed in both WT and the Bvg$^-$ phase-locked mutant but not in the Bvg$^+$ phase-locked mutant. The GFP-expressing *Bb* strains were incubated with *Ac* at an MOI of 1. The white arrows indicate the GFP-expressing *Bb* strains localized in CVs. Bar: 10 μm.

D. *Bb* WT did not support the localization of the Bvg$^+$ phase-locked mutant to CV. The mCherry-expressing *Bb* WT was mixed with the GFP-expressing Bvg$^+$ phase-locked mutant (1:1) and incubated with *Ac* at an MOI of 1. The white arrowheads indicate the CVs filled by the mCherry-expressing *Bb* WT. Bar: 10 μm.

E. The dead cells of Bvg$^+$ phase-locked mutants were accumulated within GFVs. The GFP-expressing Bvg$^+$ phase-locked mutant was incubated with *Ac* at an MOI of 1000. Dextran was added into the infection medium 4 h before microscopy. The yellow and white arrows indicated the dead bacterial cells accumulated within dextran-filled GFVs and *Ac* CV, respectively. Bar: 10 μm.

F. The percentage of *Bb* WT and its derivatives colocalized with dextran (left), localized in CV (center), and GFV (right). Values are the mean ± standard deviation (SD) (*n*=400 *Ac*). *** denotes $p<0.001$.

3.7 Development of screening strategy based on the co-culture results

The above results demonstrate that *Bb* in the Bvg^- phase survived well in the co-culture with *Ac*, compared to that in the Bvg^+ phase, supporting the hypothesis that the Bvg^- phase of *Bb* may be advantageous for survival in the environment during the life cycle outside of the mammalian hosts (*58*). These results are also consistent with the previous report mentioning that *Bb* WT is shifted to the Bvg^- phase below 26℃ which represents the environmental temperature (*142*). Furthermore, these results indicate that Bvg^- phase-related genes are involved in *Bb* survival from predation by *Ac*. In contrast, genes specifically expressed in the Bvg^+ phase (i.e., virulence genes) may be targeted for *Ac* predation.

To explore genes responsible for survival of *Bb* after co-culture with *Ac*, I designed two distinct negative and screening strategies. negative and positive. The negative screening is based on the possibility that *Bb* in the Bvg^- phase specifically expresses genes which function to prevent predation by *Ac* and support survival. Therefore, disrupting these Bvg^- phase-related genes may attenuate *Bb* survival. For negative screening, I used transposon sequencing (Tn-Seq), a method to assess the contribution of individual genes to bacterial phenotypes in question (*143*), in this case, bacterial survival after co-culture with *Ac*. This method was used for identification of

potential genes involved in the survival of *Vibrio cholerae* and *Legionella pneumophila* (*144–146*). The proposed step for negative screening using Tn-Seq is indicated (**Fig. 3.10A**).

On the other hand, the positive screening is based on the possibility that Bvg^+ phase-specific factors, which include various major virulence factors, are targeted by *Ac* predation. To perform positive screening, I generated derivatives of the Bvg^+ phase locked mutant that were deficient in multiple genes for the Bvg^+ phase-specific virulence factors (hereafter referred to as the *Bb* poly-mutants) and examined whether the absence of these virulence genes influence survivability of the Bvg^+ phase-locked mutant in the presence of *Ac* (**Fig. 3.10B**).

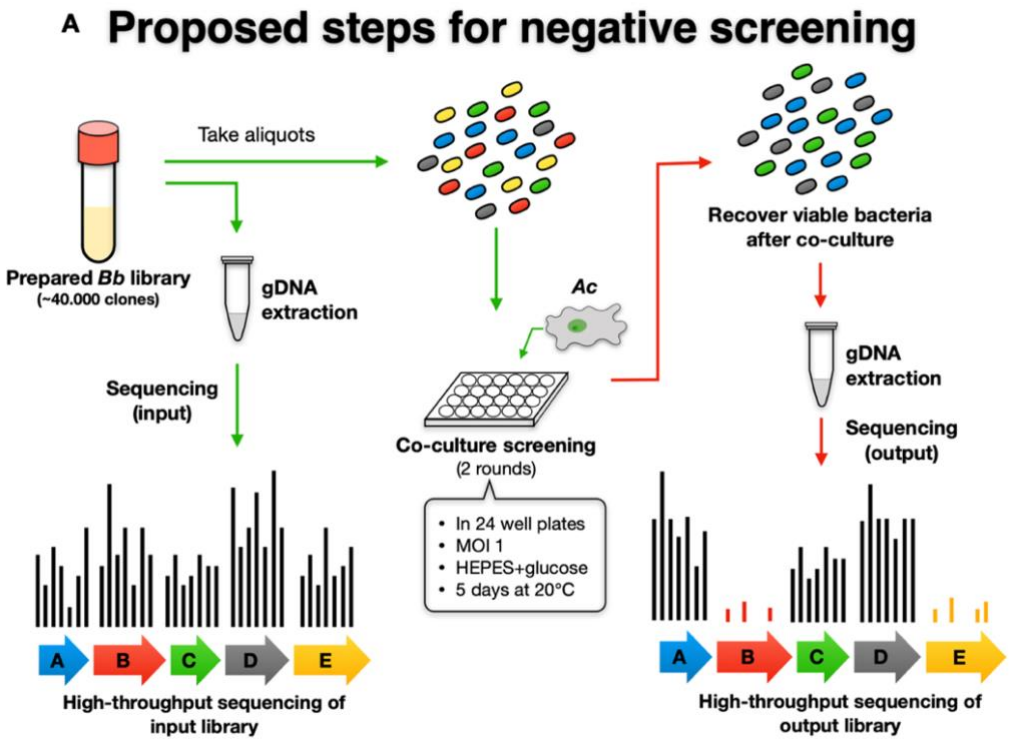

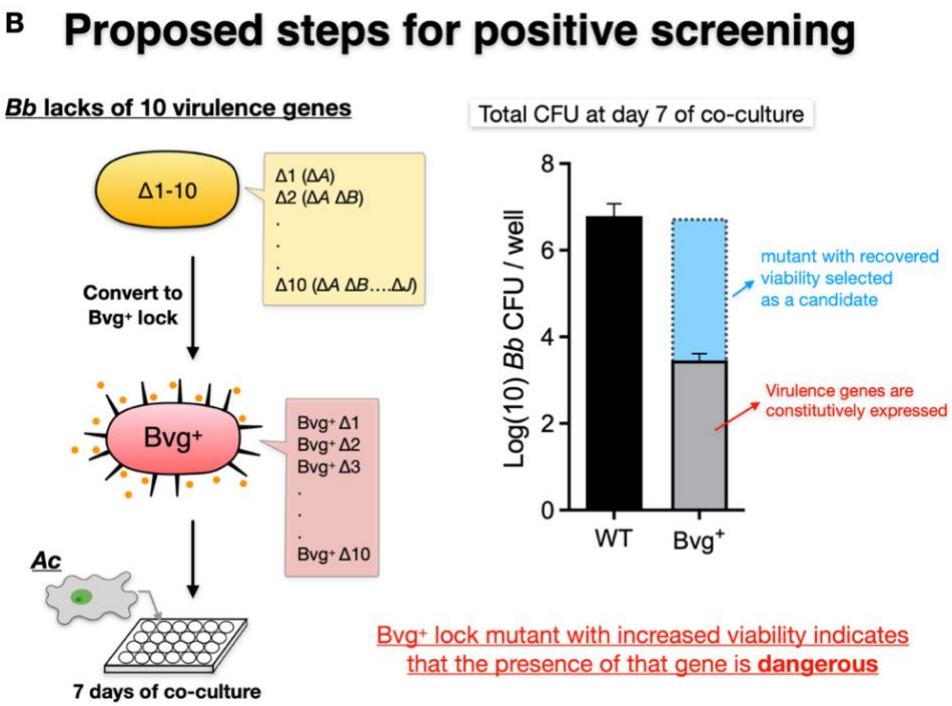

Figure 3.10 Screening strategies to elucidate key genes of *Bb* that are involved in the interaction with *Ac*

A. The *Bb* mutant library was constructed using genome-wide transposon mutagenesis. Two aliquots of the mutant library were used for co-culture assay and input genome DNA (gDNA) extraction, respectively. The co-culture assay was performed twice, and then viable bacteria were collected after co-culture and processed for the gDNA pools extraction. Extracted input and output gDNA were subjected to NGS, and the results were analyzed using EdgeR (*120*).

B. The *Bb* poly-mutants were subjected for the co-culture assay with *Ac*. The Bvg$^+$ phase-locked mutant was used as a control. The bacterial of the poly-mutants recovered after co-culture to a similar degree as WT are considered to be deficient in a gene encoding a factor (dangerous factor) that is targeted by *Ac* predation.

3.8 Tn-seq to identify 'promoting factors' for *Bb* survival in the presence of *Ac*

After negative screening, I chose gene reads that are different by 3 log-fold or over between the input and output libraries and obtained 35 genes (**Table 3.1**). These genes could be categorized as those with membrane-related transport functions, those related to TCS, others with unknown functions. In the present study, it has been shown that the bacteria in the Bvg^- phase, but not in the Bvg^+ phase survived in the co-culture with *Ac* (**Fig. 3.8A**). Therefore, I narrowed down the candidates to Bvg^- phase-specific genes by referring to the previous microarray data (*121*). Six genes were obtained (**Table 3.2**): *BB1281* encoding a histidine kinase, *BB2796*, *BB4462*, *BB3917*, and *BB0824* related to the bacterial membrane transport, and *BB0019* required for the cell wall metabolism, and performed the co-culture assays again by using the mutants deficient in each gene, which were designated as *ΔA* to *ΔF* (**Table 3.2**); however, each mutant candidate still survived in the co-culture with *Ac*, similar to WT (**Fig. 3.11**).

Table 3.1 List of selected candidate genes from the Tn-Seq screening

No.	Gene name	Locus	Product
1	AYT36_RS00790	BB0153	O-antigen biosynthesis protein WlbC
2	AYT36_RS06465	BB1281	HAMP domain-containing histidine kinase
3	AYT36_RS00100	BB0016	TssQ family T6SS-associated lipoprotein
4	AYT36_RS23450	BB4615	M61 family metallopeptidase
5	AYT36_RS16380	BB3225	TRAP transporter fused permease subunit
6	AYT36_RS25435	BB5008	Sensor histidine kinase
7	AYT36_RS00335	BB0062	DMT family transporter
8	AYT36_RS05705	BB1129	DUF2894 domain-containing protein
9	AYT36_RS07230	BB1428	LysR family transcriptional regulator
10	AYT36_RS01485	BB0295	Protein-export chaperone SecB
11	AYT36_RS10340	BB2031	TetR/AcrR family transcriptional regulator
12	AYT36_RS06735	BB1335	MFS transporter
13	AYT36_RS19715	BB3883	Lipoprotein
14	AYT36_RS14225	BB2796	Amino acid ABC transporter permease
15	AYT36_RS14615	BB2874	Hypothetical protein
16	AYT36_RS20180	BB3971	LysR family transcriptional regulator
17	AYT36_RS14975	BB2946	Fe^{3+} ABC transporter substrate-binding protein
18	AYT36_RS22240	BB4373	Lipoprotein
19	AYT36_RS01200	BB0238	Tripartite tricarboxylate transporter substrate binding protein
20	AYT36_RS00605	BB0116	Endonuclease/exonuclease/phosphatase family protein
21	AYT36_RS01475	BB0293	Tripartite tricarboxylate transporter substrate binding protein
22	AYT36_RS15400	BB3031	ABC-F family ATPase
23	AYT36_RS01645	BB0325	Cyclolysin T1SS permease/ATPase CyaB
24	AYT36_RS18285	BB3599	Outer membrane protein assembly factor BamD
25	AYT36_RS23490	BB4623	Co^{2+}/Mg^{2+} efflux protein ApaG
26	AYT36_RS22685	BB4462	TolC family outer membrane protein
27	AYT36_RS06880	BB1358	Phosphatase PAP2 family protein
28	AYT36_RS00115	BB0019	FecR domain-containing protein
29	AYT36_RS19265	BB3796	ABC transporter substrate-binding protein
30	AYT36_RS19890	BB3917	K^+-transporting ATPase subunit F
31	AYT36_RS01215	BB0241	Amino acid ABC transporter substrate-binding protein
32	AYT36_RS22485	BB4422	ABC transporter substrate-binding protein
33	AYT36_RS21470	BB4221	Tripartite tricarboxylate transporter TctB family protein
34	AYT36_RS04170	BB0824	Molybdate ABC transporter permease subunit
35	AYT36_RS01095	BB0217	Na^+/H^+ antiporter NhaA

Table 3.2 List of candidate genes that specifically expressed in Bvg$^-$ phase

Locus	Product	Mutant
BB1281	HAMP domain-containing histidine kinase	ΔA
BB2796	Amino acid ABC transporter permease	ΔB
BB4462	TolC outer membrane protein	ΔC
BB0019	FecR domain-containing protein	ΔD
BB3917	K$^+$-transporting ATPase A chain	ΔE
BB0824	Molybdate ABC transporter permease	ΔF

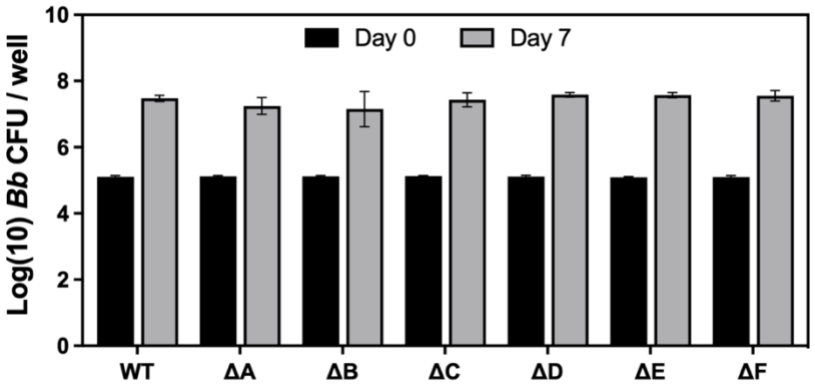

Figure 3.11 *Bb* mutants deficient in each candidate survived in the co-culture with *Ac*, similar to to WT

Ac was infected with *Bb* WT and all six mutant candidates at an MOI of 1, and the total CFU number (grey bar) after 7 days of co-culture was enumerated. Black bar indicated input bacteria number at day 0. Values are the mean ± standard deviation (SD) (n=3).

3.9 The co-culture assay using *Bb* poly-mutant strains to identify 'dangerous factors'

For the positive screening, I used a series of the *Bb* poly-mutant strains that were previously prepared in our laboratory from strain S798, a clinical isolate from a pig with atrophic rhinitis (*122*). These mutant strains were deficient in multiple virulence factors (**Table 3.3 and 3.4**). Strain S798 exhibited a similar ability as strain RB50, which was used in the first part of this study, to survive in the co-culture with *Ac* (**Fig. 3.12A**). I firstly examined the Bvg$^+$ phase-locked *Δ*5 and *Δ*10 for the survival ability and found that *Δ*5 and *Δ*10 were recovered from the co-culture

approximately 2 log-fold and 4 log-fold more than WT (**Fig. 3.12B**). Next, a series of the poly-mutant strains from *Δ*4 to *Δ*10 were examined. After co-culture, Bvg$^+$ phase-locked *Δ*6, *Δ*7, *Δ*8, *Δ*9, and *Δ*10 were highly recovered, while the number of recovered Bvg$^+$ phase-locked *Δ*4 was 4 log-fold fewer than those, similar to Bvg$^+$ phase-locked WT. Bvg$^+$ phase-locked *Δ*5 was recovered intermediately between Bvg$^+$ phase-locked WT and *Δ*6. *Δ*5 has an additional deletion of *fhaB*, compared to *Δ*4. *Δ*6 has an additional deletion of *fimBCD*, compared to *Δ*5 (**Table 3.4**). Therefore, FhaB and FimBCD were likely potential candidates for dangerous factors targeted by *Ac* (**Fig. 3.12C**).

Table 3.3 List of targeted virulence genes for the positive screening

No.	Group	Gene locus	Gene function (Based on RefSeq: AP014582)
1	Toxin	BBS798_3771	Dermonecrotic toxin (Dnt)
2		BBS798_0319	Bifunctional hemolysin-adenylate cyclase (CyaA)
3	T3SS	BBS798_1587	Type III secretion system ATPase (BscN)
4	Adhesin	BBS798_2818-20	Fimbrial adhesin (FimDCB)
5		BBS798_2822	Filamentous hemagglutinin (FhaB)
6		BBS798_2151	Filamentous hemagglutinin (FhaS)
7		BBS798_1837	Filamentous hemagglutinin (FhaL)
8		BBS798_1147	Bordetella RTX-family Adhesin (BrtA)
9	Autotransporter	BBS798_1328	Pertactin (Prn)
10		BBS798_1765	Virulence Associated Gene 8 (Vag8)

Table 3.4 List of *Bb* poly-mutant strains used for the positive screening

Strain name	Genotype
WT	Wild-type strain S798, Clinical isolate
Δ1	WT lacking *bscN* gene
Δ2	Δ1 lacking *dnt* gene
Δ3	Δ2 lacking *prn* gene
Δ4	Δ3 lacking *cyaA* gene
Δ5	Δ4 lacking *fhaB* gene
Δ6	Δ5 lacking *fimBCD* gene
Δ7	Δ6 lacking *vag8* gene
Δ8	Δ7 lacking *fhaS* gene
Δ9	Δ8 lacking *fhaL* gene
Δ10	Δ9 lacking *brtA* gene

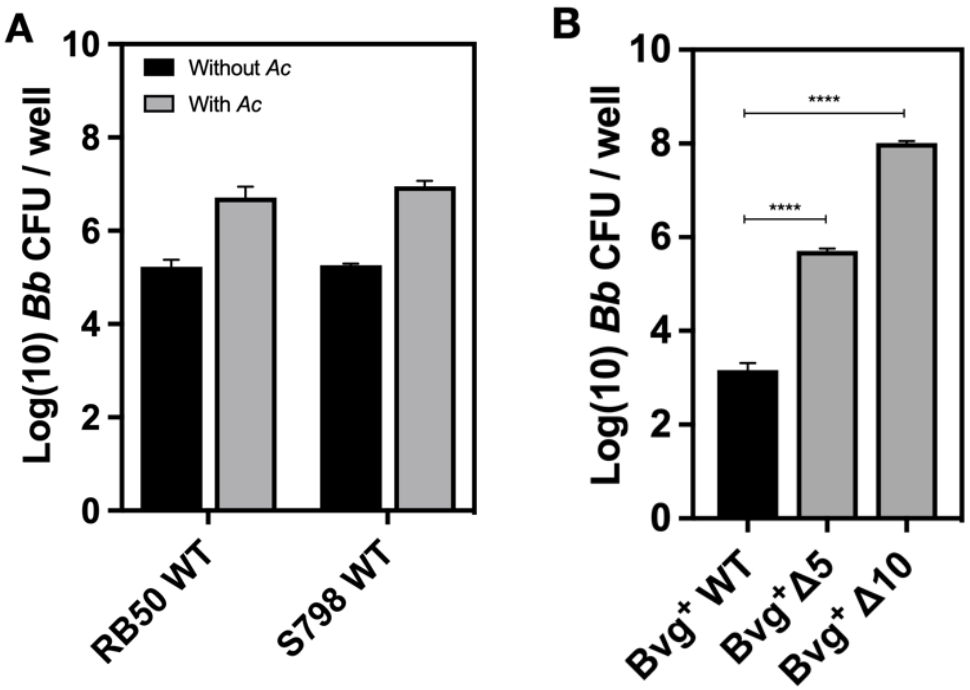

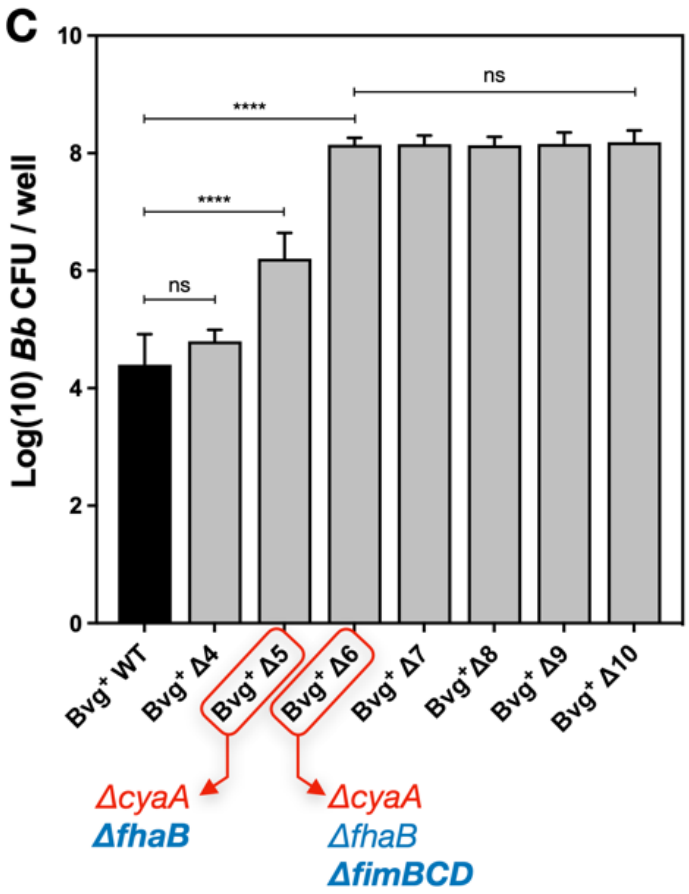

Figure 3.12 The positive screening identified *fhaB* and *fimBCD* as the dangerous factors

A. In the presence of *Ac*, *Bb* strain S798 has comparable survivability to *Bb* strain RB50. *Ac* was infected with either *Bb* S798 WT or RB50 WT at an MOI of 1, and the total bacteria recovered from the 7-day co-culture were enumerated (grey bars). The black bar indicates input bacterial number at day 0. Values are the mean ± standard deviation (SD) (n=3).

B. Bvg^+ phase-locked *Δ*5 and *Δ*10 survived well after co-culture with *Ac* compared to Bvg^+ phase-locked WT. *Ac* was infected with Bvg^+ phase-locked WT (black bar), *Δ*5 (Bvg^+ *Δ*5), and *Δ*10 (Bvg^+ *Δ*10) at an MOI of 1, and the total CFU number after 7 days of co-culture was enumerated. Compared to Bvg^+ phase-locked WT, the total CFU number of *Δ*5 and *Δ*10 was 2-log and 4 log-fold increased, respectively. Values are the mean ± standard deviation (SD) (n=3). **** denotes p<0.0001.

C. Candidate of dangerous factors was obtained after performing co-culture assay with Bvg$^+$ phase-locked *Δ*4 to *Δ*10 (Bvg$^+$ *Δ*4 to *Δ*10). *Ac* was infected with Bvg$^+$ phase-locked WT (black bar) or Bvg$^+$ *Δ*4 to *Δ*10 at an MOI of 1, and the total CFU number after 7 days of co-culture was enumerated. A similar total CFU number was obtained in the case of Bvg$^+$ *Δ*4 and WT or among Bvg$^+$ *Δ*6 to *Δ*10, indicating that gene deleted in Bvg$^+$ *Δ*5 (*fhaB*) and *Δ*6 (*fimBCD*) was the probable dangerous factors. Values are the mean ± standard deviation (SD) (n=3). **** denotes p<0.0001. ns: not significant.

3.10 Bvg$^+$ phase-locked *Bb* lacking *fhaB* or *fimBCD* survived co-culture with *Ac*

To confirm the results of the experiments using *Bb* S798, I constructed Bvg$^+$ phase-locked *Bb* RB50 lacking *fhaB* or *fimBCD* gene, and examined them for survivability in the co-culture with *Ac*. The deletion of *fhaB* or *fimBCD* rescued the low survivability of Bvg$^+$ phase-locked WT. The double knock-out (dKO) Bvg$^+$ phase-locked *ΔfhaB/ΔfimBCD* strain was recovered from the co-culture at the highest number compared to the single knock-out *ΔfhaB* and *ΔfimBCD* strains. Deletion of non-cadidate genes, *bscN* and *cyaA*, did not influence survivability of isogenic Bvg$^+$ phase-locked WT (**Fig. 3.13A**). Furthermore, Bvg$^+$ phase-locked *ΔfhaB* and *ΔfimBCD* regained the ability to reside within *Ac* to a similar extent to WT and the Bvg$^-$ phase-locked mutant (**Fig. 3.13B**). These results prove that FhaB and FimBCD are the dangerous factors targeted by *Ac* predation.

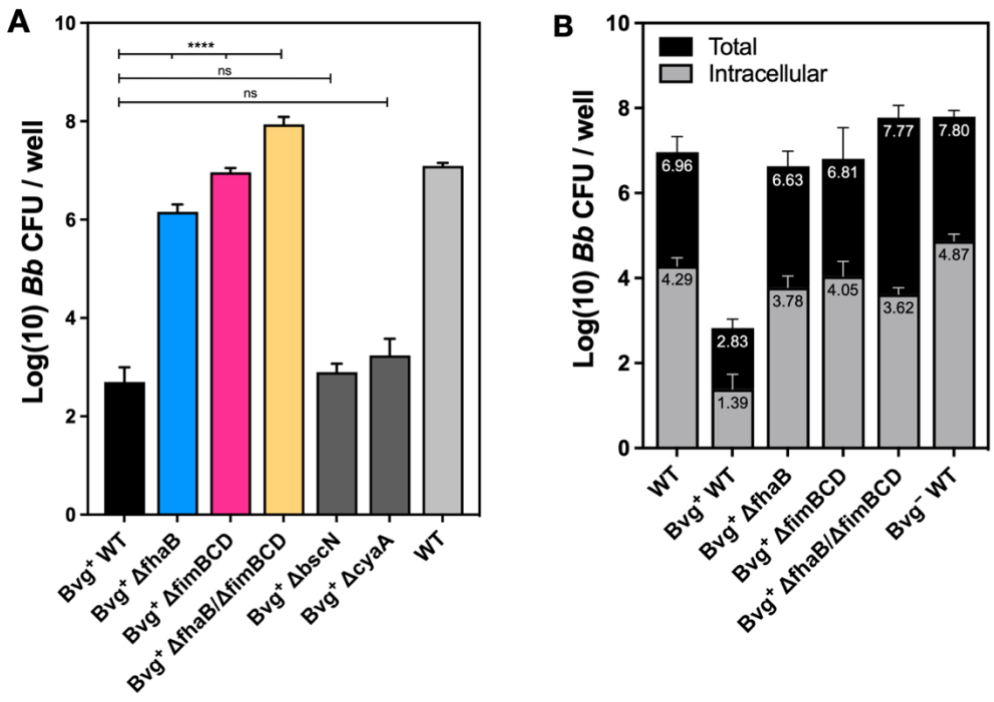

Figure 3.13 Bvg$^+$ phase-locked lacking *fhaB* or *fimBCD* had similar survivability to WT

A. Total CFU number of Bvg$^+$ phase-locked *ΔfhaB* and *ΔfimBCD* increased after co-culture. *Ac* was infected with Bvg$^+$ phase-locked WT (Bvg$^+$ WT), *ΔfhaB* (Bvg$^+$ *ΔfhaB*), *ΔfimBCD* (Bvg$^+$ *ΔfimBCD*), *ΔfhaB/ΔfimBCD* (Bvg$^+$ *ΔfhaB/ΔfimBCD*), *ΔbscN* (Bvg$^+$ *ΔbscN*), *ΔcyaA* (Bvg$^+$ *ΔcyaA*), and WT at an MOI of 1. The total CFU number after 7 days of co-culture was enumerated. Values are the mean ± standard deviation (SD) (n=3). **** denotes p<0.0001.

B. The trend of total (black) and intracellular (grey) bacterial number of Bvg$^+$ *ΔfhaB*, Bvg$^+$ *ΔfimBCD*, Bvg$^+$ *ΔfhaB/ΔfimBCD* were similar to WT and Bvg$^-$ WT. *Ac* was infected with WT, Bvg$^+$ WT, Bvg$^+$ *ΔfhaB*, Bvg$^+$ *ΔfimBCD*, Bvg$^+$ *ΔfhaB/ΔfimBCD*, and Bvg$^-$ WT *Bb* at an MOI of 1. At day 7 of co-culture, the total and intracellular bacteria numbers were enumerated. Values are the mean ± standard deviation (SD) (n=3).

3.11 Bvg$^+$ phase-locked *Bb* lacking *fhaB* or *fimBCD* was transferred to the *Ac* CV similar to WT

I investigated the localization of Bvg$^+$ *ΔfhaB* and *ΔfimBCD* in *Ac* by microscopy. The Bvg$^+$ *ΔfhaB*, Bvg$^+$ *ΔfimBCD*, and Bvg$^+$ *ΔfhaB/ΔfimBCD* did not colocalize with dextran, while Bvg$^+$ phase-locked WT was accumulated in FV of the intracellular digestion pathway (**Fig. 3.14A**). In addition, Bvg$^+$ *ΔfhaB*, Bvg$^+$ *ΔfimBCD*, and Bvg$^+$ *ΔfhaB/ΔfimBCD*, but not Bvg$^+$ WT, were also observed within a CV in 3 h (**Fig. 3.14B**). These results indicate that Bvg$^+$ phase-locked mutant lacking FhaB and fimbriae evade *Ac* predation in a similar manner to WT.

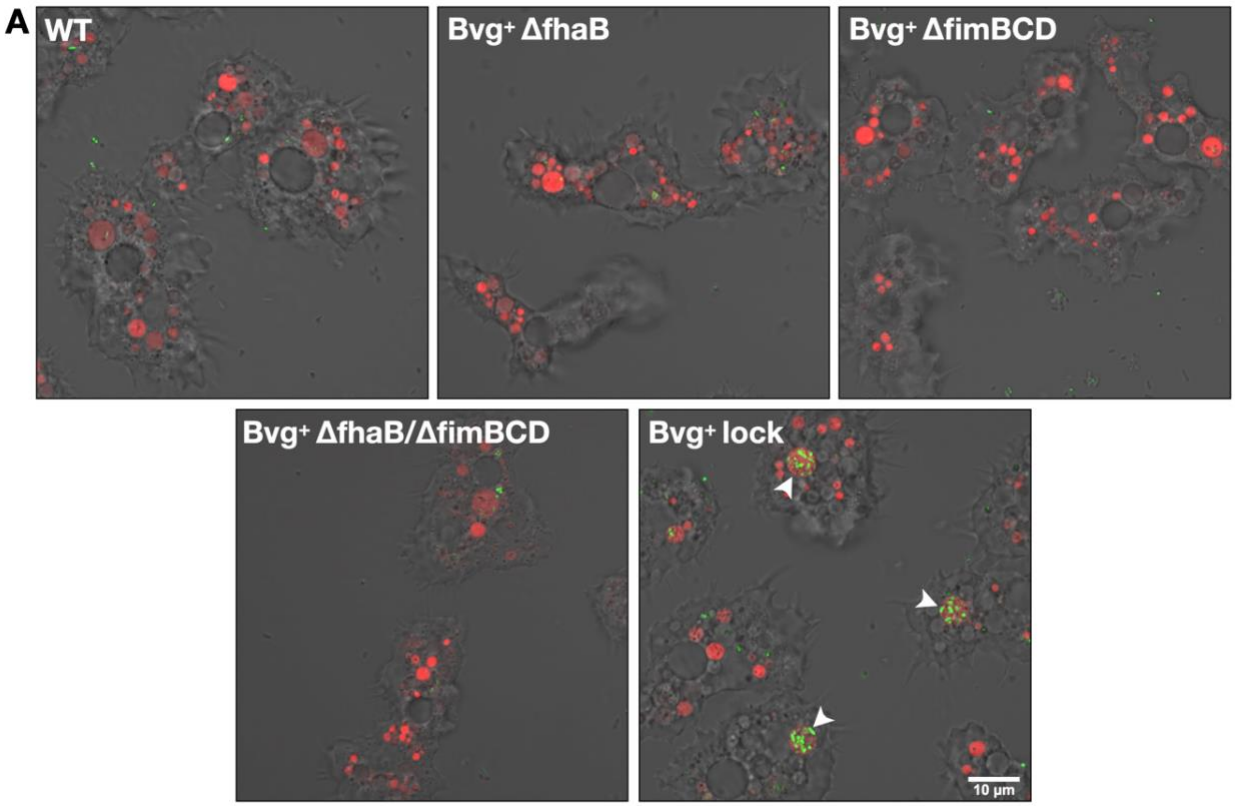

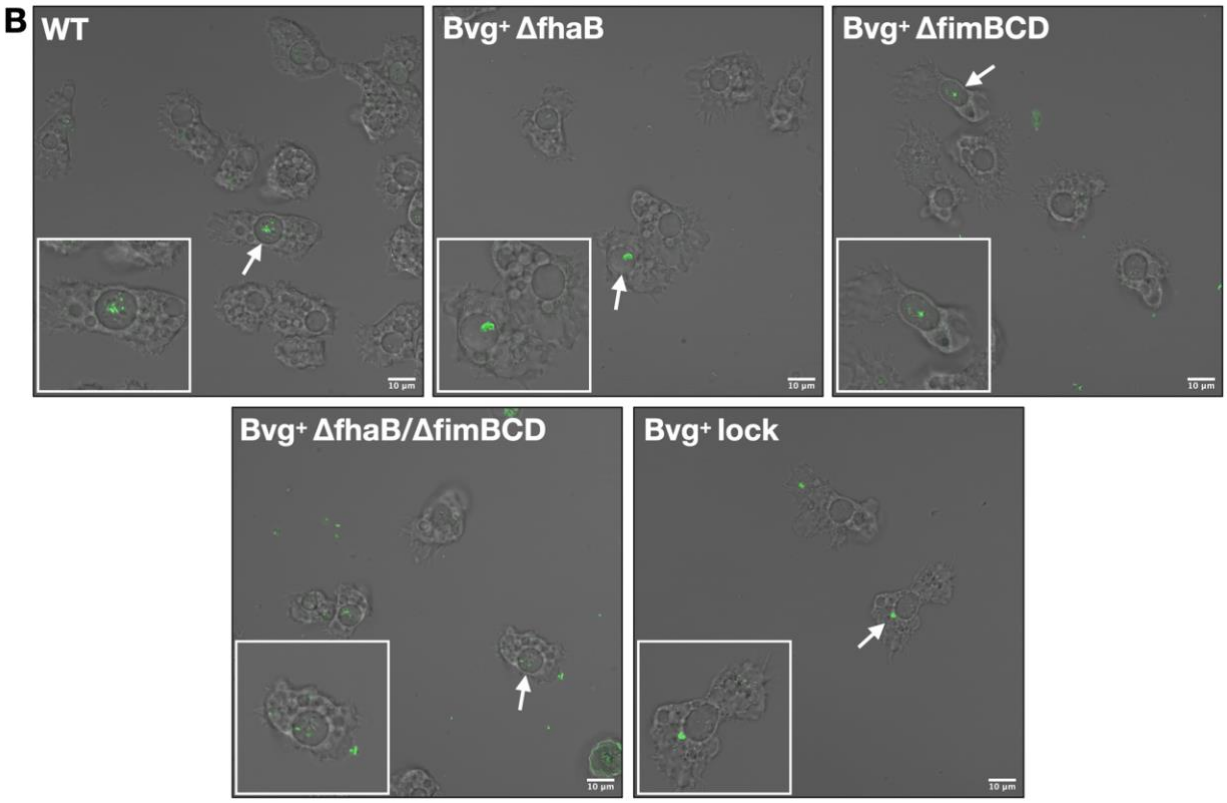

Figure 3.14 Intracellular localization of the Bvg$^+$ phase-locked mutants lacking FhaB or fimbriae

A. GFP-expressing Bvg$^+$ phase-locked *Bb* lacking FhaB or fimbriae did not colocalize with dextran. *Ac* was infected with *Bb* WT, Bvg$^+$ *ΔfhaB*, Bvg$^+$ *ΔfimBCD*, Bvg$^+$ *ΔfhaB/ΔfimBCD*, and Bvg$^+$ lock at an MOI of 1000 in HG medium supplemented with 40 µg/ml of dextran. Colocalization of GFP-expressing *Bb* strains and dextran within FV was observed at 3 h post-infection. The white arrowheads indicate the colocalization of GFP-expressing Bvg$^+$ lock *Bb* with dextran. Bar: 10 µm.

B. The CV localization was observed in Bvg$^+$ phase-locked mutant lacking FhaB or fimbriae. *Ac* was infected with *Bb* WT, Bvg$^+$ *ΔfhaB*, Bvg$^+$ *ΔfimBCD*, Bvg$^+$ *ΔfhaB/ΔfimBCD*, and Bvg$^+$ lock at an MOI of 1. The white arrows indicate the CV localization of GFP-expressing *Bb* strains at day 7 post-incubation. Bar: 10 µm.

CHAPTER 4 - DISCUSSION AND FUTURE WORK

4.1 *Bb* not only survives predation by *Ac* but also proliferates with the aid of *Ac*

It is inevitable for *Bb* that lives in the natural environments, such as soil and water, to encounter other symbiotic or predacious organisms that share the habitat. In this study, I tried to dissect the interaction between *Bb* and *Ac*, a common environmental protozoan, and to understand the lifestyle of *Bb* in the natural environment. *Ac* has a biphasic life-form consisting of the trophozoite stage and cyst stage. I demonstrated that *Bb* survived within *Ac* trophozoites as previously described (*112*), and observed *Bb* residing in dormant cysts of *Ac*. These results imply that *Ac*, both in trophozoite and cyst stage, may provide a protective niche for internalized *Bb* from harsh environmental conditions. In addition, when co-cultured with *Ac* in the nutrient-limited HG medium, *Bb* was found to proliferate without affecting the amoebae viability. These results suggest that the amoebae support the bacterial multiplication probably by providing nutritional sources for the bacteria through cell debris, metabolic end products, and so on (*124*). Alternatively, the amoebae may serve as reservoirs to feed the intracellular *Bb*. A similar feeding mechanism was reported *Vibrio mimicus* (*147*). In *Ac*, *Bb* was mainly localized in vacuoles distinct from those in the digestive pathway that are commonly transferred from the food vacuoles to the degradative phagolysosomes (*148*). Thus, I hypothesize that internalized *Bb* may interfere with phagosome maturation or phagosome-lysosome fusion and eventually evade predation by the amoebae. *Legionella pneumophila* and *Mycobacterium avium* were also reported to prevent phagosome-lysosome fusion. *Burkholderia cepacia* was shown to survive within acidic vacuoles of *A. polyphaga* by an unknown mechanism (*149–151*). I observed that *Bb* was localized within CV in 7 days after co-culture, and escaped to extracellular milieu when CV expelled its contents. However, whether *Bb* multiplies in CV remains to be determined. It was reported that *V. cholerae*

was localized in CV when incubated with *Ac*, which resulted from the vacuolar fusion between *V. cholerae*-containing vacuoles with CV (*131*). In the present study, I could not clarify if *Bb* also generates specific vacuoles containing themselves in *Ac*.

4.2 *Bb* in the Bvg$^-$ phase is advantageous in surviving in *Ac*

I further showed that *Bb* survival in the presence of *Ac* depends on the Bvg phases: *Bb* locked in Bvg$^+$ phase less survived than WT, while *Bb* locked in the Bvg$^-$ phase well survived, similar to WT. Furthermore, both *Bb* WT and the Bvg$^-$ phase-locked mutant localized within CV. These results indicate that *Bb* WT goes into the Bvg$^-$ phase and produces Bvg$^-$ phase-specific factors that allow the bacteria to survive *Ac* predation. In contrast, the Bvg$^+$ phase-locked mutant may be efficiently eradicated by *Ac* through the digestion pathway involving GFVs. *Ac* may recognize *Bb* through these factors and induce amoebic digestion.

4.3 *Bb* may conceal the FhaB and fimbriae during an encounter with *Ac*

The previous study has shown that a chemotaxis protein, *cheZ*, was highly expressed in *Bb* recovered from the *Dd* sori (*112*). Because *cheZ* is specifically expressed in the Bvg$^-$ phase (*121*), the above result may indicate that Bvg$^-$ phase-specific genes are required for *Bb* survival within the amoeba sori; however, the role of *cheZ* was not further characterized. In the present study, I tried to find genes of *Bb* required for the bacterial survival within *Ac* through the Tn-Seq technology and found 6 candidate genes specifically expressed in the Bvg$^-$ phase. However, none of these genes were found to play a role in the *Bb* survival after co-culture with *Ac*. Instead, the positive screening that I independently adopted identified FhaB and fimbriae, major adhesins of *Bb*, as the potential candidate factors that prevent the bacteria from surviving in the co-culture with

Ac. FhaB and fimbriae are known as adhesion molecules through which the bacteria colonize the upper respiratory tracts of hosts. The present results indicate that the adhesion molecules are targeted for predation by the amoeba; however, the mechanisms by which *Ac* recognize these adhesins remain to be determined. These adhesins may interact with the amoeba-specific receptors and facilitate the interaction of *Bb* with the amoeba cells. As a result, the bacteria may be efficiently transferred to the amoeba digestion pathway. *Bb* may conceal FhaB and fimbriae through the Bvg phase-conversion to prevent predation by the amoeba. Further study could be focused on identifying *Ac* receptor and molecular mechanisms by which *Ac* efficiently targets and digests FhaB- or fimbriae-expressing *Bb*.

4.4 Conclusions

To understand the lifestyle of *Bb* outside the mammalian hosts, I studied the interaction of the bacteria with *Ac*, one of the common protozoan predators in the environment. The results indicated that *Ac* could serve as a transient host for *Bb* in the natural environment and supports the propagation of the bacteria. Upon internalization, *Bb* evades *Ac* predation by utilizing CVs of the amoebae, which protect the bacteria from *Ac* digestion and expel them to the extracellular milieu through the water discharge system of *Ac*. *Bb* is considered to convert to the Bvg^- phase in the natural environment at lower temperatures. The present study revealed that the bacteria in the Bvg^- phase are advantageous to survive in *Ac* because Bvg^+ phase-specific factors, FhaB and fimbriae, are targeted by *Ac* predation.

4.5 Future work

Future work could focus on the following points:

i. It remains unknown how *Bb* enters CV. Answers to this question are necessary for further understanding of the mechanism of *Bb* escape from *Ac*.

ii. Determination of Bvg$^-$ phase-related genes (if such factors actually exist) required by *Bb* to survive within *Ac*.

iii. The molecular mechanisms by which FhaB and fimbriae of *Bb* are recognized by *Ac* are yet to be understood. Answers to this question may provide a different aspect of adhesion molecules of *Bb*, which function when the bacteria infect mammalian hosts.

REFERENCES

1. R. A Goodnow, Biology of *Bordetella bronchiseptica*. *Microbiol. Rev.* **44**, 722–738 (1980).
2. D. A. Bemis, *Bordetella* and mycoplasma respiratory infections in dogs and cats. *Vet. Clin. North Am. - Small Anim. Pract.* **22** (1992).
3. Mattoo et al., Clinical Manifestations of Respiratory Infections Due to *Bordetella pertussis* and Other *Bordetella* Subspecies. *Clin. Microbiol. Rev.* **18**, 326–382 (2005).
4. I. Rivera, B. Linz, E. T. Harvill, Evolution and Conservation of *Bordetella* Intracellular Survival in Eukaryotic Host Cells. *Front. Microbiol.* **11** (2020).
5. Mattoo et al., Molecular Pathogenesis, Epidemiology, and Clinical Manifestations of Respiratory Infections Due to *Bordetella pertussis* and Other *Bordetella* Subspecies. *Clin. Microbiol. Rev.* **18**, 326–382 (2005).
6. P. A. Cotter, M. H. Yuk, S. Mattoo, B. J. Akerley, J. Boschwitz, D. A. Relman, J. F. Miller, Filamentous hemagglutinin of *Bordetella bronchiseptica* is required for efficient establishment of tracheal colonization. *Infect. Immun.* **66**, 5921–5929 (1998).
7. E. V. Scheller, P. A. Cotter, *Bordetella* filamentous hemagglutinin and fimbriae: critical adhesins with unrealized vaccine potential. *Pathog. Dis.* **73**, (2015).
8. J. A. Montaraz, P. Novotny, J. Ivanyi, Identification of a 68-kilodalton protective protein antigen from *Bordetella bronchiseptica*. *Infect. Immun.* **47**, 744–751 (1985).
9. H. Jungnitz, N. P. West, M. J. Walker, G. S. Chhatwal, C. A. Guzmàn, A Second Two-Component Regulatory System of *Bordetella bronchiseptica* Required for Bacterial Resistance to Oxidative Stress, Production of Acid Phosphatase, and In Vivo Persistence. (1998)
10. D. Jurnecka, P. Man, P. Sebo, L. Bumba, *Bordetella pertussis* and *Bordetella bronchiseptica* filamentous hemagglutinins are processed at different sites. *FEBS Open Bio*. **8**, 1256–1266 (2018).
11. M. G. Barnes, A. A. Weiss, BrkA Protein of *Bordetella pertussis* Inhibits the Classical Pathway of Complement after C1 Deposition. *Infect. Immun.* **69**, 3067 (2001).
12. S. L. Brockmeier, K. B. Register, T. Magyar, A. J. Lax, G. D. Pullinger, R. A. Kunkle, Role of the dermonecrotic toxin of *Bordetella bronchiseptica* in the pathogenesis of respiratory disease in swine. *Infect. Immun.* **70**, 481–490 (2002).
13. E. Wehmann, B. Khayer, T. Magyar, Heterogeneity of *Bordetella bronchiseptica* adenylate

cyclase (*cyaA*) RTX domain. *Arch. Microbiol.* **197**, 105–112 (2015).

14. B. Arico, R. Rappuoli, *Bordetella parapertussis* and *Bordetella bronchiseptica* contain transcriptionally silent pertussis toxin genes. *J. Bacteriol.* **169**, 2847–2853 (1987).
15. S. Z. Hausman, J. D. Cherry, U. Heininger, C. H. W. Von König, D. L. Burns, Analysis of proteins encoded by the *ptx* and *ptl* genes of *Bordetella bronchiseptica* and *Bordetella parapertussis*. *Infect. Immun.* **64**, 4020–4026 (1996).
16. T. L. Nicholson, S. L. Brockmeier, C. L. Loving, K. B. Register, M. E. Kehrli, S. M. Shore, The *Bordetella bronchiseptica* type III secretion system is required for persistence and disease severity but not transmission in swine. *Infect. Immun.* **82**, 1092–1103 (2014).
17. A. A. Weiss, E. L. Hewlett, G. A. Myers, S. Falkow, Tn5-induced mutations affecting virulence factors of *Bordetella pertussis*. *Infect. Immun.* **42**, 33–41 (1983).
18. D. A. Relman, M. Domenighini, E. Toumanen, R. Rappuoli, S. Falkow, Filamentous hemagglutinin of *Bordetella pertussis*: Nucleotide sequence and crucial role in adherence. *Proc. Natl. Acad. Sci. U. S. A.* **86**, 2637–2641 (1989).
19. D. Relman, E. Tuomanen, S. Falkow, D. T. Golenbock, K. Saukkonen, S. D. Wright, Recognition of a bacterial adhesin by an integrin: Macrophage CR3 (αMβ2, CD11b CD18) binds filamentous hemagglutinin of *Bordetella pertussis*. *Cell*. **61**, 1375–1382 (1990).
20. S. M. Prasad, Y. Yin, E. Rodzinski, E. I. Tuomanen, H. R. Masure, Identification of a carbohydrate recognition domain in filamentous hemagglutinin from *Bordetella pertussis*. *Infect. Immun.* **61**, 2780–2785 (1993).
21. F. D. Menozzi, C. Gantiez, C. Locht, Interaction of the *Bordetella pertussis* filamentous hemagglutinin with heparin. *FEMS Microbiol. Lett.* **78**, 59–64 (1991).
22. F. R. Mooi, H. G. J. van der Heide, A. R. ter Avest, K. G. Welinder, I. Livey, B. A. M. van der Zeijst, W. Gaastra, Characterization of fimbrial subunits from *Bordetella* species. *Microb. Pathog.* **2**, 473–484 (1987).
23. B. Riboli, P. Pedroni, A. Cuzzoni, G. Grandi, F. de Ferra, Expression of *Bordetella pertussis* fimbrial (*fim*) genes in *Bordetella bronchiseptica*: *fimX* is expressed at a low level and vir-regulated. *Microb. Pathog.* **10**, 393–403 (1991).
24. S. A. Kania, S. Rajeev, E. H. Burns, T. F. Odom, S. M. Holloway, D. A. Bemis, Characterization of *fimN*, a new *Bordetella bronchiseptica* major fimbrial subunit gene. *Gene*. **256**, 149–155 (2000).

25. J. A. Edwards, N. A. Groathouse, S. Boitano, *Bordetella bronchiseptica* adherence to cilia is mediated by multiple adhesin factors and blocked by surfactant protein A. *Infect. Immun.* **73**, 3618–3626 (2005).
26. S. Mattoo, J. F. Miller, P. A. Cotter, Role of *Bordetella bronchiseptica* fimbriae in tracheal colonization and development of a humoral immune response. *Infect. Immun.* **68**, 2024–2033 (2000).
27. I. R. Henderson, J. P. Nataro, Virulence functions of autotransporter proteins. *Infect. Immun.* **69** (2001).
28. I. G. Charles, G. Dougan, D. Pickard, S. Chatfield, M. Smith, P. Novotny, P. Morrissey, N. F. Fairweather, Molecular cloning and characterization of protective outer membrane protein P.69 from *Bordetella pertussis*. *Proc. Natl. Acad. Sci. U. S. A.* **86**, 3554–3558 (1989).
29. L. J. Li, G. Dougan, P. Novotny, I. G. Charles, P.70 pertactin, an outer-membrane protein from *Bordetella parapertussis*: cloning, nucleotide sequence and surface expression in Escherichia coli. *Mol. Microbiol.* **5**, 409–417 (1991).
30. P. Emsley, I. G. Charles, N. F. Fairweather, N. W. Isaacs, Structure of *Bordetella pertussis* virulence factor P.69 pertactin. *Nature*. **381**, 90–92 (1996).
31. E. Leininger, M. Roberts, J. G. Kenimer, I. G. Charles, N. Fairweather, P. Novotny, M. J. Brennan, Pertactin, an Arg-Gly-Asp-containing *Bordetella pertussis* surface protein that promotes adherence of mammalian cells. *Proc. Natl. Acad. Sci. U. S. A.* **88**, 345–349 (1991).
32. P. Emsley, G. McDermott, I. G. Charles, N. F. Fairweather, N. W. Isaacs, Crystallographic characterization of pertactin, a membrane-associated protein from *Bordetella pertussis*. *J. Mol. Biol.* **235**, 772–773 (1994).
33. L. Coutte, R. Antoine, H. Drobecq, C. Locht, F. Jacob-Dubuisson, Subtilisin-like autotransporter serves as maturation protease in a bacterial secretion pathway. *EMBO J.* **20**, 5040–5048 (2001).
34. R. C. Fernandez, A. A. Weiss, Cloning and sequencing of a *Bordetella pertussis* serum resistance locus. *Infect. Immun.* **62**, 4727–4738 (1994).
35. T. M. Finn, D. F. Amsbaugh, Vag8, a *Bordetella pertussis* Bvg-Regulated Protein. *Infect. Immun.* **66**, 3985–3989 (1998).
36. J. Vojtova, J. Kamanova, P. Sebo, *Bordetella* adenylate cyclase toxin: A swift saboteur of

host defense. *Curr. Opin. Microbiol.* **9** (2006).

37. R. Shrivastava, J. F. Miller, Virulence factor secretion and translocation by *Bordetella* species. *Curr. Opin. Microbiol.* **12**, 88–93 (2009).
38. A. Raptis, L. Knipling, J. Wolff, Dissociation of catalytic and invasive activities of *Bordetella pertussis* adenylate cyclase. *Infect. Immun.* **57**, 1725–1730 (1989).
39. P. A. Cotter, J. F. Miller, in *Principles of Bacterial Pathogenesis* (Academic Press, 2001).
40. A. Rogel, J. E. Schultz, R. M. Brownlie, J. G. Coote, R. Parton, E. Hanski, *Bordetella pertussis* adenylate cyclase: purification and characterization of the toxic form of the enzyme. *EMBO J.* **8**, 2755–2760 (1989).
41. E. L. Hewlett, K. J. Kim, S. J. Lee, M. C. Gray, Adenylate cyclase toxin from *Bordetella pertussis*: Current concepts and problems in the study of toxin functions. *Int. J. Med. Microbiol.* **290**, 333–335 (2000).
42. E. T. Harvill, P. A. Cotter, M. H. Yuk, J. F. Miller, Probing the function of *Bordetella bronchiseptica* adenylate cyclase toxin by manipulating host immunity. *Infect. Immun.* **67**, 1493–1500 (1999).
43. T. Magyar, N. Chanter, A. J. Lax, J. M. Rutter, G. A. Hall, The pathogenesis of turbinate atrophy in pigs caused by *Bordetella bronchiseptica*. *Vet. Microbiol.* **18**, 135–146 (1988).
44. K. Kume, T. Nakai, Y. Samejima, C. Sugimoto, Properties of dermonecrotic toxin prepared from sonic extracts of *Bordetella bronchiseptica*. *Infect. Immun.* **52**, 370–377 (1986).
45. H. Nagano, T. Nakai, Y. Horiguchi, K. Kume, Isolation and characterization of mutant strains of *Bordetella bronchiseptica* lacking dermonecrotic toxin-producing ability. *J. Clin. Microbiol.* **26**, 1983–1987 (1988).
46. K. E. Walker, A. A. Weiss, Characterization of the dermonecrotic toxin in members of the Genus *Bordetella*. *Infect. Immun.* **62**, 3817–3828 (1994).
47. G. D. Pullinger, T. E. Adams, P. B. Mullan, T. I. Garrod, A. J. Lax, Cloning, expression, and molecular characterization of the dermonecrotic toxin gene of *Bordetella* spp. *Infect. Immun.* **64**, 4163–4171 (1996).
48. G. Schmidt, U. M. Goehring, J. Schirmer, M. Lerm, K. Aktories, Identification of the C-terminal part of *Bordetella* dermonecrotic toxin as a transglutaminase for Rho GTPases. *J. Biol. Chem.* **274**, 31875–31881 (1999).
49. S. Teruya, Y. Hiramatsu, K. Nakamura, A. Fukui-Miyazaki, K. Tsukamoto, N. Shinoda, D.

Motooka, S. Nakamura, K. Ishigaki, N. Shinzawa, T. Nishida, F. Sugihara, Y. Maeda, Y. Horiguchi, *Bordetella* dermonecrotic toxin is a neurotropic virulence factor that uses Cav3.1 as the cell surface receptor. *MBio*. **11** (2020).

50. Y. Horiguchi, N. Inoue, M. Masuda, T. Kashimoto, J. Katahira, N. Sugimoto, M. Matsuda, *Bordetella bronchiseptica* dermonecrotizing toxin induces reorganization of actin stress fibers through deamidation of Gin-63 of the GTP-binding protein Rho. *Proc. Natl. Acad. Sci. U. S. A.* **94**, 11623–11626 (1997).
51. T. Kashimoto, J. Katahira, W. R. Cornejo, M. Masuda, A. Fukuoh, T. Matsuzawa, T. Ohnishi, Y. Horiguchi, Identification of functional domains of *Bordetella* dermonecrotizing toxin. *Infect. Immun.* **67**, 3727–3732 (1999).
52. M. Lerm, G. Schmidt, U. M. Goehring, J. Schirmer, K. Aktories, Identification of the region of Rho involved in substrate recognition by *Escherichia coli* cytotoxic necrotizing factor 1 (CNF1). *J. Biol. Chem.* **274**, 28999–29004 (1999).
53. A. A. Weiss, S. Falkow, Genetic analysis of phase change in *Bordetella pertussis*. *Infect. Immun.* **43**, 263–269 (1984).
54. G. M. De Tejada, J. F. Miller, P. A. Cotter, Comparative analysis of the virulence control systems of *Bordetella pertussis* and *Bordetella bronchiseptica*. *Mol. Microbiol.* **22**, 895–908 (1996).
55. P. A. Cotter, A. M. Jones, Phosphorelay control of virulence gene expression in *Bordetella*. *Trends Microbiol.* **11**, 367–373 (2003).
56. J. A. Melvin, E. V. Scheller, J. F. Miller, P. A. Cotter, *Bordetella pertussis* pathogenesis: current and future challenges. *Nat. Rev. Microbiol.* **12**, 274–288 (2014).
57. P. A. Cotter, J. F. Miller, A mutation in the *Bordetella bronchiseptica bvgS* gene results in reduced virulence and increased resistance to starvation, and identifies a new class of Bvg-regulated antigens. *Mol. Microbiol.* **24**, 671–685 (1997).
58. P. A. Cotter, J. F. Miller, BvgAS-Mediated Signal-Transduction: Analysis of Phase-locked Regulatory Mutants of *Bordetella bronchiseptica* in a Rabbit Model. *Infect. Immun.* **62**, 3381–3390 (1994).
59. E. Uribe-Querol, C. Rosales, Phagocytosis: Our Current Understanding of a Universal Biological Process. *Front. Immunol.* **11** (2020).
60. A. Banemann, R. Gross, Phase variation affects long-term survival of *Bordetella*

bronchiseptica in professional phagocytes. *Infect. Immun.* **65**, 3469–3473 (1997).

61. C. A. Guzmàn, M. Rohde, K. N. Timmis, Mechanisms involved in uptake of *Bordetella bronchiseptica* by mouse dendritic cells. *Infect. Immun.* **62**, 5538–5544 (1994).
62. B. Schneider, R. O. Y. Gross, A. Haas, Phagosome Acidification Has Opposite Effects on Intracellular Survival of *Bordetella pertussis* and *B. bronchiseptica*. **68**, 7039–7048 (2000).
63. C. B. Forde, R. Parton, J. G. Coote, Bioluminescence as a reporter of intracellular survival of *Bordetella bronchiseptica* in murine phagocytes. *Infect. Immun.* **66**, 3198–3207 (1998).
64. C. A. Guzmàn, M. Rohde, M. Bock, K. N. Timmis, Invasion and intracellular survival of *Bordetella bronchiseptica* in mouse dendritic cells. *Infect. Immun.* **62**, 5528–5537 (1994).
65. K. Zimna, E. Medina, H. Jungnitz, C. A. Guzmàn, Role played by the response regulator Ris in *Bordetella bronchiseptica* resistance to macrophage killing. *FEMS Microbiol. Lett.* **201**, 177–180 (2001).
66. G. S. Chhatwal, M. J. Walker, H. Yan, K. N. Timmis, C. A. Guzmàn, Temperature dependent expression of an acid phosphatase by *Bordetella bronchiseptica*: Role in intracellular survival. *Microb. Pathog.* **22**, 257–264 (1997).
67. I. H. Soumana, B. Linz, E. T. Harvill, Environmental origin of the genus *Bordetella*. *Front. Microbiol.* **8**, 1–10 (2017).
68. J. M. Lynch, E. Mitscherlich , E. H. Marth, Microbial Survival in the Environment, Bacteria and Rickettsiae Important in Human and Animal Health. *Q. Rev. Biol.* **60**, 503–503 (1985).
69. J. F. Porter, R. Parton, A. C. Wardlaw, Growth and survival of *Bordetella bronchiseptica* in natural waters and in buffered saline without added nutrients. *Appl. Environ. Microbiol.* **57**, 1202–1206 (1991).
70. J. F. Porter, A. C. Wardlaw, Long-term survival of *Bordetella bronchiseptica* in lakewater and in buffered saline without added nutrients. *FEMS Microbiol. Lett.* **110**, 33–36 (1993).
71. N. A. Khan, *Acanthamoeba : Biology and Pathogenesis* (Caister Academic Press, **54** (2015).
72. F. Marciano-Cabral, G. Cabral, *Acanthamoeba* spp. as agents of disease in humans. *Clin. Microbiol. Rev.* **16**, 273–307 (2003).
73. R. Siddiqui, N. A. Khan, Biology and pathogenesis of *Acanthamoeba*. *Parasites and Vectors*. **5**, 6 (2012).
74. H. H. Kong, Molecular Phylogeny of *Acanthamoeba*. *Korean J. Parasitol.* **47** (2009).

75. J. R. Cope, J. S. Yoder, G. S. Visvesvara, in *Infectious Diseases* (Elsevier, 2017).
76. S. Bouyer, M. H. Rodier, A. Guillot, Y. Héchard, *Acanthamoeba castellanii*: Proteins involved in actin dynamics, glycolysis, and proteolysis are regulated during encystation. *Exp. Parasitol.* **123**, 90–94 (2009).
77. A. de Obeso Fernandez del Valle, Protein secretion and encystation in *Acanthamoeba*, 258 (2019).
78. T. M. Preston, H. Richards, R. S. Wotton, Locomotion and feeding of *Acanthamoeba* at the water air interface of ponds. *FEMS Microbiol. Lett.* **194**, 143–147 (2001).
79. P. G. Allen, E. A. Dawidowicz, Phagocytosis in *Acanthamoeba*: I. A mannose receptor is responsible for the binding and phagocytosis of yeast. *J. Cell. Physiol.* **145**, 508–513 (1990).
80. J. Iqbal, R. Siddiqui, N. A. Khan, *Acanthamoeba* can propagate on thermophilic Sulfolobus spp. *Parasitol. Res.* **112**, 879–881 (2013).
81. J. E. Strassmann, L. Shu, Ancient bacteria–amoeba relationships and pathogenic animal bacteria. *PLoS Biol.* **15**, 1–8 (2017).
82. J. L. Sinclair, J. F. McClellan, D. C. Coleman, Nitrogen Mineralization by *Acanthamoeba polyphaga* in Grazed *Pseudomonas paucimobilis* Populations. *Appl. Environ. Microbiol.* **42**, 667–671 (1981).
83. N. A. Khan, J. Iqbal, R. Siddiqui, Taste and smell in *Acanthamoeba* feeding. *Acta Protozool.* **53** (2014).
84. F. L. Schuster, M. Levandowsky, Chemosensory responses of *Acanthamoeba castellanii*: Visual analysis of random movement and responses to chemical signals. *J. Eukaryot. Microbiol.* **43**, 150–158 (1996).
85. B. Bowers, Comparison of pinocytosis and phagocytosis in *Acanthamoeba castellanii*. *Exp. Cell Res.* **110**, 409–417 (1977).
86. B. Astorga, J. Lorenzo-Morales, C. M. Martín-Navarro, V. Alarcõn, J. Moreno, A. C. González, E. Navarrete, J. E. Piñero, B. Valladares, *Acanthamoeba* belonging to T3, T4, and T11: Genotypes isolated from air-conditioning units in Santiago, Chile. *J. Eukaryot. Microbiol.* **58**, 542–544 (2011).
87. R. L. Tyndall, E. S. Lehman, E. K. Bowman, D. K. Milton, J. M. Barbaree, Home Humidifiers as a Potential Source of Exposure to Microbial Pathogens, Endotoxins, and Allergens. *Indoor Air*. **5**, 171–178 (1995).

88. H. R. Bagheri, R. Shafiei, F. Shafiei, S. A. Sajjadi, Isolation of *Acanthamoeba* spp. from drinking waters in several Hospitals of Iran. *Iran. J. Parasitol.* **5**, 19–25 (2010).

89. V. J. Maschio, F. Chies, A. M. Carlesso, A. Carvalho, S. P. Rosa, S. T. Van Der Sand, M. B. Rott, *Acanthamoeba* T4, T5 and T11 Isolated From Mineral Water Bottles in Southern Brazil. *Curr. Microbiol.* **70**, 6–9 (2015).

90. T. A. Nerad, T. K. Sawyer, E. J. Lewis, S. M. Mclaughlin, *Acanthamoeba pearcei* N. Sp. (Protozoa: Amoebida) from Sewage Contaminated Sediments. *J. Eukaryot. Microbiol.* **42**, 702–705 (1995).

91. M. Rezaeian, M. Niyyati, S. Farnia, A. Motevalli Haghi, Isolation of *Acanthamoeba* spp. from different environmental sources. *Iran. J. Parasitol.* **3**, 44–47 (2008).

92. J. Lorenzo-Morales, J. F. Lindo, E. Martinez, D. Calder, E. Figueruelo, B. Valladares, A. Ortega-Rivas, Pathogenic *Acanthamoeba* strains from water sources in Jamaica, West Indies. *Ann. Trop. Med. Parasitol.* **99**, 751–758 (2005).

93. N. A. Khan, *Acanthamoeba*: Biology and increasing importance in human health. *FEMS Microbiol. Rev.* **30** (2006), pp. 564–595.

94. P. H. H. Weekers, C. Van Der Drift, Nitrogen Metabolizing Enzyme Activities In the Free-Living Soil Amoebae *Acanthamoeba castellanii*, *Acanthamoeba polyphaga* and *Hartmannella vermiformis*. *J. Eukaryot. Microbiol.* **40**, 251–254 (1993).

95. V. E. Paquet, S. J. Charette, Amoeba-resisting bacteria found in multilamellar bodies secreted by *Dictyostelium discoideum*: Social amoebae can also package bacteria. *FEMS Microbiol. Ecol.* **92** (2016).

96. M. Horn, M. Wagner, in *Journal of Eukaryotic Microbiology*. **51**, 509-514 (2004).

97. Y. Shi, D. C. Queller, Y. Tian, S. Zhang, Q. Yan, Z. He, Z. He, C. Wu, C. Wang, L. Shu, S.-J. Liu, Ed., The Ecology and Evolution of Amoeba-Bacterium Interactions. *Appl. Environ. Microbiol.* **87** (2021).

98. N. A. Khan, R. Siddiqui, Predator vs aliens: bacteria interactions with *Acanthamoeba*. *Parasitology*. **141**, 869–874 (2014).

99. R. Rønn, A. E. McCaig, B. S. Griffiths, J. I. Prosser, Impact of protozoan grazing on bacterial community structure in soil microcosms. *Appl. Environ. Microbiol.* **68**, 6094–6105 (2002).

100. S. Adiba, C. Nizak, M. van Baalen, E. Denamur, F. Depaulis, From grazing resistance to

pathogenesis: The coincidental evolution of virulence factors. *PLoS One*. **5** (2010).

101. C. Matz, S. Kjelleberg, Off the hook - How bacteria survive protozoan grazing. *Trends Microbiol.* **13**, 302–307 (2005).
102. R. Siddiqui, N. A. Khan, War of the microbial worlds: Who is the beneficiary in *Acanthamoeba*-bacterial interactions? *Exp. Parasitol.* **130** (2012).
103. A. M. Denoncourt, V. E. Paquet, S. J. Charette, Potential role of bacteria packaging by protozoa in the persistence and transmission of pathogenic bacteria. *Front. Microbiol.* **5** (2014).
104. G. Greub, D. Raoult, Microorganisms Resistant to Free-Living Amoebae. *Clin. Microbiol. Rev.* **17** (2004).
105. W. Khunkitti, D. Lloyd, J. R. Furr, A. D. Russell, *Acanthamoeba castellanii*: Growth, encystment, excystment and biocide susceptibility. *J. Infect.* **36**, 43–48 (1998).
106. J. A. Benavides-Montaño, V. Vadyvaloo, *Yersinia pestis* Resists Predation by *Acanthamoeba castellanii* and Exhibits Prolonged Intracellular Survival. *Appl. Environ. Microbiol.* **83**, 1–4 (2017).
107. B. S. Fields, R. F. Benson, R. E. Besser, *Legionella* and legionnaires' disease: 25 Years of investigation. *Clin. Microbiol. Rev.* **15** (2002).
108. A. Magnet, R. H. S. Peralta, T. S. Gomes, F. Izquierdo, C. Fernandez-Vadillo, A. L. Galvan, M. J. Pozuelo, C. Pelaz, S. Fenoy, C. Del Águila, Vectorial role of *Acanthamoeba* in *Legionella* propagation in water for human use. *Sci. Total Environ.* **505**, 889–895 (2015).
109. M. V. Storey, J. Winiecka-Krusnell, N. J. Ashbolt, T. A. Stenström, The efficacy of heat and chlorine treatment against thermotolerant *Acanthamoebae* and *Legionellae*. *Scand. J. Infect. Dis.* **36**, 656–662 (2004).
110. M. Steinert, U. Hentschel, J. Hacker, Legionella pneumophila: An aquatic microbe goes astray. *FEMS Microbiol. Rev.* **26** (2002).
111. T. J. Rowbotham, Preliminary report on the pathogenicity of *Legionella pneumophila* for freshwater and soil amoebae. *J. Clin. Pathol.* **33**, 1179–1183 (1980).
112. D. L. Taylor-Mulneix, L. Bendor, B. Linz, I. Rivera, V. E. Ryman, K. K. Dewan, S. M. Wagner, E. F. Wilson, L. J. Hilburger, L. E. Cuff, C. M. West, E. T. Harvill, *Bordetella bronchiseptica* exploits the complex life cycle of *Dictyostelium discoideum* as an amplifying transmission vector. *PLoS Biol.* **15**, 1–28 (2017).

113. H. Abe, S. Kamitani, A. Fukui-Miyazaki, N. Shinzawa, K. Nakamura, Y. Horiguchi, Detection of genes expressed in *Bordetella bronchiseptica* colonizing rat trachea by in vivo expressed-tag immunoprecipitation method. *Microbiol. Immunol.* **59**, 249–261 (2015).
114. S. Nishikawa, N. Shinzawa, K. Nakamura, K. Ishigaki, H. Abe, Y. Horiguchi, The Bvg-repressed gene *brtA*, encoding biofilm-associated surface adhesin, is expressed during host infection by *Bordetella bronchiseptica*. *Microbiol. Immunol.* **60**, 93–105 (2016).
115. O. Edelheit, A. Hanukoglu, I. Hanukoglu, Simple and efficient site-directed mutagenesis using two single-primer reactions in parallel to generate mutants for protein structure-function studies. *BMC Biotechnol.* **9**, 1–8 (2009).
116. K. Tsukamoto, N. Shinzawa, A. Kawai, M. Suzuki, H. Kidoya, N. Takakura, H. Yamaguchi, T. Kameyama, H. Inagaki, H. Kurahashi, Y. Horiguchi, Y. Doi, The *Bartonella* autotransporter BafA activates the host VEGF pathway to drive angiogenesis. *Nat. Commun.* **11**, 3571 (2020).
117. Y. Aqeel, R. Siddiqui, H. Iftikhar, N. A. Khan, The effect of different environmental conditions on the encystation of *Acanthamoeba castellanii* belonging to the T4 genotype. *Exp. Parasitol.* **135**, 30–35 (2013).
118. Y. Hiramatsu, T. Nishida, D. K. Nugraha, F. Sugihara, Y. Horiguchi, Melanin Produced by *Bordetella parapertussis* Confers a Survival Advantage to the Bacterium during Host Infection. *mSphere* (2021).
119. T. van Opijnen, D. W. Lazinski, A. Camilli, Genome-Wide Fitness and Genetic Interactions Determined by Tn-seq, a High-Throughput Massively Parallel Sequencing Method for Microorganisms. *Curr. Protoc. Microbiol.* **36** (2015).
120. M. D. Robinson, D. J. McCarthy, G. K. Smyth, edgeR: A Bioconductor package for differential expression analysis of digital gene expression data. *Bioinformatics*. **26**, 139–140 (2009).
121. T. L. Nicholson, Construction and validation of a first-generation *Bordetella bronchiseptica* long-oligonucleotide microarray by transcriptional profiling the Bvg regulon. *BMC Genomics*. **8**, 220 (2007).
122. K. Okada, Y. Ogura, T. Hayashi, A. Abe, A. Kuwae, Y. Horiguchi, H. Abe, Complete genome sequence of *Bordetella bronchiseptica* S798, an isolate from a pig with atrophic rhinitis. *Genome Announc.* **2** (2014).

123. M. E. Kovach, P. H. Elzer, D. S. Hill, G. T. Robertson, M. A. Farris, R. M. Roop, K. M. Peterson, Four new derivatives of the broad-host-range cloning vector pBBR1MCS, carrying different antibiotic-resistance cassettes. **166**, 1–2 (2015).
124. M. A. Laskowski-Arce, K. Orth, *Acanthamoeba castellanii* promotes the survival of *Vibrio parahaemolyticus*. *Appl. Environ. Microbiol.* **74**, 7183–7188 (2008).
125. G. Sandström, A. Saeed, H. Abd, *Acanthamoeba polyphaga* is a possible host for *Vibrio cholerae* in aquatic environments. *Exp. Parasitol.* **126**, 65–68 (2010).
126. X. T. Bui, A. Winding, K. Qvortrup, A. Wolff, D. D. Bang, C. Creuzenet, Survival of *Campylobacter jejuni* in co-culture with *Acanthamoeba castellanii*: Role of amoeba-mediated depletion of dissolved oxygen. *Environ. Microbiol.* **14**, 2034–2047 (2012).
127. J. Winiecka-Krusnell, K. Wreiber, A. Von Euler, L. Engstrand, E. Linder, Free-living amoebae promote growth and survival of *Helicobacter pylori*. *Scand. J. Infect. Dis.* **34**, 253–256 (2002).
128. W. D. Dolphin, Effect of Glucose on Glycine Requirement of *Acanthamoeba castellanii*. *J. Protozool.* **23**, 455–457 (1976).
129. E. Stubblefield, G. C. Mueller, Effects of Sodium Chloride Concentration on Growth, Biochemical Composition, and Metabolism of HeLa Cells. *Cancer Res.* **20**, 1646–1655 (1960).
130. L. B. Pinheiro, M. D. Gibbs, G. Vesey, J. J. Smith, P. L. Bergquist, Fluorescent reference strains of bacteria by chromosomal integration of a modified green fluorescent protein gene. *Appl. Microbiol. Biotechnol.* **77**, 1287–1295 (2008).
131. C. Van Der Henst, T. Scrignari, C. Maclachlan, M. Blokesch, An intracellular replication niche for *Vibrio cholerae* in the amoeba *Acanthamoeba castellanii*. *ISME J.* **10**, 897–910 (2016).
132. A. Sharma, A. Puhar, Gentamicin Protection Assay to Determine the Number of Intracellular Bacteria during Infection of Human TC7 Intestinal Epithelial Cells by *Shigella flexneri*. *Bio-Protocol*. **9** (2019).
133. A. Akya, A. Pointon, C. Thomas, Viability of *Listeria monocytogenes* in co-culture with *Acanthamoeba* spp. *FEMS Microbiol. Ecol.* **70**, 20–29 (2009).
134. A. Sanchez-Hidalgo, A. Obregón-Henao, W. H. Wheat, M. Jackson, M. Gonzalez-Juarrero, *Mycobacterium bovis* hosted by free-living-amoebae permits their long-term persistence

survival outside of host mammalian cells and remain capable of transmitting disease to mice. *Environ. Microbiol.* **19**, 4010–4021 (2017).

135. M. Steinert, K. Birkness, E. White, B. Fields, F. Quinn, *Mycobacterium avium* bacilli grow saprozoically in coculture with *Acanthamoeba polyphaga* and survive within cyst walls. *Appl. Environ. Microbiol.* **64**, 2256–2261 (1998).
136. L. Y. Gao, Y. A. Kwaik, The mechanism of killing and exiting the protozoan host *Acanthamoeba polyphaga* by *Legionella pneumophila*. *Environ. Microbiol.* **2**, 79–90 (2000).
137. C. Van der Henst, A. S. Vanhove, N. C. Drebes Dörr, S. Stutzmann, C. Stoudmann, S. Clerc, T. Scrignari, C. Maclachlan, G. Knott, M. Blokesch, Molecular insights into *Vibrio cholerae*'s intra-amoebal host-pathogen interactions. *Nat. Commun.* **9** (2018).
138. R. A. Pal, The osmoregulatory system of the amoeba, *Acanthamoeba castellanii*. *J. Exp. Biol.* **57**, 55–76 (1972).
139. G. S. Visvesvara, H. Moura, F. L. Schuster, Pathogenic and opportunistic free-living amoebae: *Acanthamoeba* spp., *Balamuthia mandrillaris*, *Naegleria fowleri*, and *Sappinia diploidea*. *FEMS Immunol. Med. Microbiol.* **50** (2007).
140. T. L. Nicholson, S. L. Brockmeier, C. L. Loving, K. B. Register, M. E. Kehrli, S. E. Stibitz, S. M. Shore, Phenotypic modulation of the virulent Bvg phase is not required for pathogenesis and transmission of *Bordetella bronchiseptica* in swine. *Infect. Immun.* **80**, 1025–1036 (2012).
141. J. Olofsson, D. Axelsson-Olsson, L. Brudin, B. Olsen, P. Ellström, *Campylobacter jejuni* actively invades the amoeba *Acanthamoeba polyphaga* and survives within non digestive vacuoles. *PLoS One*. **8** (2013).
142. C. A. Cummings, H. J. Bootsma, D. A. Relman, J. F. Miller, Species- and strain-specific control of a complex, flexible regulon by *Bordetella* BvgAS. *J. Bacteriol.* **188**, 1775–1785 (2006).
143. T. van Opijnen, A. Camilli, Transposon insertion sequencing: a new tool for systems-level analysis of microorganisms. *Nat. Rev. Microbiol.* **11**, 435–442 (2013).
144. G. E. Vergara, Mechanisms of intracellular resistance and the role of the escape of *Vibrio cholerae* from protist hosts Thesis / Dissertation Sheet (2019).
145. S. L. Drennan, A. Lama, R. C. Johnson, E. D. Cambronne, G. L. Rubenstein, Identification

of Conserved ABC Importers Necessary for Intracellular Survival of *Legionella pneumophila* in Multiple Hosts. *Front. Cell. Infect. Microbiol.* **7**, 1–14 (2017).

146. S. R. Shames, L. Liu, J. C. Havey, W. B. Schofield, A. L. Goodman, C. R. Roy, Multiple *Legionella pneumophila* effector virulence phenotypes revealed through high-throughput analysis of targeted mutant libraries. *Proc. Natl. Acad. Sci.*, **114** (2017).
147. H. Abd, S. P. Valeru, S. M. Sami, A. Saeed, S. Raychaudhuri, G. Sandström, Interaction between *Vibrio mimicus* and *Acanthamoeba castellanii*. *Environ. Microbiol. Rep.* **2**, 166–171 (2010).
148. J. M. Rodriguez-Paris, K. V. Nolta, T. L. Steck, Characterization of lysosomes isolated from *Dictyostelium discoideum* by magnetic fractionation. *J. Biol. Chem.* **268**, 9110–9116 (1993).
149. J. A. Bozue, W. Johnson, Interaction of *Legionella pneumophila* with *Acanthamoeba castellanii*: Uptake by Coiling Phagocytosis and Inhibition of Phagosome-Lysosome Fusion. *Infect. Immun.* **64**, 668–673 (1996).
150. J. D. Cirillo, S. Falkow, L. S. Tompkins, L. E. Bermudez, Interaction of *Mycobacterium avium* with environmental amoebae enhances virulence. *Infect. Immun.* **65**, 3759–3767 (1997).
151. J. Lamothe, S. Thyssen, M. A. Valvano, *Burkholderia cepacia* complex isolates survive intracellularly without replication within acidic vacuoles of *Acanthamoeba polyphaga*. *Cell. Microbiol.* **6**, 1127–1138 (2004).

ACKNOWLEDGEMENTS

At the end of this Ph.D. journey, I would like to thank all the wonderful people who always supported me along the way.

First and foremost, I would like to express my sincere gratitude to my supervisor, Prof. Yasuhiko Horiguchi, for the kindness and compassionate guidance during my master and doctorate program. Without him, I would not have reached this stage.

Besides, I would like to thank my Ph.D. committee members: Prof. Toru Nakano (Graduate school of Frontier Biosciences (FBS), Osaka University), Prof. Tetsuya Iida (Research Institute for Microbial Diseases (RIMD), Osaka University), and Prof. Shiroh Iwanaga (RIMD, Osaka University) for the insightful comments and advice.

I sincerely thank the Molecular Bacteriology lab members and all my friends at BIKEN and Osaka University, who are always kind, helpful, and supportive. Because of all of them, my Ph.D. life become easier.

I would also thank to Taniguchi Scholarship Program, which was generously awarded by Research Institute for Microbial Diseases (RIMD), Osaka University. The full financial support they have provided allows me to focus on my Ph.D. program.

Without any doubt, the love and sincerity from my dear wife, Dwi Mutiara Fahmi, that arise as support is an important to motivate me constantly. Thank you for always taking care of me and staying beside me with all the encouragement.

There are not enough words to express my gratitude to my parents, my father Suharyono and my mother Mukartini. Thank you for everything they have taught me, all the prayers they have said, and for all the support and love they have given to me.

Finally, in accordance with the Islam traditions, I also would express my gratitude toward Almighty Allah SWT. With His grace, I could have the strength and ability to finish this Ph.D. program.

AUTHOR'S ACHIEVEMENTS

List of Publications

- Yukihiro Hiramatsu, Takashi Nishida, **Dendi Krisna Nugraha**, Fuminori Sugihara, Yasuhiko Horiguchi. (2021). Melanin produced by *Bordetella parapertussis* confers a survival advantage to the bacterium during host infection. *mSphere* (6):5. https://doi.org/10.1128/mSphere.00819-21.
- **Dendi Krisna Nugraha**, Takashi Nishida, Yuki Tamaki, Hiroyuki Yamaguchi, and Yasuhiko Horiguchi. Interaction between *Bordetella bronchiseptica* and *Acanthamoeba* as a transient host in the natural environment. *Manuscript in preparation*.

International and Domestic Meetings, and Award

Presentation in international conferences

Dendi K. Nugraha, Hiroyuki Yamaguchi, and Yasuhiko Horiguchi. *Bordetella bronchiseptica* utilizes *Acanthamoeba castellanii* as a temporal niche. The 19th Awaji International Forum on Infection and Immunity, Online meeting, September 28-30, 2021. (Poster)

Presentation in domestic conferences or meetings

- **Dendi K. Nugraha**, Takashi Nishida, Yuki Tamaki, Hiroyuki Yamaguchi, and Yasuhiko Horiguchi. *Bordetella bronchiseptica* utilizes *Acanthamoeba castellanii* as a temporal niche. 令和 3 年度研究業績発表会, 2022 年 1 月 21 日、阪大微生物病研究所 (oral)
- **Dendi K. Nugraha**, Takashi Nishida, Yuki Tamaki, Hiroyuki Yamaguchi, and Yasuhiko Horiguchi. *Bordetella bronchiseptica* utilizes *Acanthamoeba castellanii* as a temporal niche. BIKEN 谷口海外奨学生との交流, 2021 年 11 月 30 日, 阪大微生物病研究所 (Oral)
- **Dendi K. Nugraha**, Takashi Nishida, Yuki Tamaki, Hiroyuki Yamaguchi, and Yasuhiko Horiguchi. *Bordetella bronchiseptica* utilizes *Acanthamoeba castellanii* as a temporal niche. 第 74 回日本細菌学会関西支部総会 2021 年 11 月 13 日, オンライン (Oral)

- **Dendi K. Nugraha**, Hiroyuki Yamaguchi, and Yasuhiko Horiguchi. *Bordetella bronchiseptica* utilizes *Acanthamoeba castellanii* as a temporal niche. 第 73 回日本細菌学会関西支部総会, 2020 年 11 月 14 日, 大阪 (Oral)
- **Dendi K. Nugraha**, Hiroyuki Yamaguchi, and Yasuhiko Horiguchi. *Bordetella bronchiseptica* utilizes *Acanthamoeba castellanii* as a temporal niche. 第 93 回日本細菌学会総会, 2020 年 2 月 19 日, 名古屋 (Poster)
- **Dendi K. Nugraha**, Hiroyuki Yamaguchi, and Yasuhiko Horiguchi. *Bordetella bronchiseptica* utilizes *Acanthamoeba castellanii* as a temporal niche. 令和元年度研究業績発表会, 2020 年 1 月 16 日、阪大微生物病研究所 (Poster)
- **Dendi K. Nugraha**, Hiroyuki Yamaguchi, and Yasuhiko Horiguchi. *Bordetella bronchiseptica* utilizes *Acanthamoeba castellanii* as a temporal niche. 第 72 回日本細菌学会関西支部総会, 2019 年 11 月 16 日, 大阪 (Oral)

Award

Dendi K. Nugraha. 優秀発表賞 (Excellent Presentation Award). Dendi K. Nugraha, Hiroyuki Yamaguchi, and Yasuhiko Horiguchi. *Bordetella bronchiseptica* utilizes *Acanthamoeba castellanii* as a temporal niche. 第 93 回日本細菌学会総会, 2020 年 2 月 19 日, 名古屋